



Preventing groundwater intrusion into sheet-piled excavations using jet grouting

A literature review and a case study comparing semi-theoretical prediction models for column diameters

Master's thesis in Infrastructure and Environmental Engineering

LINNÉA JOHANSSON
FILIPPA SPÅNÉR

DEPARTMENT OF ARCHITECTURE
AND CIVIL ENGINEERING

MASTER'S THESIS ACEX30

Preventing groundwater intrusion into sheet-piled excavations using jet grouting
A literature review and a case study comparing semi-theoretical prediction models for column
diameters

Master's Thesis in the Master's Programme of Infrastructure and Environmental Engineering

LINNÉA JOHANSSON
FILIPPA SPÅNÉR

Department of Architecture and Civil Engineering
Division of Geology and Geotechnics
Research Group Engineering Geology
CHALMERS UNIVERSITY OF TECHNOLOGY

Göteborg, Sweden 2020

Preventing groundwater intrusion into sheet-piled excavations using jet grouting

A literature review and a case study comparing semi-theoretical prediction models for column diameters

Master's Thesis in the Master's Programme of Infrastructure and Environmental Engineering

LINNÉA JOHANSSON

FILIPPA SPÅNÉR

© LINNEA JOHANSSON, FILIPPA SPÅNÉR, 2020

Examensarbete ACEX30

Institutionen för arkitektur och samhällsbyggnadsteknik

Chalmers tekniska högskola, 2020

Department of Architecture and Civil Engineering

Division of Geology and Geotechnics

Research Group Engineering Geology

Chalmers University of Technology

SE-412 96 Göteborg

Sweden

Telephone: + 46 (0)31-772 1000

Cover:

Photograph from the jet grouting trial performed at the Gothenburg Port Line

Taken on March 16, 2020, by the authors

Department of Architecture and Civil Engineering

Göteborg, Sweden, 2020

Preventing groundwater intrusion into sheet-piled excavations using jet grouting

A literature review and a case study comparing semi-theoretical prediction models for column diameters

Master's thesis in the Master's Programme of Infrastructure and Environmental Engineering

LINNÉA JOHANSSON

FILIPPA SPÅNÉR

Department of Architecture and Civil Engineering

Division of Geology and Geotechnics

Research Group Engineering Geology

Chalmers University of Technology

ABSTRACT

When carrying out deep excavation projects, a common concern is inflow of groundwater. One possible solution to seal excavations is to use jet grouting technology. The practice entails an initial drilling to a pre-determined depth, followed by an injection of a cementing agent by a high-velocity jet. This stream erodes and remolds the immediate soil matrix, creating a column with improved characteristics. By merging columns into one another, a water barrier can be formed.

The overall purpose of this master's thesis was to gain an in-depth knowledge about jet grouting. This by writing a comprehensive guide about the technology, focusing on the application of sealing the toe of a sheet pile wall driven to sloping bedrock. To achieve this, a literature review was conducted followed by an analysis of three semi-theoretical prediction models and one commercial prototype model to estimate jet grouted column diameters. These models were thereafter verified through a case study of a current Swedish infrastructure project.

The main finding from this thesis was that the models generally overestimate the columns' diameter, which indicates a risk of groundwater inflows if used when determining the operational parameters. Two of the models can however be considered as adequate since they predicted the diameter mainly within the suggested error margin. This thesis also found that excavation of test columns and the so-called "painted bars" test are two suitable verification methods of column diameters. Furthermore, observations made during the trial have been described of which may be of assistance when planning future test programs.

Keywords: groundwater control, jet grouting, semi-theoretical prediction models, sheet-piled excavations, waterproofing

Förhindring av grundvatteninträngning i spontade schakter genom att använda jetinjektering
En litteraturstudie och en fallstudie som jämför semi-teoretiska modeller för att uppskatta pelardiameter

Examensarbete inom masterprogrammet infrastruktur och miljöteknik

LINNÉA JOHANSSON

FILIPPA SPÅNÉR

Institutionen för arkitektur och samhällsbyggnadsteknik
Avdelningen för geologi och geoteknik
Teknisk geologi
Chalmers tekniska högskola

SAMMANFATTNING

Vid djupa schaktarbeten är inflöde av grundvatten ofta problematiskt. En möjlig lösning för att täta schakt är att tillämpa jetinjektering. Metoden innefattar först en borrhning till ett förbestämt djup och därefter en injektion av ett cementeringsmedel via en höghastighetsstråle. Denna jetström eroderar och omformar den närliggande jorden, vilket resulterar i en pelare med förbättrade egenskaper. Genom att producera pelare intill varandra kan en barriär mot grundvatten bildas.

Det övergripande syftet med denna masteruppsats var att få en djupare kunskap om jetinjektering. Detta genom att skriva en omfattande guide om tekniken med fokus på att täta undersidan av en spontvägg som är driven till sluttande berggrund. För att uppnå detta genomfördes en litteraturstudie samt en analys av tre semi-teoretiska modeller och en kommersiell prototypmodell som förutspår jetinjekterande pelardiametrar. Dessa modeller verifierades därefter med en fallstudie i ett aktuellt svenskt infrastrukturprojekt.

Den främsta upptäckten i denna avhandling var att modellerna i allmänhet överskattar pelarens diameter, vilket antyder att en risk för vatteninflöde föreligger om dessa skulle användas för att bestämma de operativa parametrarna. Två av modellerna kan dock betraktas som tillräckliga, då de flesta av de uppskattade diametrarna befinner sig inom den föreslagna felmarginalen. Denna avhandling fann också att utgrävning av testspelare samt test med målade stålstänger är två lämpliga verifieringsmetoder för pelardiametrar. Vidare har de observationer som gjordes under fallstudien beskrivits, vilket kan vara till hjälp vid planering av framtida testprogram.

Nyckelord: grundvattenkontroll, jetinjektering, semi-teoretiska beräkningsmodeller, spontade schakter, vattentätning

Contents

1	INTRODUCTION	1
1.1	Purpose and aim	2
1.2	Method	2
1.3	Scope and limitations	3
2	GENERAL PRACTICES OF JET GROUTING	4
2.1	Modern jet grouting procedure	4
2.1.1	Treatment systems	6
2.1.2	Lifting and rotation	7
2.1.3	Overlapping and installation sequences	8
2.2	Operational parameters	9
2.2.1	Equipment set-up	9
2.2.2	Grout and spoil return	10
2.2.3	Safety	11
2.3	Applications of jet grouting	12
2.4	The significance of the soil	12
2.4.1	The mechanisms of soil and jet interaction	13
2.4.2	Swedish geology	14
2.5	Sustainability	16
3	APPLYING JET GROUTING AS A SEALING TECHNIQUE DURING DEEP EXCAVATION	17
3.1	Seepage into deep excavations	17
3.1.1	Mitigation measures	18
3.1.2	Retaining structures: steel sheet piles	19
3.1.3	Jet grouting to seal deep excavations	21
3.2	Utilizing jet grouting to seal the toe of a sheet pile wall	23
3.2.1	Number of rows and column length	23
3.2.2	The risk of the “shadow effect”	24
3.3	Column design considerations	25
3.3.1	Geometry	25
3.3.2	Position	26
3.3.3	Possible outcome due to defects	28
3.4	Quality control of water cut-offs	28
3.4.1	Direct verification methods of the column diameter	29
3.4.2	Indirect verification methods of the column diameter	30
3.4.3	Verifying the permeability of a jet grouted barrier	32
4	COLUMN DIAMETER PREDICTION METHODS	35
4.1	Wang et al. (2012)	36
4.2	Shen et al. (2013)	39
4.3	Flora et al. (2013)	42

4.4	Recent research developments	46
4.5	The revised manufacturer's prediction model	47
4.6	Summary of required variables	48
5	CASE STUDY: THE GOTHENBURG PORT LINE	50
5.1	Overall project description	50
5.1.1	Organization and main challenges	51
5.1.2	Geology and hydrogeology	51
5.2	Description of the case study site: zone 2	53
5.2.1	Geology and hydrogeology	53
5.2.2	Borehole interpretation	54
5.2.3	Site observations	56
5.3	Execution of the trial	57
5.3.1	Equipment	58
5.3.2	Excavation	59
5.3.3	Painted bars test	61
6	RESULTS	63
6.1	Theoretical predictions models	63
6.2	Field trial	66
6.2.1	Excavation	66
6.2.2	Painted bars test	68
7	DISCUSSION	71
7.1	Theoretical prediction models	71
7.2	Field trial	73
7.2.1	Excavation	74
7.2.2	Painted bars test	76
7.3	Literature and the jet grouting research community	77
8	CONCLUSION AND RECOMMENDATIONS	79
	REFERENCES	82
	APPENDICES	86
	Appendix I	86
	Appendix II	93
	Appendix III	100
	Appendix IV	102

Preface

This report is the final product of a master's thesis within the field of Civil Engineering at Chalmers University of Technology, in cooperation with Skanska Sweden Foundation projects. The report is written by two graduating students from the five-year civil engineering program with their master's within Infrastructure and Environmental Engineering (MPIEE).

The authors would like to give their most sincere gratitude to the following individuals:

Johan Thörn, researcher at the Division of Geology and Geotechnics at Chalmers, for taking your time to supervise this thesis by sharing your knowledge and insight withing geology and hydrogeology, challenging us when needed, and for leaving witty comments after each read.

Patrik Andersson, operational manager at Skanska Sweden Foundation projects, for taking your time to supervise this thesis by allowing us to take part in the geotechnical world at Skanska and for supplying us with material and contact information making the case study possible.

Lodovico Strina, operational manager at Superco France and jet grouting consultant at the Gothenburg Port Line project, for providing us with theoretical background and practical expertise regarding jet grouting technology through a series of lectures and many fruitful discussions.

All the workers, foremen, and supervisors, at Skanska Foundation projects stationed at the Gothenburg Port Line project, for sharing your experience, expertise, and support, making us feel more than welcome during the field trial.

Lars Rosén, professor and head at the Division of Geology and Geotechnics at Chalmers, for taking your time to work as the examiner for this thesis by assisting us with administrative necessities, reviewing this report, and giving concluding remarks allowing us to finalize this thesis.

Sofia Løseth, a fellow student at the master's program of Infrastructure and Environmental Engineering, for taking your time to be the opponent of this thesis by encouraging us throughout this process and critically reviewing our work.

And finally, a special thank you to our *families and friends* for your support, patience, and encouragement during our five years of studies at Chalmers.

Gothenburg, June 2020
Linnéa and Filippa

Notations

Roman upper-case letters

B_2	regression constant	[-]
B	parameter reflecting the ratio of the properties of water and grout	[-]
D	diameter of column	[m]
D_0	calculated diameter of column	[m]
D_{50}	average size of soil particles	[mm]
D_a	average diameter of column	[m]
D_{ref}	reference diameter of column	[m]
D_f	size of no. 200 sieve	[mm]
D_r	diameter of the monitor	[m]
$E(x)$	the kinetic energy at a distance x from the nozzle	[J]
E'_n	specific energy at the nozzle	[J]
E'_p	specific energy at the pump	[J]
I	spacing between two columns	[m]
J	formal parameter quantifying the action of the jet	[-]
L	length of column	[m]
M	number of nozzles on the monitor	[-]
M_c	content of fine particles as a percentage	[%]
N	number of passes of the jet	[-]
N_{SPT}	number of blows in standard penetration test (SPT)	[-]
Q	flow rate of the fluid	[m ³ /s]
R	radius of column	[m]
R_c	calculated radius of the column	[m]
R_s	rotation speed	[m/s]
S	minimum thickness of cut-off (Croce & Modoni, 2007)	[-]
S	formal parameter quantifying the resistance of the soil erosion (Flora et al., 2013)	[-]
S_t	lifting step	[m]
V_g	total amount of grout needed per m of column length	[kg/m]
W/C	water and cement ratio by weight of the grout admixture	[kg/kg]
$W(x)$	the hydrodynamic power of the jet at distance x from the nozzle	[W]

Roman lower-case letters

a_0	correction factor corresponding to the horizontal tangential velocity of the nozzle	[-]
a_1	empirical parameter	[-]
a_2	empirical parameter	[-]
b_0	regression constant	[-]
b_1	regression constant	[-]
b	new parameter related to the characteristics of the soil	[-]
c'	effective cohesion	[Pa]
c_u	undrained shear strength	[Pa]
d_0	nozzle diameter	[m]
k	dimensionless parameter	[-]
p	injection pressure at the pump	[Pa]
p_a	pressure of injected air	[Pa]
p_g	pressure of the grout	[Pa]
r	distance from the jet axis	[m]
s	minimum overlap of two columns	[m]
t	time per step	[s]
q_c	unit tip resistance of cone penetration test (CPT)	[MPa]
q_u	unconfined compressive strength (UCS) of soil	[Pa]
v_0	exit velocity of the fluid at the nozzle	[m/s]
v_g	grout flow velocity	[m/s]
v_L	critical velocity	[m/s]
v_m	horizontal tangential velocity of the nozzle	[m/s]
v_{m0}	reference horizontal tangential velocity of the nozzle	[m/s]
v_s	lifting speed of the monitor	[m/s]
$v_{x,max}$	maximum velocity of the fluid along the x-direction	[m/s]
v_x	velocity at distance x from the nozzle	[m/s]
x	distance from the nozzle	[m]
x_L	ultimate erosion distance	[m]

Greek upper-case letters

Λ	parameter quantifying the interaction between the jet and surrounding fluid	[-]
Λ^*	Λ for single-fluid jet grouting	[-]
Λ_w^*	Λ for water	[-]
ψ	parameter related to the pressure of injected air	[-]

Greek lower-case letters

α	constant parameter related to the characteristics of the fluid and the medium in the flow region (Wang et al., 2012)	[-]
α	attenuation coefficient related to the characteristics of the fluid (Shen et al., 2013)	[-]
α	factor correcting Λ^* for double and triple fluid grouting (Flora et al., 2013)	[-]
α_d	attenuation coefficient for double fluid system	[-]
α_g	attenuation coefficient for grout	[-]
α_s	attenuation coefficient for single fluid system	[-]
α_w	attenuation coefficient for water	[-]
β	characteristic velocity with a value equal to the critical velocity when the soil resistance is equal to the atmospheric pressure (Shen et al., 2013)	[-]
β	exponent quantifying the influences of jet energy on the diameter of column (Flora et al., 2013)	[-]
γ_g	specific unit weight of the grout	[-]
δ	exponent quantifying the interaction between the jet and the surrounding fluid	[-]
η	characteristic velocity with a value equal to the critical velocity when the soil resistance is equal to the atmospheric pressure (Wang et al., 2012)	[-]
η	reduction coefficient, accounting for the effect on the injection time (Shen et al., 2013)	[-]
μ_g	laminar viscosity of grout	[Pa·s]
μ_w	laminar viscosity of water	[Pa·s]
ρ_{atm}	atmospheric pressure	[Pa]
ρ	density of the injected fluid	[kg/m ³]
ρ_c	density of cement	[kg/m ³]
ρ_g	density of grout	[kg/m ³]
ρ_w	density of water	[kg/m ³]
σ'	normal effective stress	[Pa]
τ_f	shear strength of sand	[Pa]
ϕ'	effective friction angle	[°]
ω	water and cement ratio by weight of the grout admixture	[kg/kg]

1 Introduction

Estimations by the United Nations (2018) indicate that 68 percent of the world's population are expected to reside in urban areas by 2050. With this urbanization follows an increased demand for durable and safe infrastructure. As a result, innovative solutions and efforts have emerged to re-organize space in already exploited areas (World Economic Forum, 2015). One example of this is that cities now are trying to make more use of underground spaces when all other alternatives at the surface have been discarded (Broere, 2016; Kaliampakos, 2016). By locating everyday urban activities underground, for instance transportation, a more sustainable environment can be achieved, as negative consequences, such as congestion, noise, and air pollution, are mitigated at the ground surface.

When constructing these underground spaces, deep excavation is generally required. However, the encounter of groundwater frequently serves as a major challenge (Niermann et al., 2017). Therefore, seepage management and sealing of excavations are essential, as it ensures the safety of the cavity. In addition, seepage control is important to reduce adverse effects, such as soil erosion and subsidence, and consequently property damages considering that the surrounding buildings might not be designed to manage the altered stress conditions or movements (Langford et al., 2016; Lu & Tan, 2019).

A proposed solution for this problem of water intrusion is jet grouting. The method consists of an initial drilling to a pre-determined depth, followed by the injection of a cementing agent into the soil by a high-energy jet. This procedure results in mixing and partial replacement of the soil (Croce et al., 2014). The formed cemented structure, known as a *soilcrete* column, has a lower permeability as well as an increased strength in comparison to the in-situ soil. Moreover, the practice can be performed within limited space at hand and in a variety of soils.

Since its introduction in 1970s Japan, much of the advances in the jet grouting technology have been undertaken by specialist contractors and practitioners, including new types of treatment systems (Brill et al., 2003), high-performance equipment (Shibazaki, 2003), exchange of experience (Burke, 2012), as well as measures to reduce the environmental impact (Yoshida, 2012). The academic jet grouting community, on the other hand, have focused on mathematically describing the mechanisms of the jet stream (Flora et al., 2013; Shen et al., 2013; Wang et al., 2012) and investigating which factors that have the largest influence for waterproofing (Cheng et al., 2019; Ni & Cheng, 2014; Pan et al., 2017). Other researchers have focused on how to design jet grouted structures by taking the variability of the soil into account (Croce & Modoni, 2007; Modoni et al., 2016) but also other uncertainties, such as boulders (Bellato et al., 2018).

Despite the described benefits and its popularity worldwide, jet grouting is not a common practice in Sweden. The understanding and knowledge related to the technology are therefore limited among Swedish geotechnical practitioners and is instead restricted to a few, often foreign, specialist contractors. For that reason, this thesis aspires to provide a fundamental guide to the technology, focusing on how to design and practice jet grouting to seal deep excavations utilizing steel sheet piles taking place in Swedish soil conditions.

1.1 Purpose and aim

The overall purpose of this thesis is to gain knowledge and an in-depth understanding of how the geotechnical problem of groundwater intrusion into excavations may be solved by utilizing jet grouting technology. This is accomplished by employing already attained knowledge, with the support from recent research together with practical experience by collaborating with a multinational development and construction company.

Thus, the main objective of this thesis is to combine the knowledge found in the scientific literature with the construction industry praxis, as information exchange between these parties often is scarce, to create an overall study. Moreover, jet grouting is not regularly used in Sweden, partly due to inadequate communication and the belief that the method is cumbersome. The thesis therefore also aspires to provide a constructive evaluation of the technology in an on-going Swedish construction project with regards to both the design and the execution.

Hence, this thesis aims to answer the following questions:

1. What is jet grouting technology?
2. How can it be used to regulate groundwater inflows into excavations which utilize steel sheet piles driven to sloping bedrock?
3. Which are the available verification methods for column diameters that can be used for quality control purposes?
4. How well did the calculated values using the applied prediction models correlate with the measured values for column diameter in the case study?
5. What, if any, were the challenges when using jet grouting technology in the case study?

1.2 Method

To answer the questions above can be divided into three parts: a literature review, an analysis of the prediction models, and a case study.

The literature review regarding the jet grouting technology and the sealing of sheet-piled excavations included articles, conference proceedings, and books published in internationally acknowledged journals. To ensure trustworthy information, only peer-reviewed material was considered. These sources were found either in online research databases or at the library at Chalmers University of Technology. The authors considered were academics as well as practicing engineers.

The prediction models applied were three semi-theoretical approaches (Flora et al., 2013; Shen et al., 2013; Wang et al., 2012) and one commercial estimation model created by a manufacturer of jet grouting equipment. The semi-theoretical models have been developed to foresee the diameter of a soilcrete column given certain soil conditions and chosen operational parameters, whereas the commercial model estimates the fuel and cement consumption and the production time for one column. To use the latter model, the equations first had to be reversed to instead calculate the column diameter as an output. The motivation for choosing semi-theoretical models was their straightforwardness, meaning they can be solved either by hand-calculation

or computer spreadsheets. Additionally, the explanation for choosing these specific models correlates to them being developed by known scholars within the jet grouting community. The reason for verifying the accuracy of the prediction models was to provide the construction company with an initial assessment if these models can be applied in future projects. In this thesis, all calculations were performed in Microsoft Excel. The input values were determined by analyzing data from geological surveys, as well as documented values for the operational parameters used in the trial. The results obtained were then summarized in tables and figures to allow for a detailed comparison.

Lastly, a case study of the jet grouting practice was performed in a Swedish construction project. The study involved an overall assessment of the technology in practice and an evaluation of two column diameter verification methods. The methods studied were excavation and a so-called “painted bars” test. These verification methods are mentioned in the European standard of jet grouting works (SS-EN 12716:2018) and were chosen by the construction company. The evaluation involved observations, notes, and photographs concerning the treatment systems, the equipment used, and the operational parameters applied. These inputs were chosen by the construction company in consultation with the project’s jet grouting expert, Lodovico Strina. Furthermore, geometrical measurements were collected from the excavated trial columns and were used to verify the accuracy of the studied prediction models.

1.3 Scope and limitations

The scope of this thesis is limited to the application of permeability reduction. More specifically, how jet grouting can be used to seal the toe of a steel sheet pile wall driven to sloping bedrock. Furthermore, the hydrological condition investigated is a partly confined aquifer; that is, a permeable friction layer overlying hard, crystalline bedrock and partially covered by clay. This application is examined by only studying jet grouted water cut-offs and bottom plugs. Furthermore, only circular profiles, that are columns, that constitute these structures will be studied.

Only three semi-theoretical prediction models and one commercial prototype model are evaluated as there are a limited number of models developed and available. Furthermore, the verification of these is limited to the data collected in the case study.

The case study is constrained to one Swedish construction project, that being the Gothenburg Port Line [Swedish: *Hamnbanan*]. Due to the period set for the completion of this thesis, but also to comply with the project’s organization, only jet grouting taking place in one of the construction zones is assessed. The assessment is also limited to only consider test columns constructed in the field trial. Furthermore, only the single fluid and the double fluid treatment system are studied, owing to the company’s wishes to investigate potential future investments.

Finally, the literature search is restricted to documents first and foremost published within the last 25 years. This constraint was set to ensure up to date information, as the jet grouting technology constantly advances.

2 General practices of jet grouting

Before modern soil improvement techniques, problems connected to soft subsoils and groundwater inflows were often addressed by first digging a cavity (Nakanishi, 1974). This cavity was then filled with a cement-based agent or supported by driving steel plates into it. These methods were however costly, inconvenient, and usually insufficient.

In the beginning of the 1960s, a method to cut rock by using high-velocity water jets was explored. A group of Japanese geotechnical specialists took a special interest, however, they applied this technology of a high-pressure jet to instead improve the quality of the subsoil by injecting a chemical agent into it (Croce et al., 2014). Jet grouting as a soil stabilization technique is therefore considered to originate from Japan, as a patent was filed in the 1970s by Nakanishi (1974). According to the patent, was this soil improvement achieved by first driving a specialized drill into the subsoil, and thereafter withdrawing it back to the surface while simultaneously pumping a solidification agent through nozzles. This action would give rise to a column, comprising of a combination of the in-situ soil and the solidification agent, that had increased mechanical properties but also a decreased permeability, in comparison to untreated soil masses.

2.1 Modern jet grouting procedure

The modern practice of jet grouting has not changed significantly since its introduction, as illustrated in Figure 1. Still, the process can generally be divided into two actions, the first being drilling, and the second jetting and grouting. Jetting refers to the process where the injected high-velocity fluid causes the immediate soil matrix to erode, whereas the term grouting refers to the insertion of a fluid that possesses cementing properties, also known as *grout*.

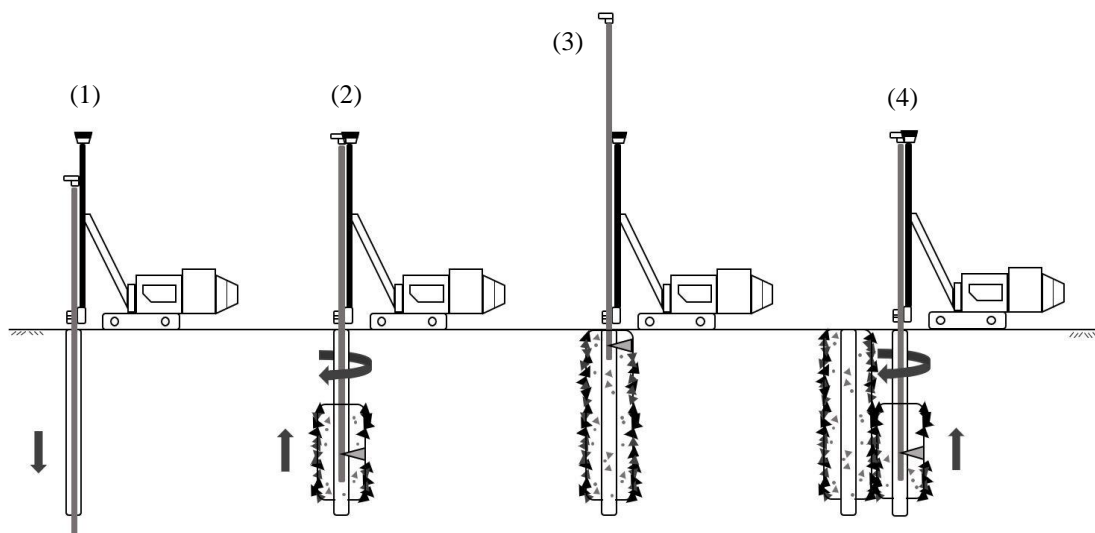


Figure 1 The general steps of the jet grouting procedure: (1) drilling, (2) jetting and grouting, (3) completion of a column, and (4) overlapping of columns (adapted from Croce et al., 2014).

The drilling is performed from the ground level to a pre-determined depth, using a rotational drilling system that is mounted at the bottom of a so-called jet grouting string. This string consists of fluid rods and a monitor, supplied with one or several nozzle(s), and a drilling tip. The drilling tip is slightly wider than the monitor, resulting in an annular borehole. Figure 2 illustrates the different components of a typical jet grouting string and the created annular borehole.

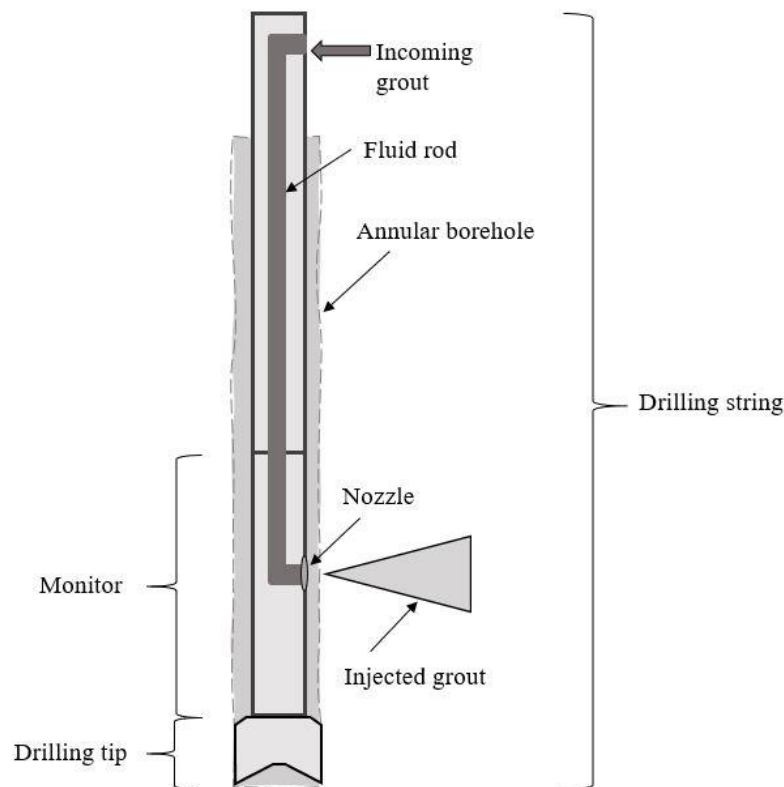


Figure 2 Graphics of a jet grouting string including the basic components. Note that the components are not to scale.

Through the nozzle(s), the jetting and grouting is executed, while the string simultaneously rotates and retreats to the surface. Note that depending on the chosen treatment system, which will be explained in more detail in Section 2.1.1, the jetting and the grouting takes place either from the same nozzle or separate nozzles. While ascending, the jet stream erodes, remolds, and injects grout into the surrounding soil matrix, producing a column. By allowing columns to overlap, jet grouted structures of different sizes and shapes can be formed, making the practice versatile and suitable for many applications (Croce et al., 2014).

Jet grouting can thus be summarized as a procedure which, by using an erosive high-velocity jet stream, mixes as well as replaces the subsoil with injected grout. The aim is therefore not to completely replace the soil but to enhance it. Still, it is suggested that jet grouting can replace up to 50 percent of the untreated soil (Burke, 2012), which is enough to improve the mechanical properties, such as its strength and stiffness. Bearing in mind that a complete substitution cannot be undertaken, the drilling tip must be wider than the jetting string for the remaining grout mixed with the replaced in-situ soil, referred to as *spoil*, to return to the ground surface. A lack of this spoil return would otherwise result in excess pore pressures and loss of control (Brill et al., 2003) resulting in adverse effects, which is further described in Section 2.2.2.

2.1.1 Treatment systems

Jet grouting treatment systems are often referred to the number of fluids that are injected into the soil. They are therefore commonly known as (a) single-, (b) double- or (c) triple-fluid systems, as illustrated in Figure 3. There are however a few other systems that recently have been developed due to new advances and are referred to as Super jetting and X-jetting (Burke, 2004; Yoshida, 2012).

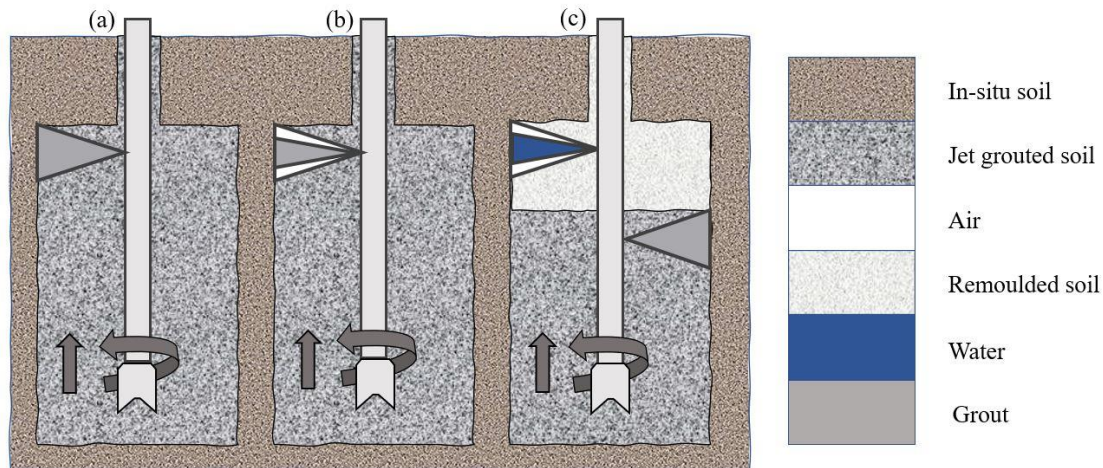


Figure 3 The different jet grouting treatment systems: (a) single fluid, (b) double fluid, and (c) triple fluid (adapted from Croce et al., 2014).

According to the definitions given in the European Standard for the execution of special geotechnical work connected to jet grouting (SS-EN 12716:2018), the broad definition for the three systems are as follows:

- **“Single system:** jet grouting with a single fluid which is the grout itself
- **Double system:** single system with the addition of an air shroud around the jet
- **Triple system:** double system using water for the jet with the optional addition of an air shroud around the jet and the concurrent addition of grout through a separate opening below the jet”

With the single fluid system, only grout is jet-injected, thus functioning both as the remolding fluid and the cementing agent. By using this treatment system, a column diameter of between 0.4-1.2 m can be obtained, depending on the soil type the treatment takes place in (Burke, 2004). More on how the characteristics of the soil influence the geometry of the column will be discussed in Section 2.3.

As described in SS-EN 12716:2018, in the double fluid system the jetted grout is covered by streams of air. This improves the performance of the grouting, as the jet of air facilitates a decrease in energy losses, resulting in an increased radius of influence and a deeper penetration of the grout (Strina, 2020). Thus, larger column diameters, up to 2.1 m, can be achieved (Burke, 2004). There is also another method of the double fluid system, where water first is injected into the ground through a nozzle located above the nozzle for grout. With this system, the remolding and erosion of the soil are carried out by the water jet, whereas the grout only functions as the cementing agent (Croce et al., 2014).

For the triple fluid system, all three mentioned injection fluids are employed. It resembles the secondly described double fluid system with water and grout injected

separately. However, in this case the water jet is coated by air as illustrated in Figure 3. With this system, the radius of influence can be increased further, due to the soil being eroded in two stages and as the performance of the water jet is increased (Croce et al., 2014). The diameter can therefore reach up to 2.5 m in sands (Burke, 2004).

Moreover, the SuperJet is a version of the double fluid system, but where high-capacity and high-efficiency pumps and compressors are used. This advanced equipment has in trials produced columns up to 7 m in diameter (Yoshida, 2012), which can be compared to the conventional tools that only reached 5 m. The X-jet, on the other hand, is an enhanced triple fluid system, where the nozzles are angled to form the shape of a cross or an X. This improves the diameter control and makes the columns more uniform, resulting in diameters of up to 2.3 m in fine-grained soils and sands (Burke, 2004).

2.1.2 Lifting and rotation

During grouting, there are two different procedures to lift and rotate the monitor while withdrawing it back to the surface, as illustrated in Figure 4. Either the lift can be performed with subsequent steps, known as (a) an intermittent or a stepwise lift, or by (b) continuously raising the jetting string, creating a spiral path, known as a steady lift (Shibazaki, 2003).

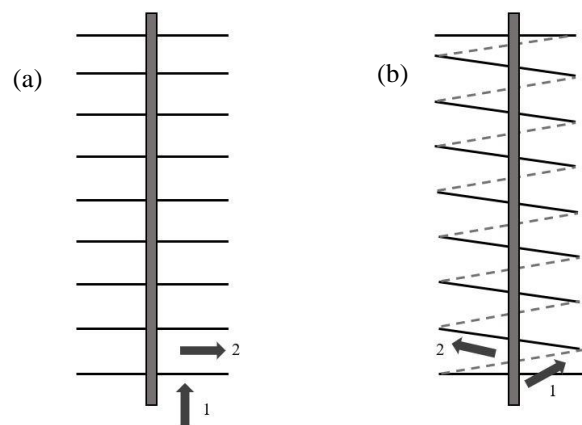


Figure 4 The different jet grouting lifting methods: (a) intermitted or stepwise lift and (b) continuous lift or spiral path (adapted from Croce et al., 2014).

With the intermitted grouting method, the height of the lifting steps and the number of rotations is pre-set. Usually, the spacing between the steps has a length of 4 cm, which is a default value for many jet grouting operation systems (Strina, 2020). Although, distances can vary between 2-10 cm. In general, 4-30 seconds are spent to rotate the nozzle(s) at least one circulation for each step, resulting in 5-40 rotations per minute (RPM) (Burke, 2004). Slower rotation speed is favorable to ensure that the full erosion distance is achieved, but also to guarantee an even mixing between the grout and the eroded soil material. However, a faster rotation reduces the production time for an individual column. Moreover, by modifying the rotational speed and its path, but also the placement of the nozzle on the monitor, it is possible to construct other shapes besides the common circular profile (Croce et al., 2014). For example, by lifting the monitor without applying any rotation, a panel or an elliptical structure can be achieved (Leoni & Pianezze, 2017). These profiles do however lie outside of the scope of this thesis. In practice the intermitted lift is preferred, as the quality of the jet grouted columns have proven to be better, in comparison to columns made using steady lifting (Shibazaki, 2003).

2.1.3 Overlapping and installation sequences

As briefly mentioned, jet grouting can be used for various applications. Many of them do however demand an arrangement of columns rather than detached single elements. These continuous geometries can be created by allowing individual columns to overlap one another. Two different approaches that can be adapted when merging columns are the so-called (a) “fresh-in-fresh” method or the (b) “fresh-in-hard” method, see Figure 5 (Croce et al., 2014).

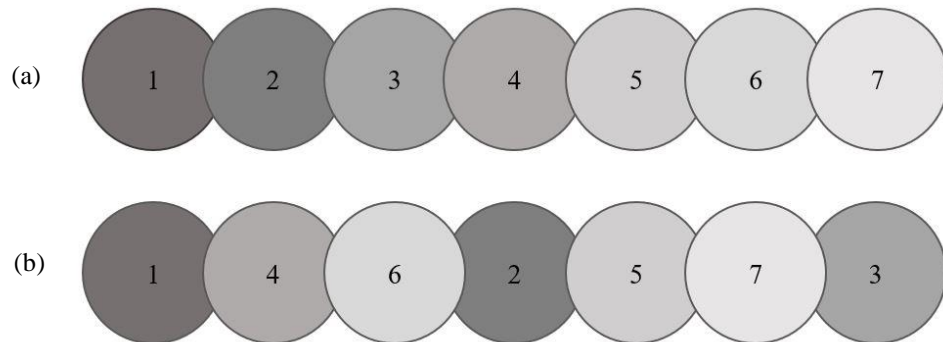


Figure 5 Graphics illustrating the different installation sequences: (a) the fresh-in-fresh method and (b) the fresh-in-hard method. The number illustrates in which order the columns were installed and shade corresponds to the hardening time.

The fresh-in-fresh method is performed with short time intervals, meaning that a series of jetted columns are formed without allowing the grout to harden before the next one is installed. By doing so, the intersection of the two columns is eroded and injected once again, merging the two columns together, ultimately creating a continuous structure (Croce et al., 2014). This method is however problematic when water is used as a drilling fluid (Strina, 2020). The reason for this is the drilling water from the formation of the second column can ‘wash out’ the grout from the first column, as it has not been permitted to fully harden. The method can therefore threaten the uniformity of the column or not allowing it to be formed at all. This can, however, be avoided if large columns are produced, since the distance between the two neighboring columns will be wide enough. When performing fresh-in-fresh with a double-jetting system, an indication of the integration of the columns is to examine the spoil. Strina (2020) states that there is a large probability that merging of columns is occurring if the spoil is accompanied by air bubbles at the area of the previously grouted column. This indicates that the jet has intersected the previous column and that the columns have joined.

In contrast, the fresh-in-hard method is based on allowing a column to harden before the adjacent column is produced, leaving little concern of fresh grout being washed out. Consequently, the fresh-in-hard method is preferred in practice. Although, there is a risk of the so-called ‘shadow-effect’, caused when the second jetting in some cases does not reach around the edges of the earlier installed column. A consequence can thereby be decreased dimensions of the second column (Croce et al., 2014) or issues with instability (Shirlaw et al., 2005). More about this impact can be found in Section 3.2.2. Furthermore, when executing fresh-in-hard, a drilling plan is necessary. This plan demonstrates the sequence in which the columns are to be constructed (Ni & Cheng, 2014). It can be more or less complex, depending on the geometry of the aspired structure. This plan should however be arranged in a rational manner, where the number of required movements has been minimized, considering that jet grouting equipment is heavy and excessive re-location should therefore be avoided.

2.2 Operational parameters

2.2.1 Equipment set-up

The equipment required to perform jet grouting is dependent on the size of the project and the chosen treatment system. All treatment systems do however require a drilling rig, a grout pump, and a cement silo including a mixing plant (Croce et al., 2014), see Figure 6. A water tank with an additional pump is also often needed, as jet grouting requires considerable amounts of water (Strina, 2020). When performing jet grouting works in urban areas, it is however common to connect to the municipal water network to ensure a continuous supply of water. If a double or triple fluid system is used, an additional air compressor and water pump, capable of high pressures, are needed.

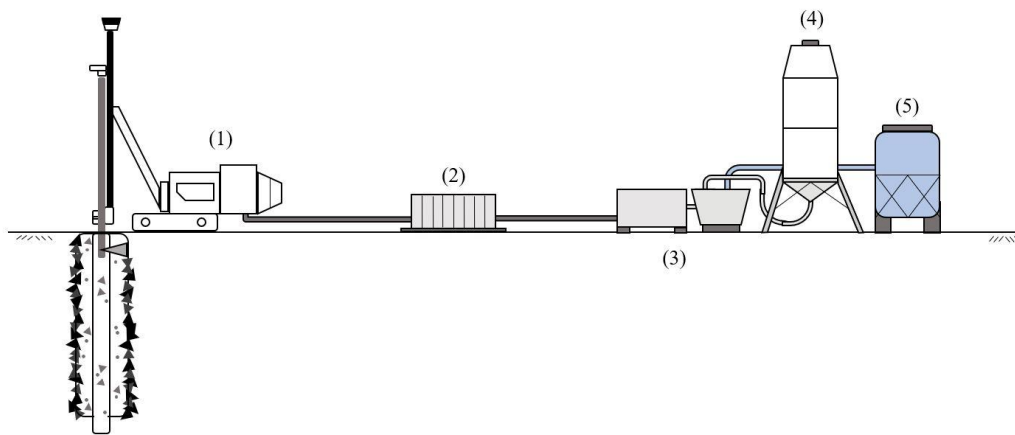


Figure 6 The basic set-up of jet grouting equipment including (1) jet rig, (2) pump, (3) mixing plant with dosage, (4) cement storage, and (5) water tank (adapted from Croce et al., 2014).

The execution of jet grouting is largely dependent on the performance of the equipment, primarily on the pressure of the injection fluid(s). In Table 1, the quantities for some jet grouting parameters for the three most common systems are displayed (Burke, 2004). As can be seen, a pressure reaching at least 400 bar is required. This high pressure is usually achieved by using a diesel-powered engine with gears to drive piston pumps. Moreover, the grout is often continuously produced in an automated plant, where all dosing is made by a dosing device. Thereafter the grout is blended in the mixer and subsequently forwarded to a storage container before it is injected into the soil (Croce et al., 2014).

Table 1 Summary of common jet grouting operational parameters and their range for the three most common treatment systems (adapted from Burke, 2004).

	Single fluid	Double fluid	Triple fluid
Grout pressure [bar]	400-700	300-700	7-100
Grout delivery [L/min]	100-300	100-600	120-200
No. of nozzles [-]	1-6	1-2	1-3
Nozzle size [mm]	1-4	2-7	5-10
Time [s/step]	4-30	4-30	4-20
Rotation speed [RPM]	7-20	2-20	7-15
Air pressure [bar]	N/A	7-15	7-15
Air delivery [m ³ /min]	N/A	8-30	4-15
Water pressure [bar]	N/A	N/A	300-400
Water delivery [L/min]	N/A	N/A	80-200

Observations made by Burke (2012) suggests that it is important to choose a drilling rig that can operate a smooth uplift and rotation in order to obtain an optimized jetting treatment. These parameters can be set manually but by investing in a data acquisition (DAQ) system the procedure can be enhanced. The DAQ system can provide with information to assure the quality of the work and quickly inform the driller if the equipment is failing. During malfunctioning, a quick response might be critical. Additionally, the operational parameters are continuously recorded, making the documentation of the work simpler and more reliable, in comparison to only having a driller's log (Strina, 2020). This is particularly of interest in projects where the client has a high demand for documentation. Another factor that Burke (2012) points out, is that it is difficult to substitute a skilled driller. A driller with proper experience in jet grouting is hard to replace without compromising the quality of the work.

2.2.2 Grout and spoil return

The cementing agent used in jet grouting practices is referred to as grout and usually consists of a mixture of water and cement. The weight ratio between these two substances, known as the W/C-ratio, normally ranges between 0.6 to 1.3 (Croce et al., 2014). Higher ratios, meaning more water than cement, are often used when a larger erosion efficiency is required. Nevertheless, by using a higher W/C-ratio a weaker soilcrete column will be formed due to a smaller amount of cement is used for a given treatment volume. This can be problematic when jet grouting is being employed as a soil stabilization technique, but of little concern for waterproofing applications when the column's strength can be negligible (Strina, 2020). On the contrary, for waterproofing purposes, a balance between the jetting and the grouting must be achieved for the treatment to be uniform and to obtain a low permeability. The permeability of a material is commonly given by the hydraulic conductivity (k). For a soilcrete column, this value generally varies between 10^{-7} to 10^{-9} m/s. In most cases, this can be considered close to waterproof. For the case when water is used as a drilling fluid, it is however wise to use a grout with a lower W/C-ratio. Because of the additional drilling water, the W/C-ratio will consequently increase. This effect should therefore be compensated for beforehand. In the worst cases when this issue is not accounted for, the columns could be "smeared" or not formed at all (Strina, 2020). Moreover, it is possible to use other materials as the cementing agent. For instance, blast furnace slag or fly-ash can be used (GI-ASCE, 2009). Hydrated bentonite is also a common additive, as well as sodium silicate which decreases the hardening time of the grout (Croce et al., 2014).

As previously mentioned, the jet grouting process entails a partial replacement of the in-situ soil and therefore will some of the grout return to the surface through the annular borehole. This flow back fluid is known as spoil and contains pristine grout but also a large share of soil particles. The volume of the spoil corresponds roughly to the same volume as the injected grout (Ni & Cheng, 2014), though the flow back is dependent on the soil type and the interaction of the jet. Having the notion of mass balance in mind, two important conclusions can be drawn from analyzing the generated spoil during the grouting operation.

Firstly, the borehole annulus must be large enough to allow a continuous backflow of fluid (Burke, 2004). A lack of spoil return can potentially result in hydrofracking of the surrounding soil due to the build-up of excess pore pressures. Adverse effects include damage to nearby structures, but also irregularities in column geometry. To avoid this,

drill casings can be installed or multiple nozzles facing different directions can be used (Brill et al., 2003).

Secondly, the volume of the spoil should theoretically be slightly greater than the injected volume (Ni & Cheng, 2014). To which extent is however dependent on the in-situ soil, as the spoil return generally decreases with increased particle size (Croce et al., 2014). For example, the spoil to grout volume ratio is about 1.3 for clays and 1.1 for sands. The fact that the ratio is lower for granular soils, is connected to that coarse soils contain more voids for the grout to saturate in comparison to clays. To be aware of is that these numbers are general design values. For instance, in a case study of a new metro tunnel performed in silty sands, Ni and Cheng (2014) reported an average spoil to grout ratio of 1.302. The authors assume that this high value could be derived from the treatment being performed below the groundwater table. Another potential explanation could be that the replaced soil particles experienced a relief in effective stress once ascending to the surface, making them increase in volume.

2.2.3 Safety

When performing jet grouting, the general safety precautions given for construction sites should be considered. All staff members and visitors should always undergo a site-specific safety introduction and wear the appropriate personal protective equipment. Also, machines should be inspected regularly and operated on surfaces with a suitable bearing capacity and set safety distances should be respected. Moreover, actions to prevent noise, vibrations, and the accumulation of dust should be taken.

There is however an European standard concerning the safety of drilling and foundation equipment which do focus on equipment used in jetting, grouting, and injection practices (SS-EN 16228-6:2014). According to this document, some additional requirements for jet grouting do exist, mainly related to the fact that the working pressure surpasses 400 bar. For instance, hoses shall be appropriately secured and have a quadruple bursting pressure, but also include a safety burst hose. Moreover, the hoses should not be lifted by using the bucket of an excavator and nor shall they be run over by any type of vehicle. The pump and the drill rig should also be equipped with emergency stops in case a pressure spike is observed.

Considering that large volumes of water are used and that leakages tend to be difficult to control; it is important to bear in mind where high voltage electrical systems are located.

Additionally, cement is a basic substance, meaning that the grout and spoil have basic characteristics. Thus, the operating personnel needs to wear protective gear, full-covered clothing, and preferably closed protective glasses or goggles, as spoil might spray or splash. This is particularly important for the treatment systems utilizing air in the grouting process, as the high-pressured air increases the risk of splashing.

Finally, it is important to keep in mind that safety should be discussed prior to trial and before production commences. For instance, when excavating columns for quality assurance, deep shafts are formed. To ensure safe working conditions, calculations related to slope stability should be completed prior to any fieldwork and excavation should not take place after, or during, unfavorable weather conditions.

2.3 Applications of jet grouting

The main purpose to implement jet grouting is to improve the mechanical properties and/or to reduce the permeability of the in-situ soil. Improved mechanical characteristics include an increased bearing capacity, shear strength, and stiffness, resulting in soil less prone to settlements (USACE, 2017). A reduced permeability can be necessary in cases when geotechnical structures are threatened by seepage, gradient flows, or erosion due to the flows of groundwater. Furthermore, jet grouting is considered to be a suitable option when access to the construction site is limited and when mass suppression must be kept low in order not to damage neighboring buildings (Niermann et al., 2017). Additionally, jet grouting can be applied in all types of soils as well as weathered rock, and be configured into various geometries of different shapes, lengths, and sizes (Croce et al., 2014).

There are several ways to construct soilcrete columns into complex structures that can be used for various applications. Jet-grouted structures are therefore commonly divided into groups depending on their shape, often defined as either one-, two-, or three-dimensional elements (Croce et al., 2014). For example, single columns secluded from other columns are characterized as a one-dimensional element. A function which can be obtained by this structure is ground stabilization, such as reinforced foundations. This is achieved by installing the columns in a similar pattern as for a conventional pile reinforcement. On the contrary, when columns are placed adjacent to one another, a two- or three-dimensional structure can be achieved. These structures, comprising of a row, or multiple rows, of columns, make up shapes of a planar line or a block corresponding to the required design (Croce et al., 2014). The most common application for these types of elements is water barriers, retaining structures, tunnel support, or as mitigation for pollution or seismic activity (Burke, 2012).

Furthermore, jet grouted structures can be installed either vertically, horizontally, or inclined, depending on the sought function and the site conditions. Common applications of vertical strips are water flow management or as retaining structures during excavations. A horizontal or inclined application can be a jet-grouted canopy in tunnels. In addition, the structures can be designed as either temporary or long-lasting solutions.

2.4 The significance of the soil

Besides the chosen treatment system and the operational parameters, do the characteristics of the in-situ soil also have a great influence on the final shape and quality of the soilcrete columns. In theory, can the design proposal be considered as adequate, but in reality will the end result differ to some degree. The reason for this is that most designs assume that the treatment is performed in relatively uniform soil conditions. However, soils are rarely homogenous, considering that the characteristics vary with both depth and direction. Comprehensive geological and hydrological surveys can provide fundamental information to improve the design, but undetected deviant physical properties might still not be estimated accurately. One parameter which cannot be completely accounted for in advance is the resistance of the soil. This means that when performing jet grouting, the soil will not be equally eroded, as visualized in Figure 7. The variability of this parameter should therefore be considered at the design stage, but also be evaluated when performing a field trial to ensure adequate quality of the treatment (Burke, 2012). For instance, gravels and sands are not

as resistant towards erosion as clays (Burke, 2004) and the column diameter will therefore vary with depth. How much is difficult to predict, but in a probabilistic design approach made by Modoni et al. (2016), it is assumed that there is a 33 percent decrease per every 10 m. This to account for the increase in confining stress and increased consolidation with depth (Croce & Modoni, 2007).

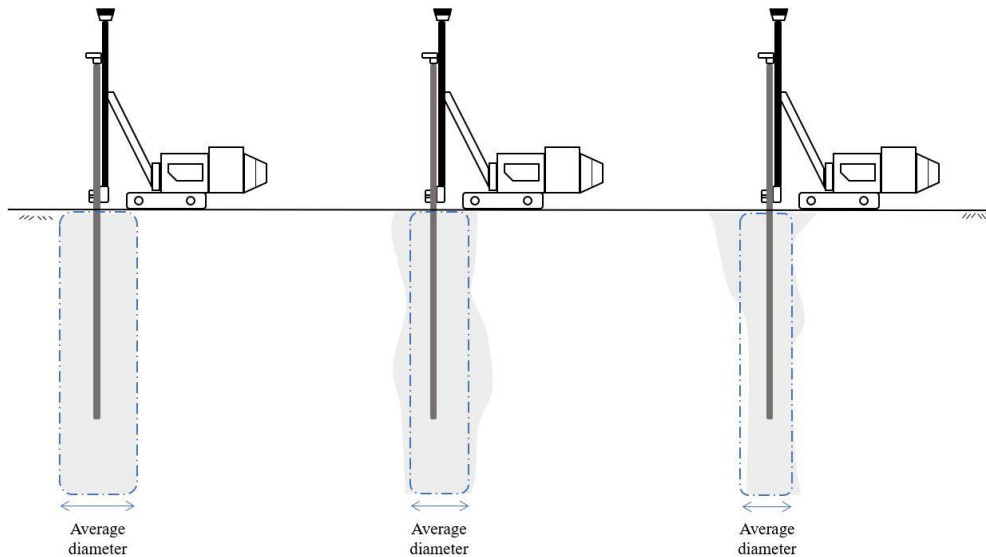


Figure 7 Graphic illustrating the variance of the uniformity for a soilcrete column and the concept of average column diameter.

Moreover, there are many other soil-related aspects which can affect the jet grouting performance and cause a poor soilcrete column. For instance, the groundwater level and how it varies over the year are important factors. What also needs to be known beforehand is the level and the quality of the underlying rock along with the soil's stress conditions and loading history (Brill et al., 2003). Furthermore, utilities and other underground objects, known and unknown, need to be taken into consideration (Brill et al., 2003). Burke (2012) also points out that it is important to ensure that the groundwater does not have a low pH or contain sewage, as this could lead to poor treatment. To summarize, it is of the highest importance to understand the interacting mechanisms between the soil and the jet, but also the geological conditions presented at the site.

2.4.1 The mechanisms of soil and jet interaction

There are three central interacting mechanisms taking place during the jetting and of which determines the treatment capability on the immediate soil matrix: erosion, cutting, and seepage, see Figure 8. All mechanisms can take place simultaneously, however, the primary mechanism is largely dependent on the soil condition and the soil's composition (Croce et al., 2014).

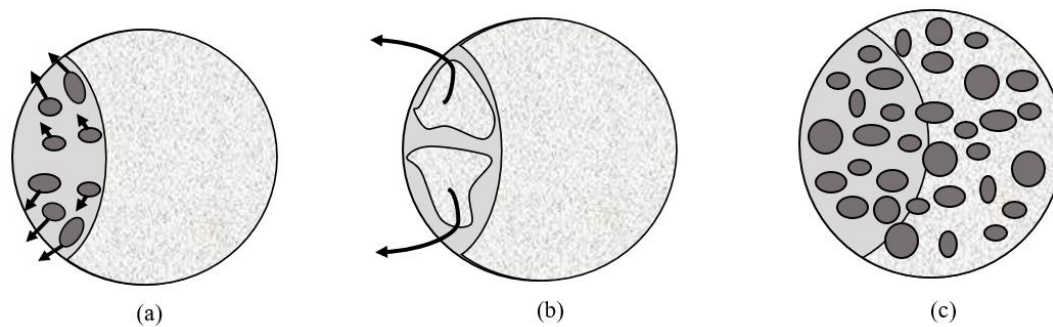


Figure 8 Graphic demonstrating the three main jet-soil interaction mechanisms; (a) erosion, (b) cutting, and (c) seepage (adapted from Croce et al., 2014).

Erosion is the primary mechanism in non-cohesive soils, those being sands and gravels. Because of the absence of binding forces between the particles, besides moisture, the jetting fluid can easily erode the immediate soil by dragging the grains from their initial position (Brill et al., 2003; Croce et al., 2014). Also, the jetting fluid reduces the grains' contact with surrounding particles due to the increased pore pressure in the soil. Consequently, the total eroding distance is dependent on the jetting time, the pressure, and the flow of the injected fluid, where an increase in all these parameters results in a larger radius of influence (Croce et al., 2014).

In soils with cohesion, those being clays or silts, the erosion and the remolding of the soil are interfered by adhesive forces. Consequently, cutting is the main interacting mechanism, as the jet cuts out larger chunks of the soil instead of individual grains (Croce et al., 2014). Therefore, in clayey soils, multiple rotations to further break down the chunks are needed in order to obtain the desired diameter and a uniform column.

The third mechanism, seepage, generally develops in permeable gravels, or soils with a high void ratio. Here, the grout fills the void between the grains as the jet is not able to erode and transport the larger individual particles from their original position (Croce et al., 2014). Longer jetting times are therefore required, rather than an increased pressure or delivery rate, to obtain larger diameters.

2.4.2 Swedish geology

To understand how jet grouting can be utilized in Sweden, it is important to be familiar with the Swedish soil conditions and how they were created. Most of the Swedish soils are largely influenced by the Quaternary period, which began about 2.6 million years ago and is characterized by dramatic changes in the climate. In the northern parts of the world, the period began with a decrease in the average temperature, resulting in increased ice formation and glaciers, and later the growth of inland ices. As the climate alternated between colder and warmer periods, the ice sheets would periodically advance or retreat. The latest cold period, taking place around 10,000 years ago is known as the Weichsel-period, and had the most impact on the present Swedish soil composition (Lindström et al., 2000). During this time, substantial amounts of material, such as weathered bedrock and loose soil, were transported with the ice, creating glacial sediments. These can therefore comprise of a mixture of deposited material, originating from vast distances. Furthermore, the deposition of the sediment depends on if the ice sheet was located below or over sea level or if it was advancing or retreating (Andréasson, 2015).

The inland ice also caused a compression of the Earth's crust, of up to 800 m, due to its self-weight. After the last inland ice had melted, large parts of Sweden were therefore situated below the sea level of that time. However, when the suppressing weight was removed, it induced an isostatic lift, which still goes on today. Because of this, regions that used to be located below sea level can today be found above, where the shoreline is referred to as the highest coastline (HC) [Swedish: *högsta kustlinjen*]. Depending on if the area was situated above or below the HC, the soil composition differs (Geological Survey of Sweden, n.d.), see Figure 9.

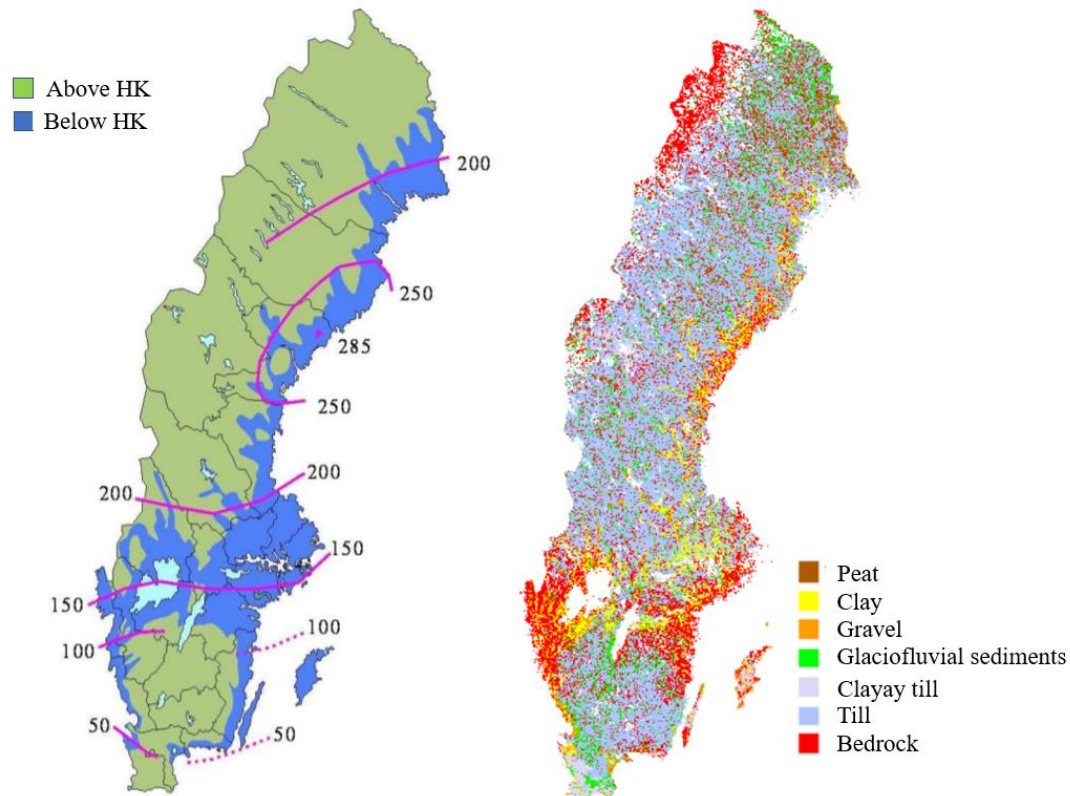


Figure 9 Maps illustrating the highest coastline (left) with numbers representing the height above today's sea level in m and the most predominant soil types (right) in Sweden (from the Geological Survey of Sweden, 2020).

One of the glacial sediments which directly originates from the ice sheet is known as till, of which appears in different forms of moraines. The soil type includes various grain sizes, ranging from blocks to clay particles. It is therefore a highly unsorted and heterogeneous soil, with varying characteristics (Andréasson, 2015). The soil could have been transported in a variety of ways, either at the surface of the ice sheet, inside the ice, or at the bottom resulting in the different types of moraine. Moreover, the deposition depends on the ice movements, staying stationary, or advancing or retreating, creating a number of different formations such as end moraine, drumlins, etc. (Andréasson, 2015). Considering that Sweden to a large extent was covered by an inland ice sheet, till is the most common soil type, covering almost 75 percent of the country's land surface (Geological Survey of Sweden, n.d.)

When the ice sheet melted, large glacier rivers were formed. These rivers would primarily transport and sort larger rock fragments, later deposited as relatively homogenous layers of gravel and sand (Andréasson, 2015). These fragments are for the

most part rounded and deposited with large voids, giving these soils a particularly high permeability. The smaller particles could on the other hand not deposit near the glacier river mouth where the water outflow velocity was too high. Instead, these particles settled in calmer environments located at some distance from the ice sheet, forming layers of clay or silt. These deposits are also well sorted but have low permeability. In addition, if the fine clay particles were deposited in the presence of saltwater, the electrolytes have caused this type of marine clay to be especially prone to settlements and sensitive to disturbances (Schoning, 2016). This is the case for many clays deposited in the western parts of Sweden, which was located below HC.

2.5 Sustainability

In the scientific literature, only a few studies discussing sustainability aspects related to jet grouting have been found. This despite the current global awareness with regards to climate change and the positive effects lowered carbon footprints entails. One article, written by Yoshida (2012), discusses some recent ecological advances in the Japanese jet grouting community. According to this study has the amount of released CO₂ emissions decreased to about one-third of the emitted quantities ten years ago. The reason for this is derived by the author to two distinct factors.

The first is upgrades in technology. For instance, modern nozzles provide more focused jets, improving the jet's erosion ability and reduces overall energy consumption. Secondly, it is believed that the increased re-use of spoil has made the largest contributions to the decreasing emissions in kg·CO₂ per treated m³ of soil. This is explained by the decreased consumption of carbon-intensive materials, that being cement. The re-circulation of spoil has also proven to generate economic savings. This is however limited to projects and regions where the spoil is classified as hazardous waste. Substantial savings can therefore be made if a reduced volume needs to be transported for disposal and treatment at landfills. Even though Yoshida (2012) provides important insights regarding the environmental impacts of the jet grouting practice, the presented results are debatable. This mainly because the lack of transparency in the data, and more on this will be discussed in Section 7.3.

3 Applying jet grouting as a sealing technique during deep excavation

In Chapter 1, urbanization was briefly explained and how it has intensified the densification of cities. Moreover, decision-makers and contemporary urban planners see densification as an opportunity to promote sustainable development (Swedish National Board of Housing, 2017). For instance, by allowing the growth of communities to take place inwards rather than into urban sprawls, travel times can be shortened, and emissions reduced. However, following that many metropolises experience a shortage in available space, construction is more often taking place in the subsurface (Ergun, 2008). This in the form of foundations and basements for high-rise buildings, underground parking garages, rapid transit systems, etc. As a result, deep excavation is generally required.

A common issue related to deep excavation projects is the encounter of groundwater. In an overview written by Lu and Tan (2019), it is proposed that out of fifteen distinct excavation failure modes, five derive from water being the driving mechanism. Those are scoring of anchors and propping elements, erosion of surrounding soil, hydraulic fracturing, sand boiling, and hydraulic heave. These malfunctions can result in catastrophic consequences, including property damage, massive subsidence, and loss in human life.

Besides stability issues, intrusive groundwater can also reduce the pore pressures in the surrounding soil. This is a particularly difficult problem in granular soils connected to layers of clay. The reason for this is that granular soils can contain and transport large volumes of water, increasing the risk of significant inflows into excavations (Niermann et al., 2017) and consequently, lead to a reduction of the pore pressures in the area. However, depending on the site conditions, even the smallest of inflows can cause a large reduction in porewater pressure. This will ultimately cause the clay to consolidate, as the pre-consolidation pressure will be exceeded by the effective stress. This results in settlements that can damage nearby infrastructure and lead to substantial operational and financial complications (Holmøy et al., 2019).

3.1 Seepage into deep excavations

Seepage can enter an excavation through many different routes, as demonstrated in Figure 10. The paths that mainly are responsible for reduced pore pressures, and eventually a lowering of the groundwater table, are given by; leakages through the retaining structure or the drilled connections to anchors or other constructions, through gaps at the toe of the retaining structure if driven to bedrock, or through water-bearing faults in the bedrock (Langford et al., 2016).

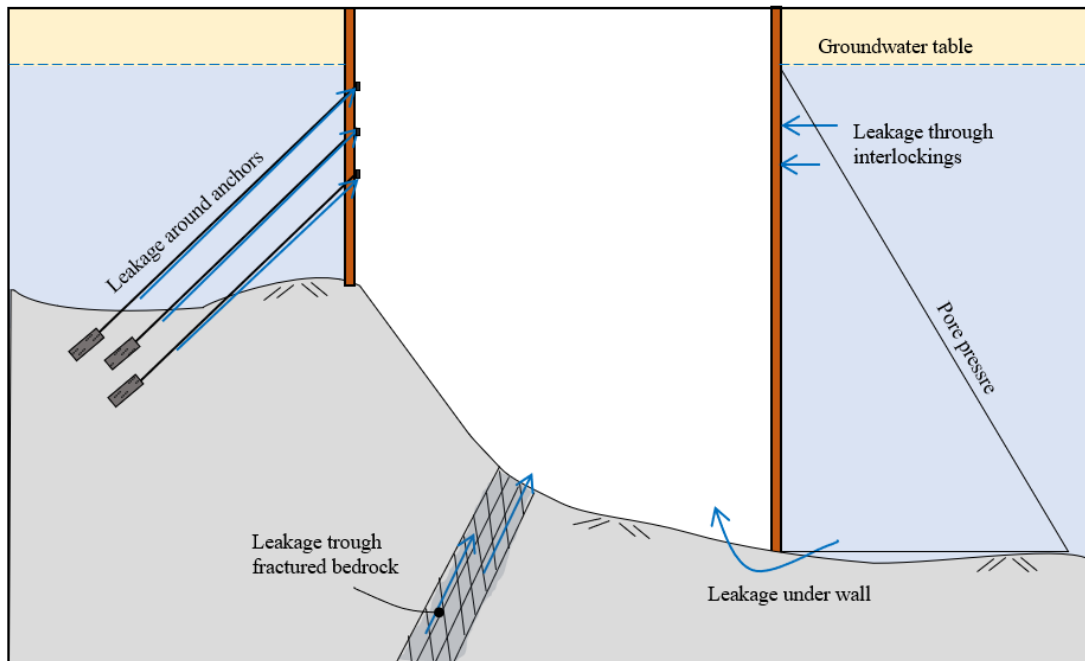


Figure 10 Illustration of different seepage routes into a deep excavation (adapted from Langford et al., 2016)

In an article by Langford et al. (2016), it is suggested that for excavations performed in a confined or partially confined soil layer, the hydrological conditions are similar to those for tunnels. Therefore, it is implied that for a 100 m x 100 m excavation the drainage from the permeable layer should not exceed 5-10 L/min. Although, depending on the established requirements for drawdown or settlements, reductions of pore pressures at the bedrock level can be stricter.

3.1.1 Mitigation measures

To prevent the described consequences from happening, actions against seepage must be adopted. According to Niermann et al. (2017) can three different types of solutions be implemented.

One option is to simply allow the water to fill the excavation. This alternative is however strongly dependent on the depth of the pit and the strength of the soil to allow the excavation to be performed in a safe manner.

The second option is to deliberately lower the groundwater level to below the bottom of the excavation by pumping out water from neighboring wells. Thereafter the excavation can proceed “in the dry”. Many contractors prefer dry conditions as it supports safer working conditions; however, this option is not an ideal solution due to several reasons. Primarily because of the mentioned settlements that can be induced. Secondly, in many countries, for example Sweden, the lowering of the groundwater table is unwarranted and is therefore strictly regulated in the environmental legislation (Miljöbalk 1998:808, chapter 29). In some cases, exceptions can be made and permits be granted, allowing such practices (Miljöbalk 1998:808, chapter 11). However, a compelling argument must be made that the adverse effects can be mitigated by other means. For the case of deep excavations, it is difficult to make those arguments, considering that a lowered groundwater table is required over a long period of time. A

decrease of the water table is likewise not a viable option for soils with high hydraulic conductivity, as these would require vast dewatering efforts. This is also not an alternative when the groundwater is contaminated as the contamination could spread and lead to expensive treatment actions (Niermann et al., 2017).

The third option is to install a dewatering system or an impermeable cut-off, allowing the excavation to be performed “in the dry”. Here jet grouting can be considered as an advantageous technology since an impermeable structure can be constructed.

3.1.2 Retaining structures: steel sheet piles

Steel sheet pile walls are one of the most common retaining systems used in Sweden to prevent soil and water from entering a deep excavation. The reason for its popularity is related to its versatility, as the sheet piles can be installed in all types of soils and can function as a temporary as well as a permanent structure (Puller, 2003). The exception may be in soil layers comprising of a large share of boulders or dense gravel. Other advantages are the rapid installation and the possibility to recover and re-use the piles, making the method economical in most projects.

The product availability of steel sheet piles is extensive, as a wide range of designs with different shapes, lengths, and widths is offered by numerous manufacturers (Ergun, 2008). The two most common types of sheet piles are the Larssen sheet pile and the Frodingham sheet pile, making up the shape of a U or a Z, as illustrated in Figure 11. The maximum recommended length for both shapes is about 30 m, and the width of the piles is usually in the range of 0.6-0.8 m (Puller, 2003).

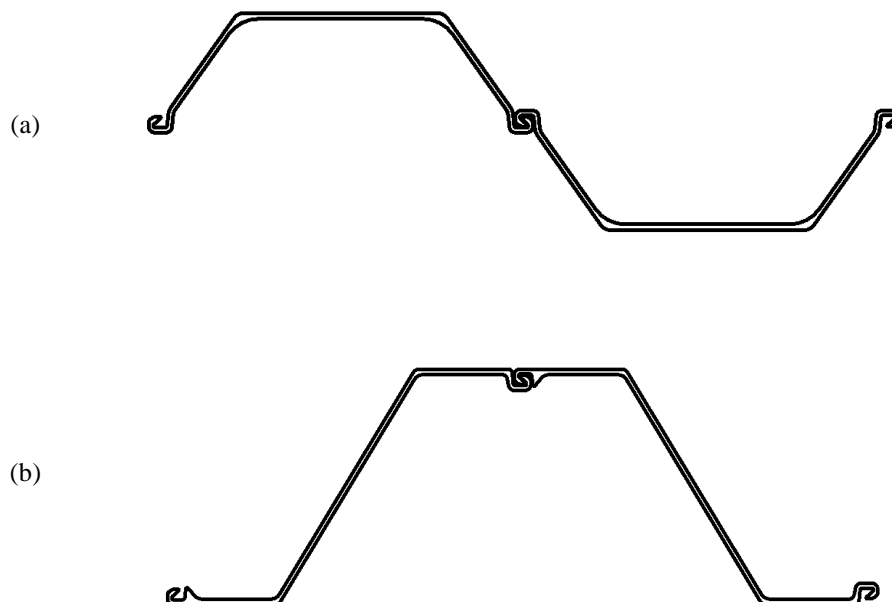


Figure 11 Illustration of the two most profiles of steel sheet piles used in Sweden: (a) U-profile and (b) Z-profile.

A retaining sheet pile wall is formed when several sheet piles are connected into a sequence, stretching along a defined perimeter. The interlocks are designed to be narrow and tight. However, if installed incorrectly or if the integrity of the interlock in some way has been compromised, for example when re-using piles or during transport, seepage can occur (Ergun, 2008). Great care is therefore essential during installment. Moreover, to mitigate the risk of seepage different interlock sealants, fillers, as well as some welding practices can be implemented (Langford et al., 2016; SS-EN 12063:1999).

The primary disadvantage of utilizing steel sheet piles is related to the environmental impacts, serving as noise and induced vibrations during the installment (Puller, 2003). This can restrict its applicability in densely urbanized areas. Technological advances have however resulted in a new generation of impact and vibratory hammers, of which to some degree can reduce the disturbances (Ergun, 2008).

The second disadvantage is that sheet pile walls cannot be considered completely impermeable. Seepage can take place either through flaws in the interlocking between two adjacent sheet piles (Ergun, 2008) or as a result of driving difficulties (Telling, 1975). The latter is especially troublesome.

Some soil conditions are particularly challenging and require considerable precision during the installment. In these soils, it is probable that the piles start to incline, or even split and curl upwards. Another issue is the triangular gaps formed at the toe of the sheet piles when driven to an inclined bedrock surface (Telling, 1975). As illustrated in Figure 12, gaps are formed between the edge of the sheet pile and the sloping bedrock. Depending on the degree of the inclination, more or less sizable gaps are formed facilitating the inflow of groundwater into the excavation. In these cases, sealing is required. Here a jet grouted cut-off from can be considered as a suitable solution.

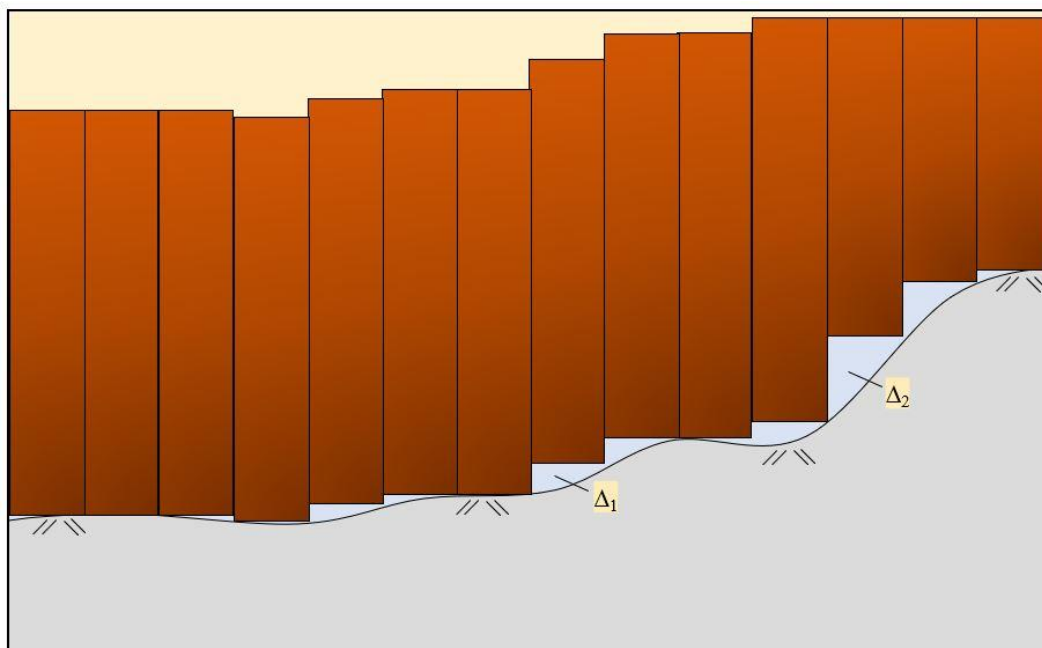


Figure 12 Illustration of the triangular gaps formed when driving sheet piles to a sloping bedrock.

Moreover, for deep excavation projects in the Nordic countries, it is common practice to secure the toe of the sheet pile into the bedrock by using a rock dowel, or rock bolt, as illustrated in Figure 13. These are installed to manage the horizontal reaction forces at the bedrock level. The installation process of the dowel is given by an initial drilling into the bedrock through a pre-welded casing, mounted on the excavation side of the sheet pile prior to the driving (ArcelorMittal, 2018). Thereafter the soil inside the casing is removed, followed by the hole being filled with grout. The rock bolt is thereafter installed before the hardening is completed.

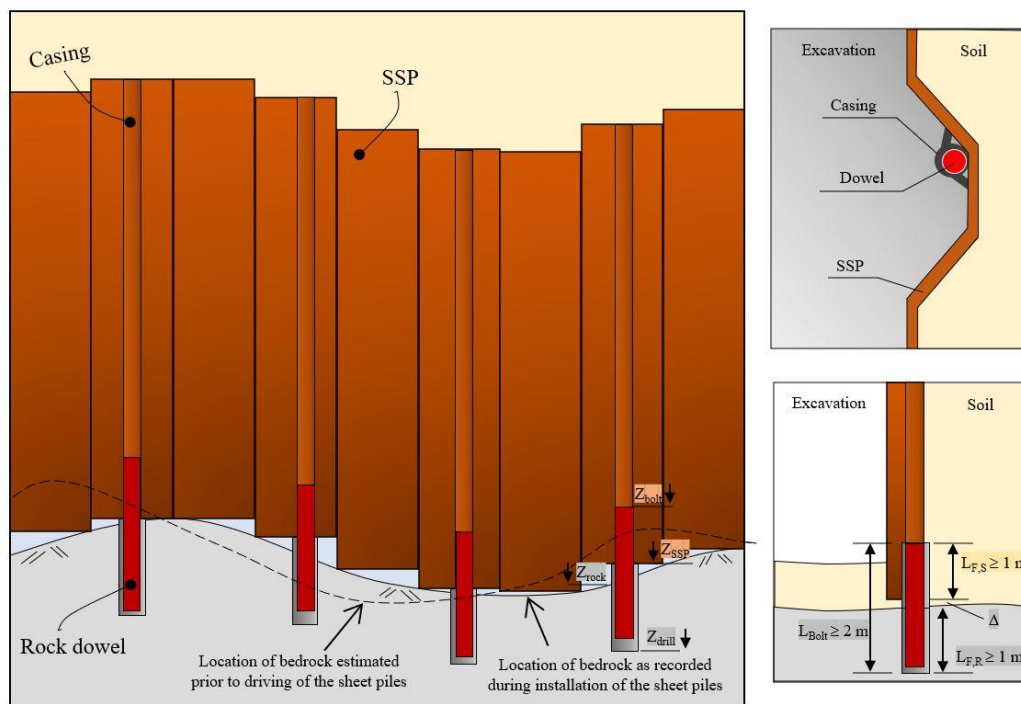


Figure 13 Illustration of rock dowels; front view (left), top view (top right), and side view (bottom right) (adapted from ArcelorMittal, 2018).

3.1.3 Jet grouting to seal deep excavations

Common jet grouted structures with the purpose of sealing are cut-offs (Croce & Modoni, 2007) and bottom plugs (Modoni et al., 2016) as illustrated in Figure 14. A cut-off is a type of two-dimensional structure, often consisting of simply one row of columns. Bottom plugs, on the other hand, are a type of three-dimensional structure containing multiple rows of columns, forming a slab at the bottom of an excavation. This type of structure is mainly used when overcoming buoyancy is necessary.

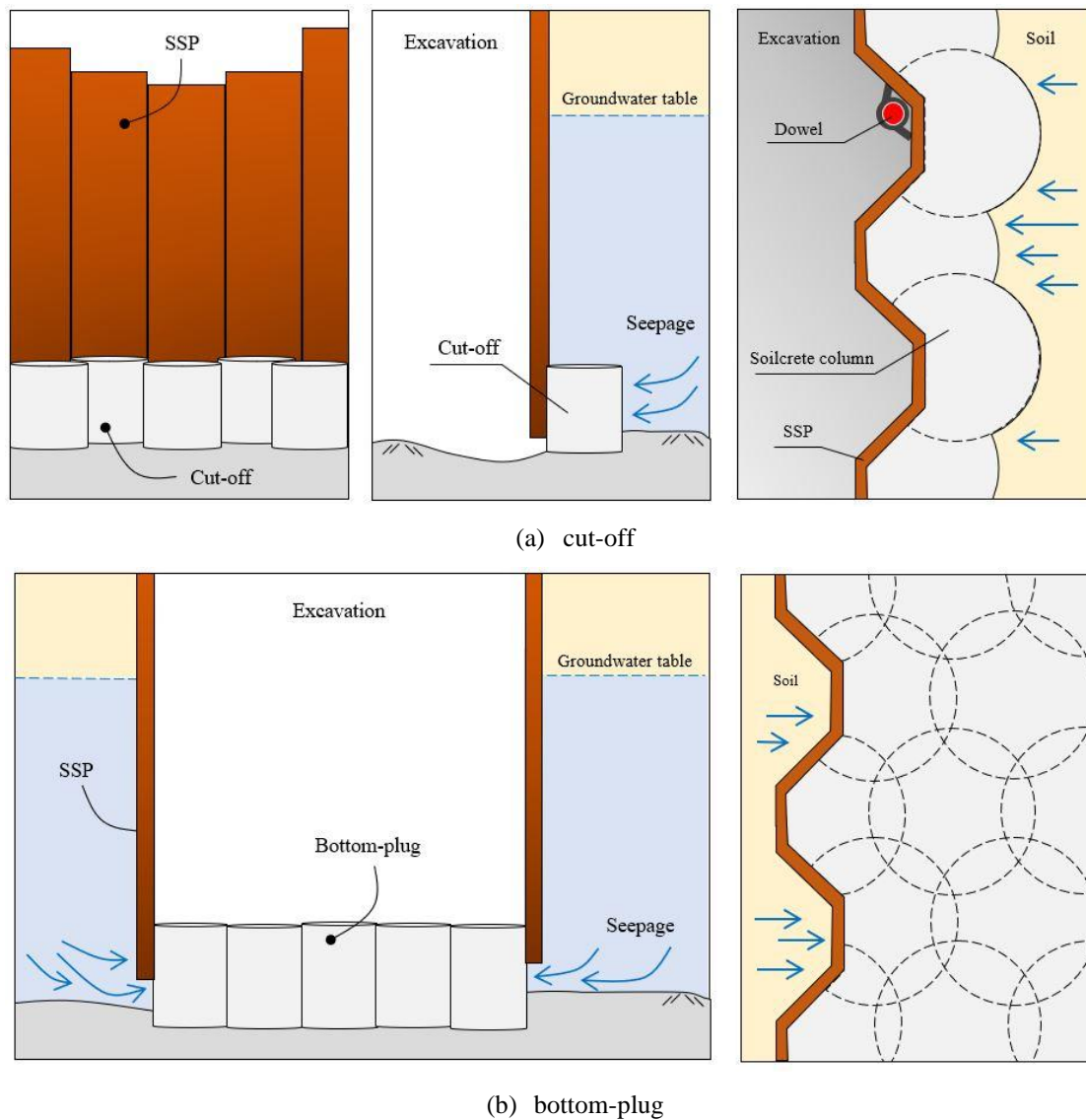


Figure 14 Illustrations of different perspectives for a cut-off (a) and a bottom plug (b) used to seal a sheet-piled excavation.

As described and illustrated in Section 2.4, the Swedish geology has been influenced by the inland ice sheet and its deposits. This means that depending on the soil stratigraphy found at the considered site, either a cut-off or a bottom plug is the best-suited option to seal the excavation. However, as stated in Section 1.3, this thesis is limited to deep excavations utilizing steel sheet piles in coarse-grained soils overlying hard bedrock. For this condition, a vertical cut-off is the most appropriate choice, considering that the horizontal groundwater flow along the bedrock is the main issue and not buoyancy forces or leakages through fractured bedrock. Thus, the emphasis in the upcoming sections will be on the design of a water cut-off comprising of one single row of columns.

3.2 Utilizing jet grouting to seal the toe of a sheet pile wall

A jet grouted water cut-off can serve as a solution to ensure the water-tightness of a sheet pile wall. The dimensions of this structure do however vary with the prerequisites of the site and the established project requirements. Several potential layouts can thus serve as a solution to the same problem and it is not possible to formulate explicit design requirements. Therefore, considerations ought to be made for the individual case. Still, the aspects and issues that are discussed in the upcoming sections serve as a good starting point.

3.2.1 Number of rows and column length

A single row of columns is usually enough to prevent groundwater seepage. However, if the pore water pressure in the soil is high or if the discharge into the excavation is substantial, multiple rows are required. For instance, in case projects reviewed by Croce and Modoni (2007) it is suggested that at least two rows are needed for applications where there exists a major risk of groundwater seepage or mass transport. That often includes applications of which are exposed to flows of surface water, for example earth dams, cofferdams, and diversion weirs. Additionally, multiple rows might also be needed if the inflow requirements are exceptionally strict or if a potential leakage would result in significant economic losses. Ultimately, the degree of confidence in the effectiveness of the jet grouting determines the thickness of the cut-off (Croce & Modoni, 2007).

The column length is dependent on the slope of the bedrock, as illustrated in Figure 12, where the height of the triangular gaps varies with the bedrock surface. Some sections might therefore call for longer columns than others to guarantee a complete treatment of the opening. It is possible to obtain an overall idea of the rock level by examining information related to the stratigraphy gathered in the preliminary geological survey. Likewise, as the sheet pile is installed prior to the jet grouting, a more exact level can be identified through the driving log. The design height of the cut-off can therefore be adjusted for certain segments and to be optimized with regards to production time and material use.

When reviewing Swedish construction projects that used jet grouting to seal the sheet pile toe when driven to bedrock, two projects were found (Swedish Transportation Agency, 2010, 2017). The blueprints for these projects states that grouting is to be performed from a depth of 0.5 m into the bedrock to at least 0.3 m above the sheet pile toe. A minimum column length in these projects is therefore given by adding the length of the gap with the required depth into the bedrock and the length above the sheet pile toe. Also, if there is a risk of blocks on the bedrock surface, it might be necessary to treat some distance into the rock if it cannot be considered as impermeable. In the general standard of grouting works (SS-EN 12715:2000) it is stated that the strength properties, the extent of the weathering, as well as the direction and degree of fissuring of the rock should be determined. Therefore, grouting some distance into the bedrock should prevail if the bedrock is concluded as weathered or fractured. The blueprints did not specify the reason for the required lengths, however, the reason for grouting at least 0.3 m above the sheet pile toe might be connected to the interlinkage of the column and the sheet pile.

Moreover, a theoretical computation performed by Tanaka and Yokoyama (2006) has investigated the required column length of a cut-off underneath a sheet pile wall constructed completely in the soil at some distance from the bedrock. This type of cut-off hinders the horizontal flows but is also designed to prohibit vertical flows and uplifting forces similarly to bottom plugs. However, in this study Tanaka and Yokoyama (2006) investigated the column lengths, that being 0.5 m, 1.0 m, or 1.5 m, and their effect on the critical hydraulic head. The scholars concluded that a height of 0.5 m should suffice, yet 1.0 m is recommended in practice. It is therefore of future interest to study if these columns' lengths are recommended for cut-offs intended to seal sheet piles driven to bedrock as well.

3.2.2 The risk of the “shadow effect”

One deficiency which can affect the impermeability of a cut-off is known as the “shadow effect”. This term refers to the untreated zones that may emerge, as demonstrated in Figure 15, when earlier installed columns, or other obstacles, blocks the jet stream from reaching all sections of the intended treatment area. In the case of using jet grouting to seal sheet piles, the sheet pile itself can come to serve as an obstacle. This is described in an article by Shirlaw et al. (2005) where a jet grouted bottom plug was constructed to support a long and narrow corridor of sheet piles during an extension of the transit system in Singapore. During the installation of the struts, it was discovered that the sheet piles had started to tilt, as the span between the opposing walls was smaller than given in the blueprints. Upon closer inspection, it was found that there were untreated zones in the immediate area of the sheet piles due to inadequate implementation. The blueprint of the bottom plug demonstrated that a center to center space of 1.8 m between columns was to be employed, though for the row closest to the sheet pile, a distance of 1.6 m was specified. Against the directives, the larger spacing was applied for all columns which lead to the jet stream being blocked by the convex part of the sheet pile. Thus, a “shadow” of untreated soil was cast in the concave portion of the wall. For some concave segments, the contact surface between the sheet pile and the plug was reduced with as much as 70 percent. This ultimately resulted in failure and the sheet piles began to tilt as the necessary support was not achieved.

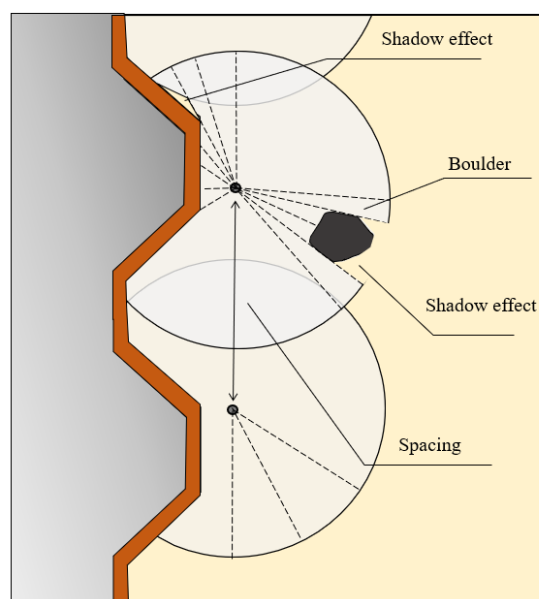


Figure 15 Illustration of the so-called “shadow effect”.

The lesson to be learned from this project is that the spacing between the column must be chosen with care and must be implemented correctly. The center of a column, which is the starting point of the jet, should be aligned with the center of the concave portion of the sheet pile, as illustrated in the original design in Figure 15. In some projects, there might be financial incentives to select a larger spacing, as a reduced number of columns would result in a shorter construction. If that is the case, appropriate compensating actions must be taken, such as increasing the column diameter and moving the center-point further from the wall, for “shadow effects” not to prevail.

3.3 Column design considerations

It is a challenge to ensure water-tightness of a jet grouted cut-off. As indicated in Chapter 2, the shape, and the quality of the soilcrete columns are greatly dependent on the performance of the chosen treatment systems and operational parameters, but also the properties of the in-situ soil. A successful design should therefore consider the influence of all these variables to prevent untreated zones. Previous studies (Cheng et al., 2019; Modoni et al., 2016; Pan et al., 2017) have identified two types of defects being the most significant ones. Those being alterations in column geometry and position.

3.3.1 Geometry

In cut-off designs, the geometry of a soilcrete column is given by the diameter (D), the minimum thickness (S), the minimum overlap (s), and the spacing between the columns (I), see Figure 16. For the ideal case, that is when the operational parameters stay constant and the soil is relatively homogenous with depth, the columns will attain a circular shape with a similar diameter. The relationship between the described geometrical variables can then be defined as follows, see Equations 1 (Croce & Modoni, 2007) and 2.

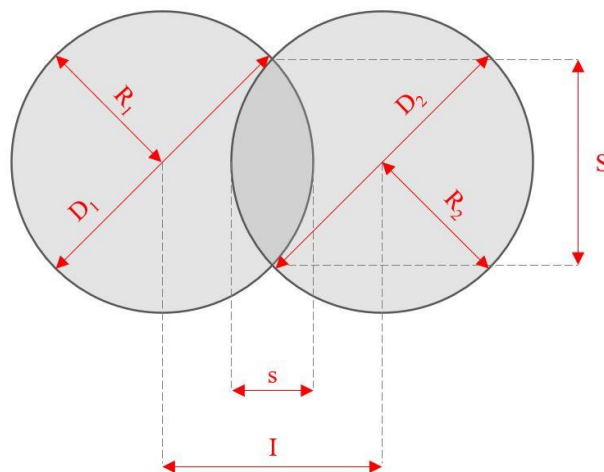


Figure 16 Illustration showing the geometrical variables for two overlapping columns with the same diameter.

$$S = \sqrt{D^2 - I^2} \quad (1)$$

$$s = 2R - I \quad (2)$$

Although, the diameter of the soilcrete columns will vary. Former studies based on experimental data (Arroyo et al., 2012; Croce & Modoni, 2007) have found that the variation in diameter is normally distributed for columns installed in the most common soil types. However, the variability coefficient (CV), or the scatter, varies between the soils. Table 2 summarizes proposed CV-values for different soil types. Generally, for cohesion soils the variance is relatively small, ranging from 0.02 to 0.05, whereas in non-cohesive soils can the diameter become up to 0.25 m larger, or smaller, than originally intended (Croce et al., 2014). When designing cut-offs, one should therefore consider this variation. To which extent will however depend on the chosen acceptable risk level (Croce and Modoni, 2007) and the engineers' knowledge and expertise (Pan et al., 2019). According to Pan et al. (2019) and Strina (2020), a common design rule is to select a minimum overlap of at least 0.2-0.3 m.

Table 2 Summary of the suggested coefficient of variation, $CV(D)$ for common soil types.

Type of soil	Clay-silt	Sandy clay	Silty sand	Sands	Sandy gravel	Gravels
Arroyo et al. (2012)		0.13-0.17				
Croce et al. (2014)	0.02-0.05			0.02-0.10		0.05-0.25
Croce and Modoni (2007)			0.06		0.19	
Langhorst et al. (2007)		0.06-0.19				

When the two adjacent columns obtain different diameters, Equation 1 and 2 are no longer valid. Instead, Equations 3 and 4 are to be used to ensure sufficient spacing and enough overlap.

$$S = \frac{1}{I} \sqrt{4 \cdot I^2 \cdot R_1^2 - (I^2 - R_2^2 + R_1^2)^2} \quad (3)$$

$$s = R_2 + R_1 - I \quad (4)$$

Note that for Equation 4, a positive value for variable s suggests that an overlap exists, whereas a negative value indicates no overlap.

3.3.2 Position

The positioning of the soilcrete columns is another aspect to bear in mind. It relies on the drilling method and the equipment used (Cheng et al., 2019). However, the operator's experience of the procedure along with the characteristics of the soil are also important factors (Pan et al., 2017). If the execution is not managed properly, the position or alignment can diverge considerably and exceed the required specifications.

A frequently used tool to measure the alignment of jet grouted columns is inclinometers which can be directly installed into or onto the drilling rod (Cheng et al., 2019). According to SS-EN 12716:2018, shall the drilling string's inclination be measured before and repeatedly during drilling for every column, to ensure that the design requirements are fulfilled. As illustrated in Figure 17, a jet grouted column can deviate in two different directions, given by the azimuth (α) and the inclination (β), ranging between 0° to 180° and -90° to 90° , respectively.

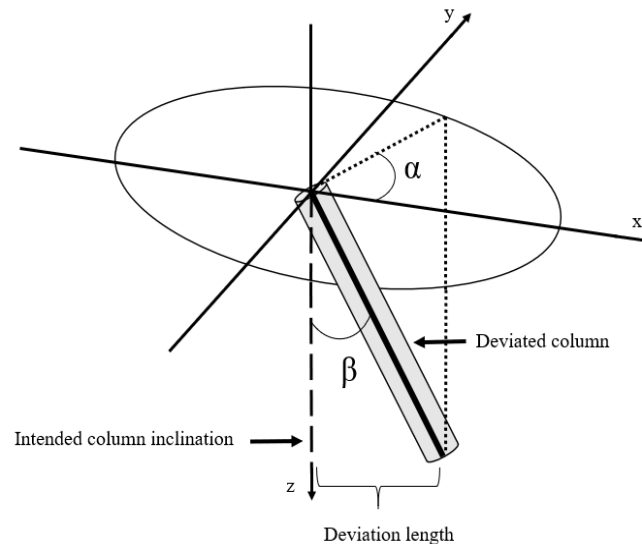


Figure 17 The possible deviation directions for a jet grouted column; azimuth (α) and inclination (β) (adapted from Pan et al., 2017).

According to experimental data gathered in silty sands and sandy gravels by Modoni et al. (2016) does the azimuth follow a uniform distribution. This means that the probability is the same for any deviation in the azimuth direction. In a water-proofing context, this is not of particular concern as gaps are formed when there are deviations in the inclination.

Research studies of the inclination found it to be normally distributed around the vertical axis, which is around 0° , see Table 3. According to SS-EN 12716:2018 shall a vertical jet grouted column not deviate more than 2 percent of the maximum drilling length from the column axis. This value might be perceived as conservative. However, when constructing longer columns or columns at greater depths, even a small inclination would result in a significant deviation. For instance, Comodromos et al. (2018) exemplify in an article that a divergence of 0.5 percent at a depth of 20 m, corresponds to a shift of 0.10 m from the intended position. This distance might even increase further if a similar alternation also arises for the adjacent column but in the opposite direction. It is therefore understandable that the guideline written by the American Society of Engineers (GI-ASCE, 2009), recommends an inclination of just 1 percent. In degrees, these mentioned limits correspond to a maximum deviation of 1.15° and 0.57° .

Table 3 Statistical summary of deviations in inclination.

Source	Soil	Diameter	No. of columns	$\overline{\Delta\beta}$	SD(β)
Arroyo et al. (2012)	Silt	0.75 m (Average)	5	0.68°	0.17°
Eramo et al. (2012)	Silty sand	2.5 m	44	Median = 0.37°	0.16°
Croce and Modoni (2007)	Silty sand	0.71-0.11 m (Average)	N/A	N/A	0.07°
Cheng et al. (2019)	Silty sand	3.6 m	8	0.43°	0.11°
Modoni et al. (2016)	N/A	N/A	N/A	Max = 0.15°	0.27°

N/A: Not stated or clearly defined by authors

The values presented in the table indicate that the mean divergences in inclination vary between 0.15° - 0.68° , which are within the limit given in the European standard. Furthermore, the standard deviation (SD) from these studies are found to be 0.07 - 0.27° , which can be considered as small. A small SD indicates consistency in the construction process, which possibly can be explained that a jet grouting project often uses the same driller and equipment. Still, fluctuations in mean deviation can be related to the equipment and the accuracy of the driller, but also the soil properties. Another probable explanation is the bending of the drilling rods caused by the self-weight (Arroyo et al., 2012), where the deviations tend to increase with depth. Although, this effect has been proven to have a greater impact in cases when inclined or horizontal drilling is performed, as the rods tend to bend in the gravity direction (Cheng et al., 2019). For these applications, it is challenging for the driller to overcome the bending forces and thereby control the deviation.

3.3.3 Possible outcome due to defects

The amount of groundwater inflow is in the end governed by the continuity and uniformity of the entire cut-off. This continuity is directly determined by the degree of defects in column geometry and position, which cannot alter too much from the design proposal. Figure 18 illustrates a case where the divergences have jeopardized the capability of the structure to function as a water barrier. Here, the soilcrete columns alternate from their intended position, both regarding inclination as well as having a varying diameter. This has resulted in gaps of untreated zones between neighboring columns, making it possible for groundwater to flow through the intended barrier.

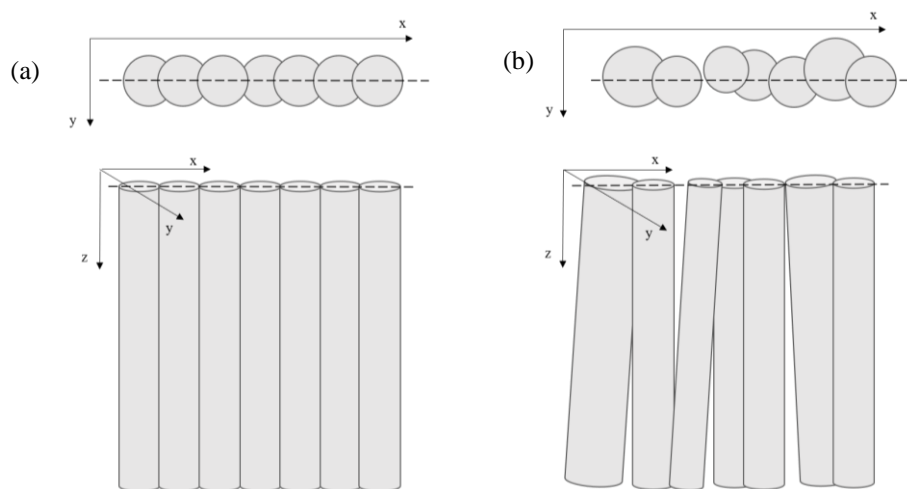


Figure 18 Illustration of the (a) original cut-off design and (b) a possible outcome.

3.4 Quality control of water cut-offs

When producing a jet grouted structure, the final result and the effectiveness of the procedure is not visible for inspection, due to it being constructed below the surface level. Therefore, it is difficult to establish an ideal quality control strategy to ensure that the overall design requirements are fulfilled. Nevertheless, when choosing the verification method(s) aspects such as project requirements, budget, required certainty, and the purpose of the jet grouting, for instance ground enforcement or a water barrier, are of importance. The choice also depends on to what extent quality control is possible

to perform. For instance, specific conditions such as grouting at great depth or within proximity to sensitive facilities and buildings can limit the choice of verification method (Kimpritis et al., 2018). Furthermore, it is a challenge to not damage the jet grouted structure during the verification. Several different methods have therefore been developed over the years.

The geometry of soilcrete columns shall, according to SS-EN 12716:2018, be tested by either direct and/or indirect measures. However, the direct method of visual inspection by excavation is always preferable, considering that the completed jet grouted element can be examined. Other necessary information related to the quality of the column, besides its diameter, can then also be disclosed. Additionally, direct methods are considered to be the most accurate ones, as the column diameter is measured in-situ (Croce et al., 2014). Indirect methods, on the other hand, record other variables to estimate the diameter, such as temperature or seismic waves.

A summary of the most common verification methods, including their main advantages and disadvantages, is displayed in Table 4. A more detailed description of these is presented in the upcoming sections.

Table 4 An overview of the most common quality assurance tools to verify column diameters.

Method	Type	Advantages	Disadvantages
Caliper	Direct	+ Non-invasive + The probe can be re-used	- Accuracy and reliability
Coring <i>Vertical or inclined</i>	Direct	+ Considered to be one of the most accurate methods + Retrieved data can be used when evaluating and developing prediction approaches + Laboratory tests can be performed on samples to determine mechanical properties and the permeability	- Expensive - Invasive
Excavation	Direct	+ Considered to be one of the most accurate methods + Retrieved data can be used when evaluating and developing prediction approaches	- Invasive - Time-consuming and costly - Limited to shallow depths
Geophysical methods	Indirect	+ Non-invasive + Probes can be re-used + Can be applied within a short timeframe from when columns were made	- Expert knowledge required to interpret results - Special equipment is required
Painted bars <i>Alt. radius bars</i>	Indirect	+ Non-invasive + Simple and easy set-up + Inexpensive	- Accuracy and reliability
Thermal methods	Indirect	+ Non-intrusive	- Sensors cannot be re-used - One needs to wait for at least 30 h for results

3.4.1 Direct verification methods of the column diameter

Direct methods to verify the column diameter can be difficult to implement in practice since they often are time-consuming and invasive. These are therefore usually applied on a few restricted numbers of columns, known as test columns, that are separated from the final structure. These are also produced before construction to calibrate the performance of the equipment with regards to the specific site conditions (Croce et al., 2014). The most common direct methods are excavation and core drilling (SS-EN 12716:2018).

Excavation involves the removal of the surrounding soil, resulting in a pit exposing the jet grouted elements (Kimpritis et al., 2018). Subsequently, measurements of the diameter can be collected by measuring the average diameter of the column. These measurements are considered to be reliable, therefore this type of data is frequently used when evaluating and verifying the predicted diameter (Flora et al., 2013; Shen et al., 2013; Wang et al., 2012). However, the method is time-consuming, expensive, and insensitive, meaning that it is in practice only employed in test schemes. For projects, the validity of the measurements is therefore closely linked to the test columns being performed nearby, or in a soil of which have similar characteristics as the soil where the production takes place. This is important to bear in mind, considering that many urban constructions sites today have limited access to space and incentives to perform the trial elsewhere prevails. Furthermore, as always with excavations, a risk assessment concerning soil stability and workers' safety is a necessity.

Another method is inclined core drilling. In this method, drilling is performed through the column at a known angle to a known depth from the ground surface. By measuring the length of the retrieved core sample and by using basic trigonometric expressions, the column diameter can be calculated (Kimpritis et al., 2018). Another version of core drilling is to retrieve a sample at the edge of where the diameter is expected to be located. By visually studying the core, the performance of the jet grouting can be determined, depending on whether it is soilcrete or in-situ soil that has been collected (Strina, 2020). Furthermore, core drilling is a common procedure used in the geotechnical field to determine the characteristics of soil and rocks. For jet grout applications, a sample is retrieved by vertically drilling through the column, which is then sent to a laboratory where various tests can be performed. This can include a classification of the quality of the jet grouted core but also its mechanical properties. In addition, can the permeability of the specific sample be assessed. Core drilling is, like excavation, an expensive and invasive method, limiting the method from being used on elements that constitute the final jet grouted structure. The method is also constrained to only provide a diameter at one section of the column where the sample was retrieved. Thus, the variations with depth or at all locations of the periphery of the whole column cannot be identified.

Another direct verification method is to use a caliper. This device consists of two arms connected with a hydraulic jack that can be opened and is inserted into the unhardened column. (Croce et al., 2014). With depth, the pressure at the caliper's arms are recorded. It will vary with the resistance on the surrounding pressure. If a sudden flux or change is observed, the arms have encountered untreated soil and the diameter of the column can be derived. The advantage of this method is that calipers can be retrieved, and no significant damages are made to the column. There is however an uncertainty with the method, and there is the risk of the caliper being misaligned to the column axis and consequently a smaller diameter is recorded.

3.4.2 Indirect verification methods of the column diameter

In terms of indirect verification techniques, the most straightforward procedure is known as the "painted bars" method. In this approach, a minimum of three rebars are evenly dyed and installed vertically into the ground, within proximity of where the column's edges are to be expected (Kimpritis et al., 2018), see Figure 19. Usually, one bar is placed at a distance of 0.1 m inside the expected radius, one at the expected radius, and one at 0.1 m outside the radius (Strina, 2020). These bars should be at least 0.5 m

longer than the desired column length, to ensure that enough length remains to remove the bars. Once the bars have been installed, jet grouting can be performed followed by the immediate removal and cleaning of the bars. Given the location of where the bars initially were installed and if the paint has been scratched and removed by the eroding jet, it is possible to approximate the column diameter (Kimpritis et al., 2018). An assessment of the diameter with depth can also be derived from the scraping marks. Strina (2020) motivates that the main advantage with this method is that the set-up is easy but most importantly cheap, in contrast to the previously mentioned direct methods. However, it is critical that the bars are installed at the correct distance and that they do not shift or bend during the treatment. The accuracy of the practice is therefore debatable, and the result can therefore only be considered as an estimation.

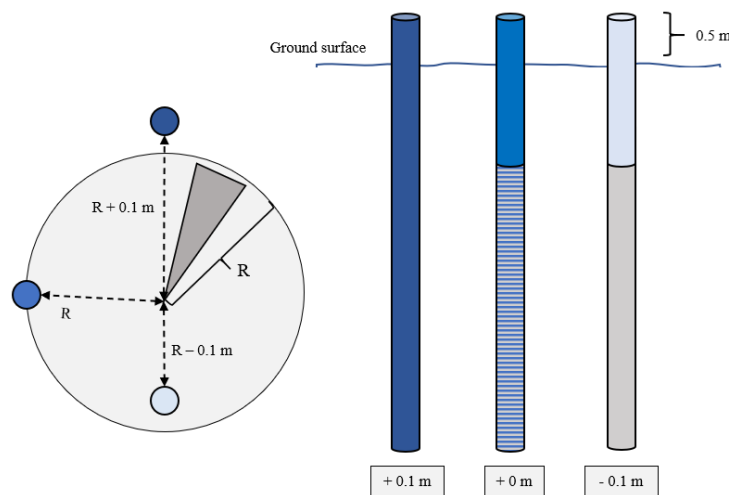


Figure 19 Principal sketch of the painted bars method.

An alternative indirect evaluation practice of column diameters, which also is relatively simple and non-destructive, is the thermal method. This approach is centered on the solidification process of the grout, which is the exothermal reaction transpiring when the cement-based agent reacts with the water, resulting in a temperature increase in the soil (Kimpritis et al., 2018). Accordingly, with a larger temperature difference, a larger diameter can be expected. The temperature sensors are installed at the center of the column during the jetting process, and measurements are recorded at a given time interval. These recordings are then compared to hydration curves for different grouts and thermal properties of soils found in software databases. The thermal method is considered to be reliable, and a case study performed by Meinhard et al. (2010) suggests that deviations of only ± 10 percent are to be expected. The method is however time-consuming, as it takes at least 30 hours before the minimum number of temperature recordings has been reached.

In recent years, advances have been made within the field of geophysical methods, allowing many of them to now be applicable in a jet grouting context. For instance, in a case study performed by Bearce et al. (2015), column diameters were estimated by measuring the electrical resistivity in the soil. Newly grouted soils have a much lower resistance towards an electric current, in comparison to saturated soils. This makes it possible to determine the column diameter, as it is simply given by the boundary between the two recorded key resistivities.

Another example is to use seismic measurements to indirectly estimate the column diameter, see Figure 20. In a field study conducted by Niederleithinger et al. (2015),

cross-hole and downhole data, comprising of velocities and traveling times for P- and S-waves taken before and after the jetting process, were compared. They found that the traveling time of the waves decreased after the jetting was performed, but also as the grout starts to harden. By exploiting this difference in velocity and traveling time, the column diameter could be estimated by using analytical relationships. Despite the method has proven to be consistent and cost-effective; it is still sensitive to surrounding disturbances and noise. Niederleithinger et al. (2015) do point this out in their article, saying this could pose a potential threat to its applicability, considering that modern construction sites often are found in urban areas of which are exposed to induce ground movements by various of activities.

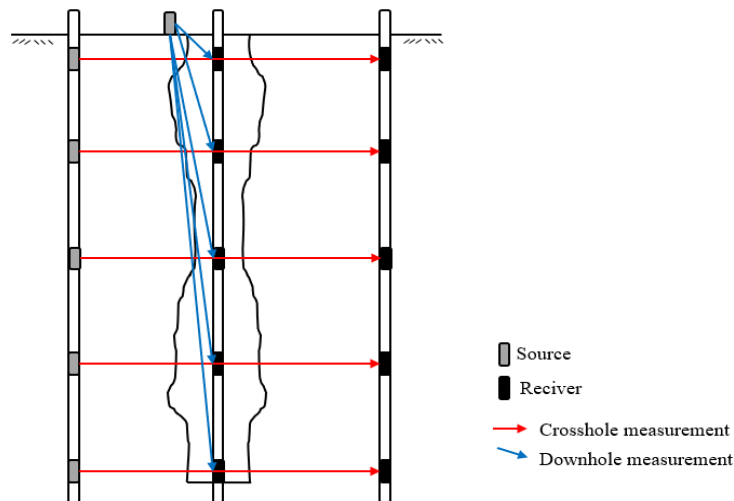


Figure 20 Principal sketch of cross-hole measurements (red) and downhole measurements (blue) of a jet grouted column.

In summary, geophysical methods are non-invasive and provide adequate results within a reasonable time frame. They can be considered as cost-efficient as retractable probes have been developed, in comparison to the thermal method of which still do not allow sensors to be recovered without jeopardizing the quality of the column. Geophysical practices do however require specialized equipment and personnel of whom can perform and interpret the test results.

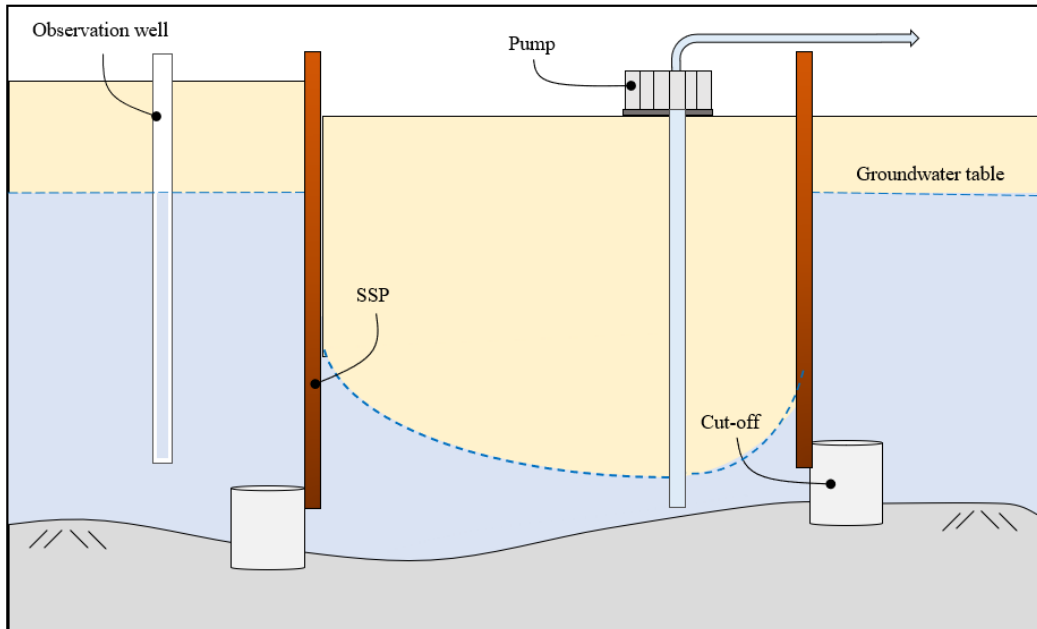
3.4.3 Verifying the permeability of a jet grouted barrier

When constructing a water cut-off, not only the column diameter needs to be verified. It is also essential to validate the water-tightness of the structure, in order for the barrier to fulfill its purpose. According to SS-EN 12716:2018 can the permeability be assessed by hydrogeological methods such as pumping tests, borehole tests, piezometric readings, or laboratory tests.

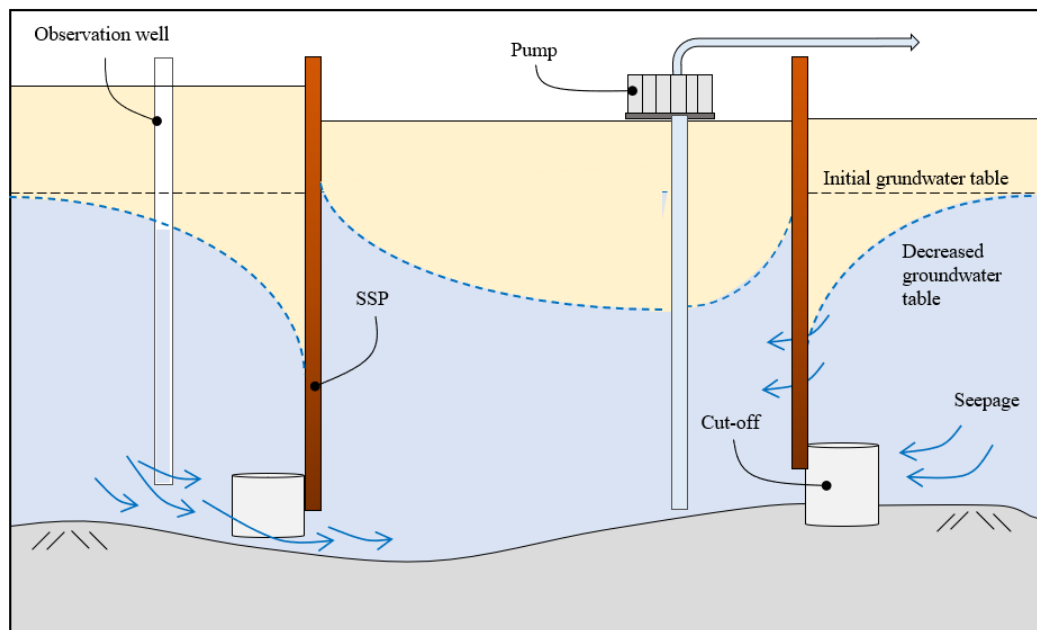
A pumping test is performed by pumping a known flow of water out of an area of interest, which, in this case, is an excavation that employs jet grouting to seal the toe of a sheet pile wall. As water is removed, the disturbances in the groundwater table due to the pumping is continuously and carefully registered in groundwater pipes or piezometers at various distances from the excavation. Considering that a pumping test registers the drawdown as a function of time, it is important to register the starting time of the pumping and when measurements were recorded (Carlsson & Gustafson, 1997).

From these recordings, the permeability of the whole structure can be estimated. Depending on the project requirements, some degree of leakage can be acceptable.

Figure 21(a) illustrates the case of a completely sealed excavation, that is; despite the pumping, no drawdown in the groundwater table outside the excavation is recorded. Figure 21(b), on the other hand, illustrates a failing cut-off with seepage and consequently a drawdown in the groundwater table.



(a) Pumping test of a completely sealed excavation



(b) Pumping test of a not completely sealed excavation

Figure 21 Graphics of pumping test for a (a) completely sealed excavation, in comparison to a (b) not completely sealed excavation. A decreased groundwater table is therefore recorded in the observation well in the second case.

Borehole water tests can also be used to estimate the permeability of a cut-off. As described in the standard of geohydraulic sampling (SS-EN ISO 22282-2:2012), the method involves either injecting or withdrawing water from a borehole in the jet-grouted structure. This generates a hydraulic head in the borehole where the changes are measured with time. Although, if the permeability is expected to be high, the test can be executed by maintaining a constant head and instead measure the required flow rate. This will however affect the jet grouted column of which is being drilled into, as it will be weakened. This type of test is consequently limited to only being performed on test columns.

To evaluate the permeability of the soilcrete, laboratory experiments can be performed on core samples. This by placing the core in a triaxial test apparatus and thereafter subject it to water pressure. By recording the pressure difference, the permeability of the specimen can be determined (USBR, 2009). It is however of importance to remember that the sample only represents a piece of the column (Croce et al.,2014). Hence, there could be defects or variations in the soilcrete quality which can result in the jet grouted structure's permeability to be lower than the value measured of the core sample in the laboratory

4 Column diameter prediction methods

As described in Chapter 3, several factors are to be associated with the waterproofing efficiency of a water cut-off. Nonetheless, the column diameter has proven to be a particularly crucial variable and will therefore form the basis of the assessment made of the jet grouting performed at the cast study site.

Authors Ribeiro and Cardoso (2017) recently published a chronological review where different mathematical models to predict the column diameter, depending on the soil conditions and the chosen operational parameters, were identified and discussed. All the mentioned approaches were formulated within the past decades and with reasonable error margins. Also, the authors grouped the studied theories into three main categories: those being either (i) empirical, (ii) conceptual, and (iii) semi-theoretical or theoretical.

Empirical relationships are expressions developed from observational and experimental data. The considered variables have a black-box relation to one another, meaning that no thought to why a given input results in a certain output is taken into consideration. The calculations are therefore strongly dependent on the context. For the case of jet grouting, empirical models are restricted to the specific soil conditions at the site. This has to do with the expressions being based on empirical data only accurate for the site where it originally was retrieved. The applicability of these models is therefore limited.

Conceptual models can be considered as a generalized description of a studied process or system. In contrast to the empirical models, is the aim of the conceptual models to increase the understanding of the input variables and how they correlate. According to Ribeiro and Cardoso (2017) are conceptual models designed to predict column diameters either based on the principle of mass conversation or the balance of volumes. More specifically, these expressions consider the equilibrium between the amount of injected grout, and the amount of grout required to produce the soilcrete column plus the generated spoil. The downside with these models is that they are restricted to quality control purposes. This has to do with the fact that the geometry of the column cannot be estimated before the execution, as spoil volumes and correction factors are required.

Finally, semi-theoretical and theoretical models aim to provide a more sophisticated and comprehensive explanation of the jetting mechanisms and their acting forces. This is achieved by using mathematical theorems which portray the injection of the jetted fluids as well as the resistance of the in-situ soil. The benefit of using a semi-theoretical or theoretical model is their relative straightforwardness, allowing them to be solved either by simple hand-calculations or computer spreadsheets. These models have over time also proven to be advantageous as they predict column diameters within proposed error margins in both coarse and fine soils. However, this only applies to jet grouting performed using a single fluid system. Deviations are still noteworthy for the double and triple fluid systems, as will be disclosed in Section 4.4. This suggests that the semi-theoretical and theoretical approaches still lack in mathematical terms to describe all acting mechanisms in the injection process.

With the benefits and disadvantages concerning each calculation method in mind, this thesis will apply three different semi-theoretical prediction model (Flora et al., 2013; Shen et al., 2013; Wang et al., 2012) and one commercial prototype model. In the upcoming sections, each model will be explained in more detail.

4.1 Wang et al. (2012)

The first semi-theoretical prediction model was developed by the Asian research group Wang et. al. in 2012. With their work, the scholars aimed to present a simple mathematical relationship to describe the jetting process. This was achieved by considering the jet grouting procedure as two acting phenomena: being (i) the turbulent kinematic flow within the jetting fluid and (ii) the erosion of the soil matrix. This approach is however limited to jet grouting performed by using a single fluid system, as the derived expressions only consider grout being the acting jetting fluid. A more generalized prediction method, which can be applied for both the double and triple fluid system, was developed by many of the same authors a year later, see Section 4.2 discussing Shen et al. (2013)

Wang et. al. (2012) begin their calculation approach by firstly referring to previous research within the kinematic flow theory presented by Abramovich (1963) and Hinze (1975). This theory is illustrated in Figure 22, where the flow of grout can be divided into two zones. In the initial zone, the maximum velocity of the jet in the x-direction, $v_{x,max}$, is the same as the exit velocity of the grout, v_0 , whereas in the main zone the maximum velocity will alter according to Equation W1.

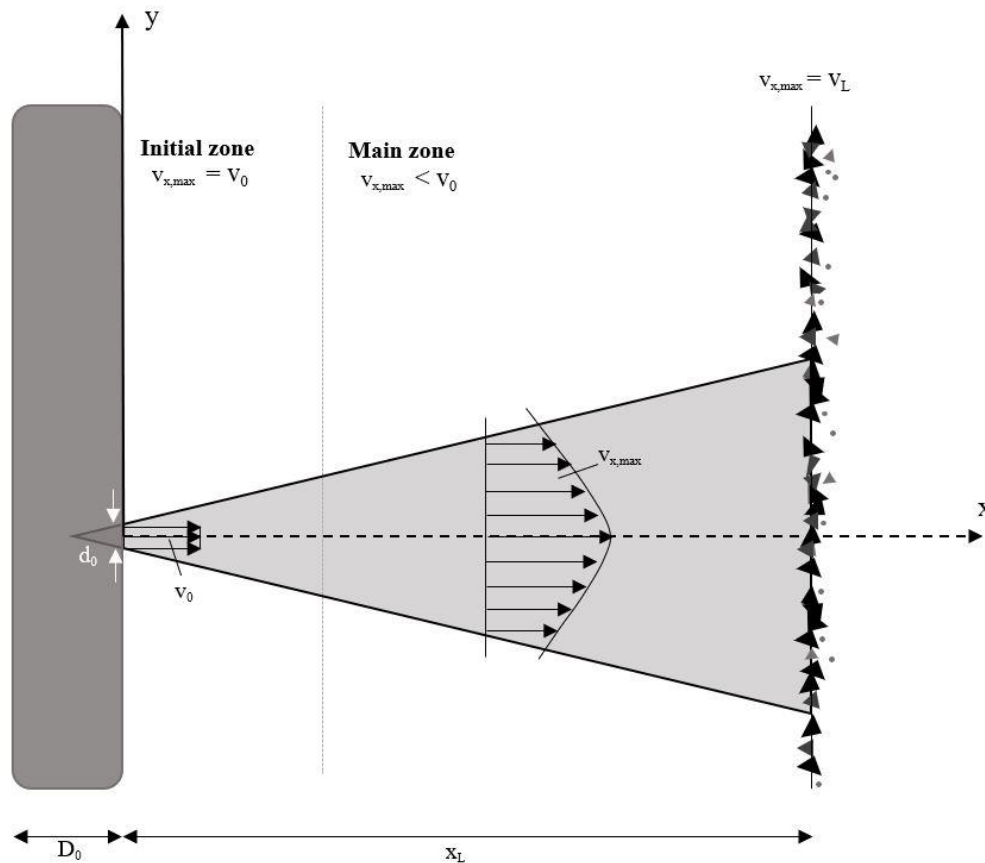


Figure 22 Principal sketch of a free jet from a round nozzle (adapted from Wang et. al., 2012).

$$\frac{v_{x,\max}}{v_0} = \alpha \cdot \frac{d_0}{x} \quad (\text{W1})$$

where: $v_{x,\max}$ = maximum velocity of the fluid along the x-direction [m/s]
 v_0 = exit velocity of the fluid [m/s]
 α = a constant parameter, related to the characteristics of the fluid and the medium in the flow region [-]
 d_0 = nozzle diameter [m]
 x = distance from the nozzle [m]

The velocity which ultimately causes erosion of the immediate soil is described as the critical velocity, v_L , given by Equation W2a. It differs between soil types and was originally described by Debbagh et al. in 2002.

$$v_L = \eta \cdot \left(\frac{q_u}{p_{\text{atm}}} \right)^k \quad (\text{W2a})$$

where: v_L = critical velocity [m/s]
 η = a characteristic velocity with a value equal to the critical velocity when the soil resistance is equal to the atmospheric pressure, related to the characteristics of the soil [-]
 q_u = unconfined compressive strength (UCS) of soils [Pa]
 p_{atm} = atmospheric pressure [Pa]
 k = a dimensionless parameter [-]

The value of the parameter k equals to 0.5, as originally suggested by Debbagh et. al. (2002). The unconfined compressive strength (UCS), q_u , can be calculated by using relationships found in soil mechanics:

$$Q_u = \begin{cases} 2 \cdot c_u & \text{For cohesion soils} \\ 2 \cdot \tau_f = 2 \cdot \sigma' \tan \phi' & \text{For non-cohesive soils} \end{cases} \quad (\text{W2b})$$

where: c_u = undrained shear strength [Pa]
 τ_f = shear strength of sand [Pa]
 σ' = normal effective stress [Pa]
 ϕ' = effective friction angle [°]

Taking the above into consideration, Wang et. al. (2012) then argues that when the soil matrix no longer can be eroded by the grout, the critical velocity will be the same as the maximum velocity of the fluid along the x-direction, that is, $v_L = v_{x,\max}$. By combining Equation W1 and W2a, the penetration distance, x_L , caused by the jet can be calculated using in Equation W3a:

$$\rightarrow x_L = \frac{\alpha}{\eta} \cdot \frac{d_0 v_0}{\sqrt{\frac{q_u}{p_{\text{atm}}}}} \quad (\text{W3a})$$

where: x_L = penetration distance [m]

The exit velocity, v_0 , for a circular nozzle can be estimated as:

$$v_0 = \frac{4 \cdot Q}{M \cdot \pi \cdot d_0^2} \quad (\text{W3b})$$

where: Q = flow rate of the fluid [m³/s]
 M = number of nozzles on the monitor [-]

By inserting the exit velocity into Equation W3a, the penetration distance is now given by Equation W3c:

$$\rightarrow x_L = \frac{\alpha}{\eta} \cdot \frac{4Q}{M\pi d_0 \sqrt{\frac{q_u}{p_{atm}}}} \quad (W3c)$$

This leads to the total diameter of a jet grouted column to be estimated as:

$$D_j = D_0 + 2 \cdot x_L = D_0 + 2 \frac{\alpha}{\eta} \cdot \frac{4Q}{M\pi d_0 \sqrt{\frac{q_u}{p_{atm}}}} \quad (W4a)$$

where: D_j = diameter of the jet grouted column [m]
 D_0 = diameter of the rod [m]

For parameters α and η , Wang et. al. (2012) combined the two into a new parameter, which is referred to as parameter b:

$$b = \frac{\alpha}{\eta} \quad (W4b)$$

where b = new parameter related to the characteristics of the soil [-]

Parameter b has been empirically estimated by Wang et al. (2012) by using existing datasets where the slope of b is plotted against the calculated penetration distance, x_L , and the penetration distance, that is $(D_m - D_0)/2$. To be noted is that the data used in the datasets were retrieved from only four different case studies, which were performed in different soil conditions as well as gathered by other researchers. From the plots, Wang et al. (2012) concluded that parameter b is influenced by either the characteristics of the grout or the soil. According to Wang et. al. (2012) were the grouts used in all the studied datasets comparable to each other. Therefore, the scholars determined that the parameter varies with respect to the properties of the soil matrix.

Considering that size and the distribution of particles is the main feature separating one soil from the other and that non-cohesive soils erode more easily, as described in Section 2.3.1, the parameter b should generally be larger for soft clays, in comparison to sands. Thus, Wang et. al. (2012) advocates that b should be approximated as follows:

$$b = 0.35 \cdot M_c^{0.41} \quad (W4c)$$

where: M_c = the content of clay, particle size $< 5\mu\text{m}$ [%]

In more general terms, Wang et. al. (2012) suggest that $b = 1.2-2.0$ for very soft clay, $b = 0.75-1.4$ for clayey silt, and $b = 0.25-0.75$ for sands.

4.2 Shen et al. (2013)

As the method of Wang et al. (2012) is only applicable for jet grouting practices of which utilizes a single fluid system, Shen et al. developed a more general approach in 2013. The predicted diameter is in this model given as by the following expression, see Equation S1:

$$D_0 = 2 \cdot R_c = 2 \cdot \eta x_L + D_r \quad (S1)$$

where: D_0 = calculated diameter of the column [m]
 R_c = calculated radius of the column [m]
 η = reduction coefficient, accounting for the effect on the injection time [-]
 x_L = ultimate erosion distance [m]
 D_r = diameter of the monitor [m]

This equation resembles Equation W4a in Section 4.1, however, the penetration distance, or the ultimate erosion distance, x_L , is in this case is defined slightly differently. In this model, the different treatment systems are taken into consideration but also the effect of the injection time.

In Shen et al. (2013), the erosion caused by the jet is still based on established theories connected to kinematic flow theory, as given by Figure 22 and Equation W1 in Section 4.1. However, the ultimate erosion distance is expressed as:

$$x_L = \frac{\alpha \cdot d_0 v_0}{v_L} \quad (S2)$$

where: x_L : ultimate erosion distance [m]
 α : attenuation coefficient, which is related to the characteristics of the fluid [-]
 d_0 : nozzle diameter [m]
 v_0 : exit velocity of the fluid at the nozzle [m/s]
 v_L : critical velocity, i.e. the minimum value of jet velocity that will initiate soil erosion [m/s]

When grout is used as a jetting fluid, which is the case for the single fluid system, the attenuation coefficient, α_s , can be calculated by using Equations S3a-S3d. When predictions are made for other jet grouting fluids and systems, Shen et al. (2013) apply other expressions that are more complex. For the case of jet grouting utilizing a double fluid system, the attention coefficient, α_d is calculated by using Equations S3e-S3f.

$$\alpha_s = \alpha_g = \frac{\alpha_w}{B} \quad (S3a)$$

where: α = attenuation coefficient, which is related to the characteristics of the fluid [-]
 α_g = attenuation coefficient for grout [-]
 α_w = attenuation coefficient for water [-]
 B = parameter reflecting the ratio of the properties of water and grout [-]

The value of the attenuation coefficient for water is given by $\alpha_w = 16$ in Shen et al. (2013) and it is based on experimental data originally presented by Shibazaki (2003). Due to the lack of detailed information concerning nozzle configuration, the effect of the nozzle shape has been assumed by Shen et al. (2013). Moreover, the parameter B , which reflects the characteristics of the grout, is suggested to be calculated according to Equation S3b:

$$B = \frac{\sqrt{\mu_g/\rho_g}}{\sqrt{\mu_w/\rho_w}} \quad (S3b)$$

where: B = parameter reflecting the ratio of the properties of water and grout [-]
 μ_g = apparent laminar viscosity of grout [Pa·s]
 ρ_g = density of grout [kg/m³]
 μ_w = apparent laminar viscosity of water [Pa·s]
 ρ_w = density of water [kg/m³]

and

$$\mu_g = 0.007 \cdot (W/C)^{-2} \quad (S3c)$$

$$\rho_g = \frac{\rho_w \rho_c [1 + (W/C)]}{\rho_w + \rho_c (W/C)} \quad (S3d)$$

where ρ_c = density of cement [kg/m³]
W/C = water and cement ratio by weight of the grout admixture [kg/kg]

The values for the density of water and cement as well as the laminar viscosity of water are given as generic values, where $\mu_w = 0.001$ Pa·s, $\rho_w = 1,000$ kg/m³ and $\rho_c = 3,150$ kg/m³.

As mentioned, for the double fluid system, Equations S3e and S3f are used instead:

$$\alpha_d = y \cdot a_g \quad (S3e)$$

$$y = 1 + 0.054 \cdot \frac{p_a}{p_{atm}} \quad (S3f)$$

where ψ = parameter related to the pressure of injected air [-]
 p_a = pressure of injected air [Pa]
 p_{atm} = atmospheric pressure [Pa]

The next parameter to be determined is the critical velocity, v_L . Shen et al. (2013) have defined the velocity as the following:

$$v_L = \beta \cdot \left(\frac{q_u}{p_{atm}} \right)^k \quad (S4a)$$

where: v_L = critical velocity, i.e. the minimum value of jet velocity that will initiate soil erosion [m/s]
 β = characteristic velocity with a value equal to the critical velocity when the soil resistance is equal to the atmospheric pressure [m/s]
 q_u = erosion resistance of soil [Pa]
k = dimensionless exponent [-]

This equation is similar to Equation W2a found in Wang et al. (2013). Here, the exponent k also equals 0.5 and the erosion resistance of the soil, q_u , is still given by relationships describing basic soil mechanics:

$$Q_u = \begin{cases} 2 \cdot c_u, & \text{For clayey soils} \\ 2 \cdot \tau_f = 2 \cdot (c' + \sigma' \tan \phi'), & \text{For sandy soils} \end{cases} \quad (\text{S4b})$$

where: c_u = undrained shear strength [Pa]
 τ_f = shear strength of sand [Pa]
 c' = effective cohesion [Pa]
 σ' = normal effective stress [Pa]
 ϕ' = effective friction angle [°]

However, the characteristics of the soil are further considered in Shen et al. (2013), as the clay content of the soil is considered to affect the characteristic velocity, β , according to the following equation:

$$\beta = \begin{cases} b_0 \cdot \left(\frac{M_c}{100}\right)^{b_1} \cdot \left(\frac{D_{50}}{D_f}\right)^{b_2}, & 5 \leq M_c \leq 100 \\ b_0 \cdot \left(\frac{5}{100}\right)^{b_1} \cdot \left(\frac{D_{50}}{D_f}\right)^{b_2}, & 0 \leq M_c \leq 5 \end{cases} \quad (\text{S4c})$$

where: β = characteristic velocity [m/s]
 b_0 = regression constants [-]
 b_1 = regression constants [-]
 b_2 = regression constants [-]
 M_c = the content of fine particles less than 75 μm in size as a percentage (%)
 D_{50} = the average size of the soil particles [mm]
 D_f = the size of no. 200 sieve [mm]

The regression constants b_0 , b_1 , and b_2 are determined by Shen et al. (2013) to be 2.87, 0.4, and -0.4, respectively. These are based on fitting measures of values originally reported by Dabbagh et al. (2002). Furthermore, the standard size of a no. 200 sieve is 0.075 mm.

Finally, the exit velocity of a circular nozzle, v_0 , is familiarly described as:

$$v_0 = \frac{4 \cdot Q}{M \cdot \pi \cdot d_0^2} \quad (\text{S5})$$

where: Q = flow rate of the fluid [m^3/s]
 M = number of nozzles on the monitor [-]
 d_0 = nozzle diameter [m]

All the required parameters to determine the ultimate erosion distance have now been defined. However, to predict the diameter of a soilcrete column, the reduction coefficient, η also needs to be calculated to consider all operational factors:

$$\eta = a_0 \left(\frac{v_{m0}}{v_m}\right)^{a_1} \cdot N^{a_2} \quad (\text{S6a})$$

where: η = reduction coefficient, accounting for the effect on the injection time [-]
 a_0 = correction factor corresponding to the horizontal tangential velocity of the nozzle [-]
 a_1 = empirical parameters [-]
 a_2 = empirical parameters [-]
 v_{m0} = reference horizontal tangential velocity of the nozzle [m/s]
 v_m = horizontal tangential velocity of the nozzle [m/s]
 N = number of passes of the jet [-]

Shen et al. (2013) have defined the correction factor, the empirical parameters, and the reference horizontal tangential velocity to be $a_0 = 0.09$, $a_1 = 0.14$, $a_2 = 0.20$ and $v_{m0} = 0.071$ m/s, respectively. These determinations were based on previous papers and trials published by other research teams. Furthermore, the horizontal tangential velocity of the nozzle, v_m , and the number of passes of the jet, N can be determined considering the following operational relations:

$$v_m = \sqrt{(\pi R_s D_r)^2 + v_s^2} \quad (S6b)$$

$$N = M \cdot \frac{R_s}{v_s} \cdot \Delta S_t \quad (S6c)$$

where: R_s = rotation speed [1/s]
 D_r = diameter of the monitor [m]
 v_s = withdrawal rate of the rod [m/s]
 M = the number of nozzles on the monitor [-]
 ΔS_t = lift step [m]

4.3 Flora et al. (2013)

The third prediction model was also developed in 2013, however, by an Italian group of researchers referred to as Flora et al. They have also based their prediction approach on kinematic flow theory and soil resistance, similarly to Wang et al. (2012) and Shen et al. (2013). Although, they express their computational arguments in relation to the notion of energy required to perform the jetting process.

The prediction approach begins in the same way as the Asian models, with a similar illustration of a submerged jet like the one presented in Section 4.1, see Figure 22. However, Flora et al. (2013) emphasizes that the shape of the submerged jet is dependent on two velocity profiles: the longitudinal and the transverse. The longitudinal is the radius of the jet stream, whereas and the transverse is the forward direction which is given by the rotational radius of the jet. This suggests that the eroding jet has more of a bell-shape, decreasing in velocity with distance from the nozzle, x . The distance from the jet axis, r , where the velocity at each point, x , is therefore described by Flora et al. (2013) as:

$$\frac{v_{x,r=0}}{v_0} = A \cdot \frac{d_0}{x} \quad (F1a)$$

$$\frac{v_{x,r}}{v_0} = \frac{1}{\left[1 + 1.33 \cdot A^2 \cdot \left(\frac{r}{x}\right)^2\right]^2} \quad (F1b)$$

where: r = distance from the jet axis [m]
 x = distance from the nozzle [m]
 v_x = velocity at distance x from the nozzle [m/s]
 v_0 = outlet velocity [m/s]
 A = parameter which quantifies the interaction between the jet and surrounding fluid [-]
 d_0 = nozzle diameter [m]

By using these two equations, it is possible to mathematically describe the hydrodynamic power of the jet through a certain cross-section at a specified distance x from the nozzle. A more complete derivation of this equation can be found in the appendix of the original paper (Flora et al., 2013).

$$W(x) = \int_0^{\infty} \rho(v_{x,r})^3 \pi r \, dr = \frac{\pi A \rho \cdot d_0^3 v_0^3}{13.3 \cdot x} \quad (F2)$$

where: $W(x)$ = hydrodynamic power of the jet at distance x from the nozzle [W]
 ρ = density of the injected fluid [kg/m³]

Considering the operational parameters, such as the number of nozzles used and the time it takes to create a column of a certain length, the kinetic energy of the jet at distance x from the nozzle can be written as:

$$E(x) = M \int_{t_1}^{t_2} W(x) \, dt = \frac{\pi A \rho \cdot M d_0^3 v_0^3 L}{13.3 \cdot x \cdot v_s} \quad (F3)$$

where: $E(x)$ = kinetic energy at a distance x from the nozzle [J]
 M = number of nozzles [-]
 L = length of columns [m]
 v_s = lifting speed of the monitor [m/s]

In an earlier paper (Croce & Flora, 2000), the authors have defined the specific energy at the nozzles, E'_n , as the following:

$$E'_n = \frac{\pi \cdot \rho \cdot M d_0^2 v_0^3}{8 \cdot v_s} \quad (F4)$$

where: E'_n = specific energy at the nozzles [J]

By combining Equations F3 and F4, Flora et al. (2013) express the specific energy at distance x as:

$$E'(x) = 0.6A \cdot \frac{d_0}{x} \cdot E'_n \quad (F5)$$

Here, the authors claim that Equation F5, in comparison to their initial derivation given by Equation F4, is more conclusive. They argue that the latter expression more conclusively describes the alteration in available energy, which decreases with distance x from the nozzle. It also acknowledges the hydrodynamic interaction between the jet and the surrounding fluid with a unitless parameter A . The equation is however not applicable if one does not know the specific energy at the nozzle. Often the specific energy for the pump can be calculated (Tornaghi, 1989), see Equation F6a, assuming an energy loss of about 10 percent (Flora & Lirer, 2011), see Equation F6b:

$$E'_p = \frac{p \cdot Q}{v_s} \quad (F6a)$$

where: E'_p = specific energy at the pump [J]
 p = injection pressure at the pump [Pa]
 Q = flow rate [m³/s]

$$E'_n = 0.9 \cdot E'_p \quad (F6b)$$

The parameter Λ is strongly connected to the characteristics of the injection and the jetting fluid, in other words, to the chosen treatment system:

$$\Lambda = \alpha \cdot \Lambda^* \quad (\text{F7a})$$

where: α = factor correcting Λ^* for double and triple fluid jet grouting

$\Lambda^* = \Lambda$ for single fluid jet grouting [-]

For the case of jet grouting using a single fluid treatment system, $\alpha = 1$ whereas for the double and triple fluid system $\alpha \approx 6$. Again, the authors refer to previous research by Mondoni et al. (2006), suggesting that $\Lambda_w^* = 16$ for a submerged jet of water. Therefore, when using grout as the jetting fluid, Equation F7b and F7c are to be used:

$$\Lambda^* = \Lambda_w^* \sqrt{\frac{\mu_w \cdot \rho_g}{\mu_g \cdot \rho_w}} \quad (\text{F7b})$$

$$\rho_g = \frac{\rho_c (1 + \omega)}{\omega + \left(\frac{\rho_c}{\rho_w}\right)} \quad (\text{F7c})$$

where: $\Lambda_w^* = \Lambda$ for water [-]

μ_w = laminar viscosity of water [Pa·s]

μ_g = laminar viscosity of grout [Pa·s]

ρ_w = density of water [kg/m³]

ρ_g = density of grout [kg/m³]

ρ_c = density of cement [kg/m³]

ω = water and cement ratio by weight of the grout [kg/kg]

To determine the laminar viscosity of the grout, μ_g , Flora et al. (2013) suggest using the graph presented below, see Figure 23.

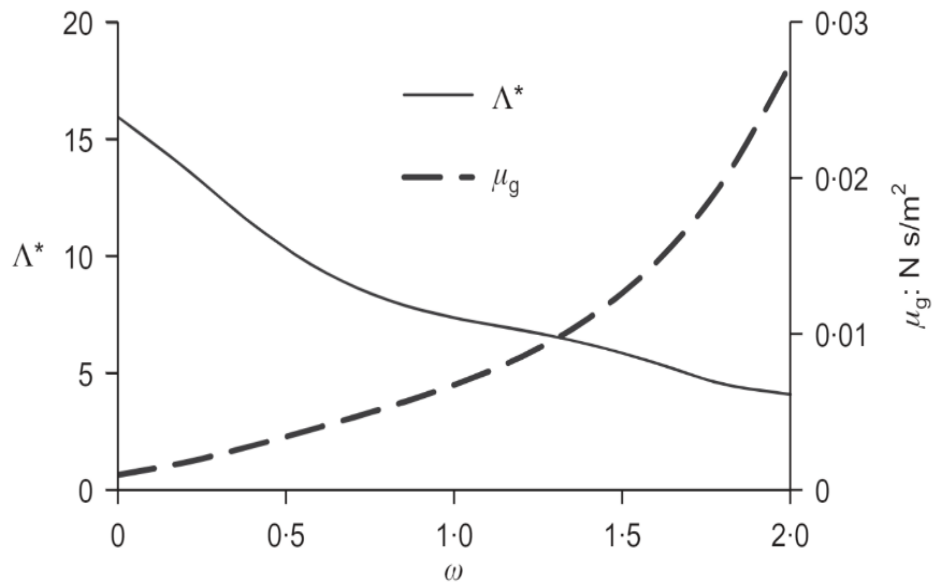


Figure 23 Graph illustrating how the parameter Λ^* and the laminar viscosity of the grout varies with the water/cement-ratio (from Flora et. al., 2013)

As the energy required to perform the jetting process now has been expressed, the average diameter is in the end proposed by Flora et al. (2013) to as:

$$D_a = D_{ref} \cdot J^\beta \cdot S^\delta \quad (F8)$$

where: D_a = average diameter of column [m]
 D_{ref} = reference diameter of column [m]
 J = formal parameter quantifying the action of the jet [-]
 β = exponent quantifying the influence of jet energy on the diameter of column [-]
 S = formal parameter quantifying the resistance of the soil erosion [-]
 δ = exponent quantifying the interaction between the jet and the surrounding fluid [-]

The parameters β and δ have been determined to be 0.20 and -0.25, respectively, from experimental field data. The reference diameter, D_{ref} , does, on the other hand, vary with the soil type. Flora et al. (2013) have estimated this variable to vary according to the values presented in Table 5.

Table 5 Proposed values for D_{ref} depending on the soil type (adapted from Flora et al., 2013).

Soil type		ASTM D2487 classification	D_{ref} [m]
Coarse-grained	Without fines	Gravels and sands with less than 5 percent fines	1.00
	With fines	Gravels and sands with more and 5 percent fines	0.80
Fine-grained		Silts, clay, and organic soils	0.50

The eroding action of the jet, J , is given by the ratio between the specific kinetic energy as described previously and the reference value of the specific energy:

$$J = \frac{E'(x)}{E'_{ref}(x)} = \frac{\alpha A^* E'_n}{\alpha_{ref} \Lambda^*_{ref} E'_{n,ref}} = \frac{\alpha A^* E'_n}{1 \cdot 7.5 \cdot 10E^6} \quad (F9)$$

Finally, the soil resistance, S , is calculated by using the results obtained during the geological investigation, either in the form of a standard penetration test (SPT) or a cone penetration test (CPT), see Equation F10a or F10b:

$$S = \frac{N_{SPT}}{N_{SPT,ref}} = \frac{N_{SPT}}{10} \quad (F10a)$$

$$S = \frac{q_c}{q_{c,ref}} = \frac{q_c}{1.5} \quad (F10b)$$

where N_{SPT} = number of blows in SPTs [-]
 q_c = unit tip resistance of CPTs [MPa]

4.4 Recent research developments

The beginning of this chapter briefly indicated that the three semi-theoretical prediction approaches to some extent provide deviant results. This despite being verified by the scholars through comparisons between the predicted diameters versus the measured diameters collected from excavations and core drillings made in field trials. As stated in Flora et al. (2013) “*an effective design procedure should [...] comprise of two subsequent steps: (a) definition of an average column diameter and (b) the prediction of scattering from the mean value*”. Recent studies have therefore begun to focus on identifying the cause-effect relationships in the jet grouting practices by applying advanced statistical approaches.

For instance, Ochmański et al. (2015) used the concept of artificial neural networks (ANN) in an attempt to predict column diameters, utilizing four different types of inputs. Those included jet grouting injection parameters, specific energy at the nozzle, soil characteristics, and the number of blows in SPTs. The predicted diameters using ANN were then compared to the measured diameters, as well as calculated diameters using the methods of Shen et al. (2013) and Flora et al. (2013). For the smaller diameters, that being less than 1.5 meters, and soilcrete columns created using a single jet system, ANN predicted diameters in the same error margin as for the two theoretical models. However, for the larger diameters utilizing a double or a triple system, the ANN model demonstrated mean absolute errors of ± 13 and ± 15 percent, respectively. This can be compared to errors of about ± 30 percent for the triple fluid system reported by Shen et al. (2013) and roughly ± 20 percent for both systems reported by Flora et al. (2013). Similar research has also been performed by Tinoco et al. (2018). Although, being a trans-disciplinary team with knowledge in both the geotechnical field as well as information system technologies, three different data mining (DM) algorithms were used. Those being multiple regression (MR), support vector machines (SVM), and ANN. Their plots of measured diameters versus predicted diameters suggested successful results, as the coefficient of determination, R^2 was 0.92 for the MR model and 1.00 for SVM and ANN. To be noted is that the dataset used in this study was not as large and varied as for the case of Ochmański et al. (2015). This had to do with the fact that the data was supplied by only one contractor, operating in similar soils. Also, fewer input variables were used, that being no more than eight variables and the majority related to the operation of the jetting fluid. These limitations in the data are something that the researchers also point out and future research related to the verification of these algorithms is called for. However, Tinoco et al. (2018) do report the relative importance of the input variables for the different algorithms. What is interesting is that not the same factors are considered to be the most significant one, despite that two of the models have an R^2 value of 1.00. For the SVM model, the withdrawal speed is regarded as the most influential parameter, followed by the flow rate of the grout slurry and the jetting system used. In contrast, for the ANN model, the grout pressure and the dynamic impact of the grout are of most importance, thereafter the operational parameters.

Another approach to tackle the uncertainties related to column geometry is to instead consider the probability of the failure mechanisms. This is exemplified in the work undertaken by Modoni et al. (2016) and Bellato et al. (2018). In the earlier paper, a semi-probabilistic approach is accounted for in the design of jet grouted bottom plugs. Here, Modoni et al. (2016) performed Monte Carlo simulations by assuming that the azimuth of the column followed a uniform distribution, the inclination pursue a normal distribution, and the coefficient of variation for column diameters is 0.1. The motivation

for these trends is described in Chapter 3 and similar observations have also been reported by Cheng et al. (2019). Bellato et al. (2018), on the other hand, utilizes probability density functions (PDFs) to create a mathematical model that predicts the likelihood of unexpected boulders to cause shadow effects. Both studies are of interest, as they propose innovative improvements in the design of jet grouting structures. No reports of these models being applied in a construction project have to this date been found, therefore, the legitimacy of these schemes remains to be answered.

4.5 The revised manufacturer's prediction model

As mentioned in Chapter 1, most of the advances within the jet grouting technology have been made by a few specialist contractors and the manufacturers. Some of these companies have developed models to predict the column diameter or other approaches to evaluate the performance of the technology. Many of these are however only available, and used, internally.

A commercial Excel-based model has been provided by a jet grouting manufacturer and will be evaluated in this thesis. This model uses the column diameter as an input parameter to estimate the fuel and cement consumption but also the time to construct one column. By rearranging the equations, it is possible to instead use the model to predict the diameter. This model does however only consider operational parameters and a single fluid treatment system.

In the revised calculation approach of the manufacturer's estimation the column diameter can be predicted according to Equation M1:

$$D = \sqrt{\frac{4}{\pi} \cdot \frac{V_c}{CT}} \quad (M1)$$

where D = predicted column diameter [m]
 V_c = cement per m of column length [kg/m]
 CT = cement per m³ treated soil [kg/m³]

The input parameters are the total amount of cement used per m of column, which is dependent on the characteristics of the grout and the amount of cement required for every m³ meter of treated soil. The CT-value is a project-specific value, often ranging between 400-800 kg/m³ depending on the desired column strength. In this case study a value of 350 kg/m³ was used. V_c can be calculated according to Equation M2:

$$V_c = \frac{1,000 \cdot V_g}{[(1,000/\rho_c)+W/C]} \quad (M2)$$

where V_g = total amount of grout needed per m of column length [kg/m]
 ρ_c = density of cement [kg/m³]
 W/C = water and cement ratio by weight [kg/kg]

The total amount of grout needed per m of column length can be calculated by using Equation M3 below:

$$V_g = \frac{1}{100 \cdot \Delta S_t} \cdot Q \cdot t \quad (M3)$$

where ΔS_t = lift step [m]
 Q = delivery of the grout [m³/s]
 t = time per step [s]

To calculate the amount of grout, the grout flow needs to be calculated by multiplying the velocity of the grout with the area of the nozzle(s), as described in Equation M4:

$$Q = v_g \cdot M \cdot N_{\text{area}} = v_g \cdot \frac{M d_0^2 \pi}{4} \quad (\text{M4})$$

where Q = flow rate of the grout [m^3/s]
 v_g = grout flow velocity [m/s]
 M = number of nozzles on the monitor [-]
 d_0 = diameter of nozzle [m]

The flow velocity of the grout can in turn be calculated based on Bernoulli's equation:

$$v_g = \sqrt{\frac{2 \cdot 9.81 \cdot 10 \cdot p_g}{\gamma_g \cdot 100,000}} \quad (\text{M5})$$

where p_g = pressure of the grout [Pa]
 γ_g = specific gravity of the grout [-]

Lastly, the specific gravity of the grout can be calculated according to Equation M6:

$$\gamma_g = \frac{W + C}{W + (C/\rho_c)} \quad (\text{M6})$$

where W = weight of water [kg]
 C = weight of cement [kg]

4.6 Summary of required variables

The three prediction models presented by Wang et al. (2012), Shen et al. (2013), and Flora et al. (2013) are similar to one another, considering that they all are semi-theoretical. Although, they do require different input parameters to predict the diameter of a soilcrete column. Table 6 summarizes all the required inputs for the respective approach. Some of these parameters had to be recorded during the case study and more on this will be presented in Chapter 5.

Table 6 Overview of the required input parameters for the studied prediction models.

Wang et al. (2012)			
<i>Operational parameters</i>		<i>Soil parameters</i>	
d_0	nozzle diameter [m]	c_u	undrained shear strength [Pa]
M	number of nozzles on the monitor [-]	M_c	content of clay, particle size $<5\mu\text{m}$ [%]
Q	flow rate of the fluid [m^3/s]	σ'	normal effective stress [Pa]
		ϕ'	effective friction angle [$^\circ$]
Shen et al. (2013)			
<i>Operational parameters</i>		<i>Soil parameters</i>	
d_0	nozzle diameter [m]	c'	effective cohesion [Pa]
D_r	diameter of the monitor [m]	c_u	undrained shear strength [Pa]
M	number of nozzles on the monitor [-]	D_{50}	average size of the soil particle [mm]
Q	flow rate of the fluid [m^3/s]	M_c	content of clay, particle size $<75\mu\text{m}$ [%]
R_s	rotation speed [m/s]	σ'	normal effective stress [Pa]
ΔS_t	lift step [m]	ϕ'	effective friction angle [$^\circ$]
v_s	withdrawal rate of the rod [m/s]	<i>Grout parameters</i>	
p_a	pressure of injected air [Pa]	W/C	water-cement ratio by weight [kg/kg]
Flora et al. (2013)			
<i>Operational parameters</i>		<i>Soil parameters</i>	
d_0	nozzle diameter [m]	D_{ref}	reference diameter of column [m]
p	injection pressure at the pump [Pa]	N_{SPT}	number of blows in SPTs [-]
Q	flow rate [m^3/s]	q_c	unit tip resistance of CPTs [MPa]
v_s	lifting speed of the monitor [m/s]	<i>Grout parameters</i>	
		ω	water-cement ratio by weight [kg/kg]
Manufacturer's model			
<i>Operational parameters</i>		<i>Grout parameters</i>	
d_0	nozzle diameter [m]	W/C	water-cement ratio by weight [kg/kg]
M	number of nozzles on the monitor [-]		
ΔS_t	lift step [m]		
t	time per step [s]		
p_g	pressure of the grout [Pa]		

5 Case study: The Gothenburg Port Line

The Gothenburg Port Line [Swedish: *Hamnbanan*], is a single-track railway line that currently extends between the Göta River Bridge in the east and the Skandia Harbor within the port of Gothenburg in the west (Swedish Transport Administration, 2016). The port is the largest in northern Europe, facilitating container and bulk logistics to all of Sweden. The Skandia Harbor is a quay entirely dedicated to container cargo and 60 percent of these leave the port by rail. This corresponds to around 70 trains per day (Port of Gothenburg, 2019), making the 10-km long Port Line one of the most important railway links in the country. To meet the future demands from trade and industry, but also to stay competitive on the global market, the capacity of the railway line must increase. Following earlier investigations, the Swedish Transport Administration decided in 2012 that the best solution was to expand to a double-track, and that tunneling was the most suitable alternative.

Constructing in the subsurface is however expensive. Yet, by allowing the expansion to take place underground, it is believed that this otherwise densely populated area would not be affected negatively by the increasing volumes of cargo (Swedish Transport Administration, 2016). Considering that the trains would operate in tunnels, less sound pollution and vibrations are also to be expected. Furthermore, land can instead become available for future property developments and no physical boundary will exist, which would be the case for a railway at surface level.

5.1 Overall project description

The construction of the new and improved Gothenburg Port Line has been divided into three parts (Swedish Transport Administration, 2016), taking into consideration its complexity and range. Figure 24 demonstrates phase number three, consisting of a 1.9 km double-tracked railway running from *Eriksberg* in the east to *Pölsebo* in the west. The section involves several geotechnical structures, including 300 m of tunneling in bedrock, 810 m of concrete tunnel, and 400 m of open concrete trough.

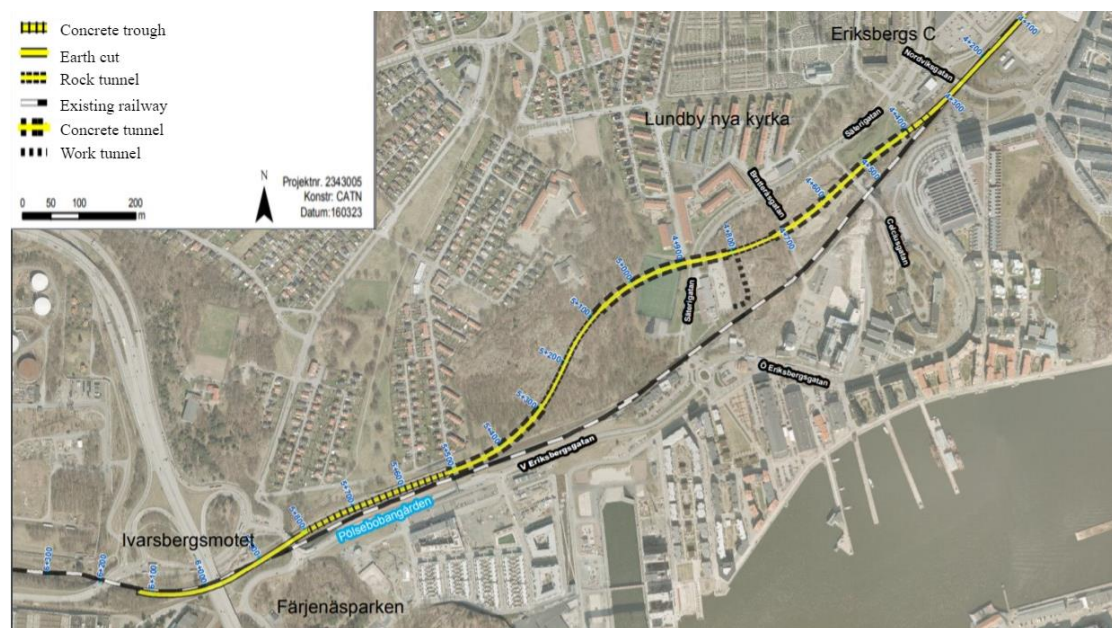


Figure 24 Map demonstrating the extension of the Gothenburg Port Line phase Eriksberg-Pölsebo (adapted from Swedish Transportation Administration, 2016)

5.1.1 Organization and main challenges

In August 2019, the project development and construction enterprise, Skanska (2019) announced that they acquired the contract for phase three, with the Swedish Transport Agency serving as the client. In total 1,100 m of tunneling will be carried out, likewise, other projects such as demolishing of existing buildings, redirecting of provisional traffic, and a stormwater service tunnel, amongst others are included. The project is valued to 1.3 billion SEK and is expected to be finished in 2024. Due to the size and complexity of the phase, it has been divided into eight zones as illustrated in Figure 25.

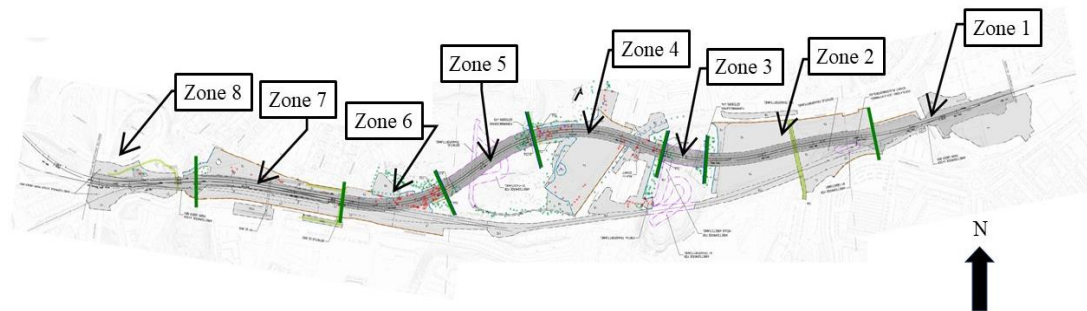


Figure 25 Map demonstrating the different production zones for phase Eriksberg-Pölsebo (unpublished material, Skanska, 2020b).

In the environmental impact assessment published by the Swedish Transport Administration (2016), a handful of likely disturbances throughout the construction stage have been identified. Frequently unfavorable outcomes related to construction works, such as noise and increased traffic, are anticipated throughout the entire production phase. Moreover, considering that the infrastructure is to be built underground, challenges related to excavation works, such as blasting and hauling of masses are also expected. Two project-specific challenges have however been identified in the overall assessment.

Firstly, the section contains parks and recreational areas including trees of noble kinds, such as oak and beech, which acts as habitats to insects and birds. Due to their high ecological and cultural value, the Swedish Transport Administration (2016) has set claims to protect certain trees, and substantial fines will be seized if these trees are damaged.

Secondly, there are also hydrological claims concerning the groundwater level. Considering that the section runs through dense residential areas, groundwater levels need to be kept relatively constant in order to not affect these existing buildings.

5.1.2 Geology and hydrogeology

The geological and hydrogeological conditions in the city of Gothenburg can in some regards be considered as particularly difficult, due to the variations between steep and hard bedrock and vast layers of clay (Swedish Transport Administration, 2016). The section between *Eriksberg* and *Pölsebo* is no exception, as illustrated in Figure 26. In this map it is evident that the intended railway expands over multiples types of soil, including glaciofluvial sediments, sands, rock, and clay.



Figure 26 Map demonstrating the soil types along with the proposed railway extension (adapted from the Geological Survey of Sweden, 2020). The construction area is marked in purple.

The stratigraphy is defined by multiple valleys filled with clay or friction material located between hills of crystalline gneiss and granite. The valley near *Sannegården* includes layers of sand and gravel which are post-glacial deposits. These glacial deposits are located directly on top of the rock, but layers of clay have been found interspersed within the sand. Furthermore, the other nearby valleys are filled with clay as well as friction material, such as sand. These clay layers are anticipated to reach up to 25 m deep and are regarded as particularly sensitive to disturbances, therefore also prone to cause settlements (Swedish Transport Administration, 2016). Laboratory tests of collected soil samples have found the clay to be normally consolidated or slightly overconsolidated. The over consolidation ratio, (OCR) was derived to vary between 1.1-1.8, making it very sensible to strains and loading. If loaded, creep up to 3 mm per year will occur, especially in those areas where the clay is deep (Swedish Transport Administration, 2015).

The sections of sand and glaciofluvial sediments, also known as friction material, are water-bearing, meaning they have a large permeability and acts as aquifers for groundwater. Additionally, most of these layers are covered by either clay or clay-rich filling material, making them closed aquifers. The hydraulic conductivity of the friction material has from investigations been found to be high, ranging from 10^{-5} to 10^{-3} m/s (Swedish Transport Administration, 2015). Transition zones between bedrock and porous materials are therefore regarded as especially troublesome, considering that groundwater flows on top of the impermeable rock can be very high (Swedish Transport Administration, 2016). When excavating these zones, seepage control is consequently necessary.

Previous surveys of the groundwater table have recorded decreased levels during construction in the nearby area (Swedish Transport Administration, 2016). This indicates that the area is sensitive to activities that can disrupt the natural groundwater conditions. Nonetheless, most fluctuations are caused by seasonal variations and are

normally found to be 2-3 m. For the case of excavations, actions to seal the pit should be implemented to prevent the lowering of the groundwater table. However, considerations should also be made to hinder damming by installing drainage where it is needed.

Due to the hydrogeological conditions described, jet grouting has been suggested as an applicable solution to seal excavations where sheet piles have been driven down to sloping bedrock. For the Port Line project, Skanska Geotechnics and Skanska Foundation Projects are responsible for the design and the execution of the jet grouting works, respectively. Jet grouting is planned to be performed in zone 2, 4, 6, and 7 (Skanska, 2020). This thesis will however only consider the jet grouting trial performed in zone 2.

5.2 Description of the case study site: zone 2

The area of zone 2 is located in the eastern parts of the project, near *Sannegården* and *Eriksberg*. This location was chosen as the trial site due to the following reasons. Firstly, because of production convenience, considering that this location at the time allowed for little interference by other on-going construction activities. Secondly, it was assumed that this area has similar soil conditions as the other zones where jet grouting also is to be performed. Therefore, the obtained results are believed to be representative for all jet grouting works made in phase three.

5.2.1 Geology and hydrogeology

As indicated in the soil map below, see Figure 27 (Geological Survey of Sweden, 2020), the expected soil conditions in zone 2 are post-glacial sands and/or glaciofluvial sediments. There is however also a possibility to find boulders in the area since it in the past has served as a quarry (Swedish National Land Survey, 2020; Swedish Transport Administration, 2015)

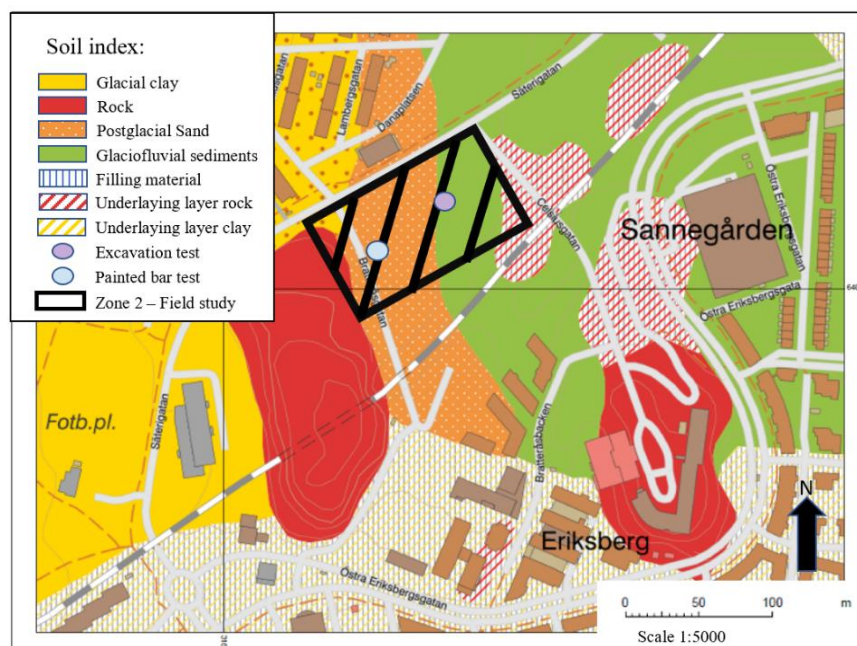


Figure 27 Map illustrating the soil types in zone 2 (adapted from the Geological Survey of Sweden, 2020).

Since the site consists of mainly coarse soils, the area is important for groundwater recharge. As it to an extent is overlaid by filling material and silt, the area can furthermore be categorized as a partially opened aquifer (Swedish Transport Administration, 2015). The regions where the sand meets rock are of particular concern, due to the hydrological factors making them important for recharge. Moreover, by studying the contour lines, it is believed that the groundwater flows from the northern parts towards the Göta River in the south.

5.2.2 Borehole interpretation

A comprehensive geotechnical survey for the phase was compiled in 2018, including CPTs, SPTs, and laboratory tests, to name a few (Swedish Transport Administration, 2018). By studying the interpreted results, it was possible to develop a soil profile for the locations where the case study was to be performed.

Figure 28 illustrates the stratigraphy for borehole 4705 and 4714, located in the proximity of the locations of the field. As illustrated, the boreholes confirm that the area mainly comprises of vast sand layers down to bedrock. A depth of 4 m to 2 m was chosen by the construction company to be jet grouted for the excavation test, whereas for the painted bars test, a depth of 8 m to 6 m was chosen. The reason to perform jet grouting at different depths was to investigate whether the design diameter could be achieved despite different stress conditions. Also, by allowing the excavation columns to be constructed closer to the surface level, the removal of masses could be reduced. Furthermore, the tests were performed in sand that resembles the expected conditions in the other zones where jet grouting will be employed. More on this will be discussed in Section 7.2.

From the data presented in the geotechnical survey (Swedish Transport Administration, 2018) it was also possible to determine the input values for the soil in order to apply the semi-theoretical prediction models. Table 7 summarizes the determined values used in the calculations. Appendix I provides the documents of which the interpretation was derived from. Due to no analysis considering the effective cohesion or the clay content of the sand has been reported, these values had to be approximated.

Table 7 Overview of the soil parameters used when applying the studied prediction models. Based on interpretations of data from borehole 4705 provided by the Swedish Transport Administration (2018).

	Borehole 4705 <i>At a depth of 4 m</i>	Motivation
Friction angle, ϕ [°]	36	Interpretation of CPTs and SPTs, see Appendix I
Effective cohesion, c' [MP]	0	Assumed a non-cohesive sand
Clay content, M_c [%]	15	Assumed value based on the soil texture triangle by USDA (2017)
Average particle size, D_{50} [m]	0.3	Interpretation from sieve analysis, see Appendix I

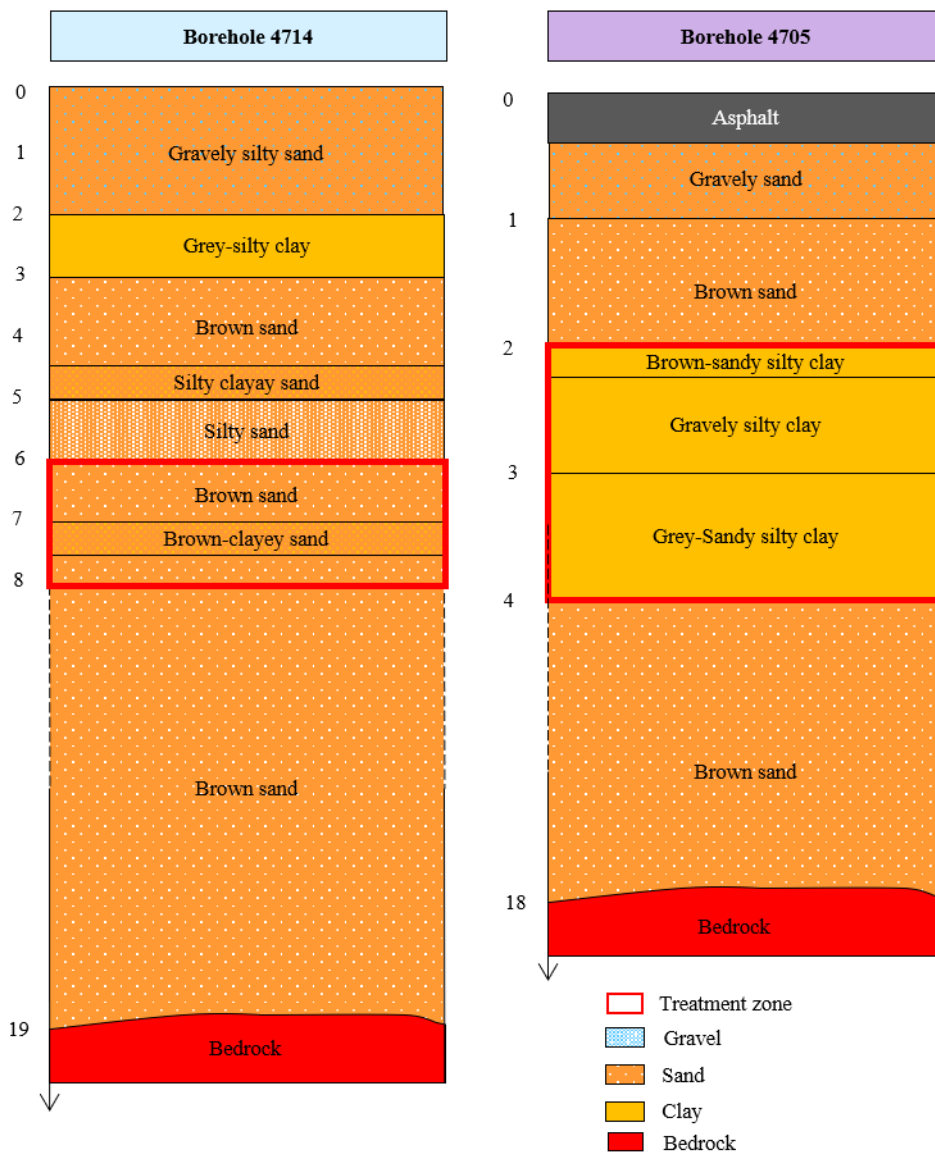
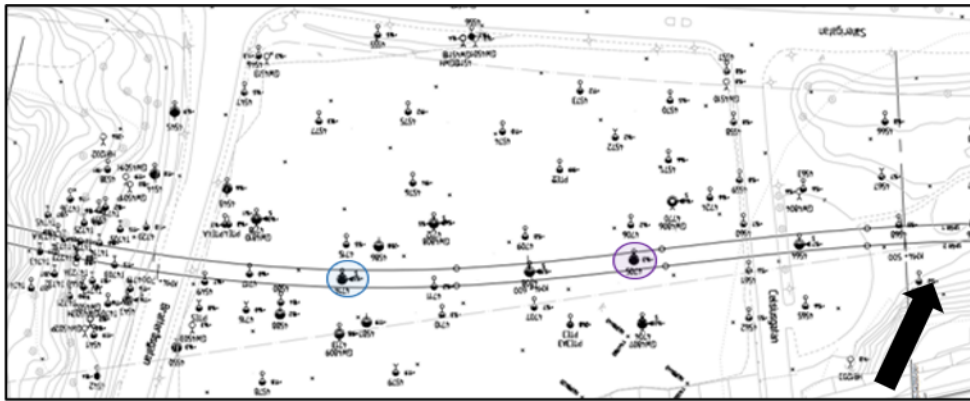


Figure 28 Soil profile for borehole 4705 (excavation) and 4714 (painted bars). Based on the SPT results reported by the Swedish Transport Administration (2018).

5.2.3 Site observations

Excavation of zone 2 had already started when the trial began and continued throughout the trial week. Filling material and glaciofluvial sands are present, but also prominent layers of clay are interspersed with the sand were found, as demonstrated in the photographs below, see Figure 29.



Figure 29 Photograph of early excavation works in zone 2; the layer of clay marked between the red lines and a close-up of the clear distinction of different soil layers at the site. This area is located in between the two test locations.

Moreover, the top sand layer has a distinct orange color, indicating that the iron concentration is high in the soil closest to the surface. This was supported by the smell of the sand, as it had a metallic odor, and that several pieces of metallic scrap were found in the excavated soil masses. According to Strina (2020), will the high concentration of iron not have an impact on the quality of the soilcrete columns. Strina (2020) does however emphasize the importance of determining if the soil contains chemicals or substances which could have a negative impact on the jet grouting process. For example, sulfur is especially troublesome as it affects the hardening process of the grout. If there are indications that the soil is contaminated, it is recommended that soil samples are analyzed in the laboratory before the jet grouting practices begin. It is also of interest to know if the soil is contaminated to ensure safe working conditions and if special consideration is required during the disposal of the soil masses.

Another observation made at the site was that when walking across the excavated sand layer, no footprints were left behind. This suggests that the sand is relatively compact, and therefore a larger jetting pressure will most likely be needed to attain the design diameter (Strina, 2020). Additionally, the clay at the site could easily be rolled in the palm and considerable amounts of shells were found, indicating that the clay was formed in a marine environment. This is however something to be expected from clays in the Gothenburg area (Schoning, 2016).

5.3 Execution of the trial

Two different assessments were performed in this trial: an excavation of test columns and a painted bars test. The motivation for performing two kinds of tests was to verify if the design diameter could be achieved for different stress states, but also to evaluate two different methods. Furthermore, excavation is recognized as the most accurate direct verification method according to SS-EN 12716:2018, whereas the painted bars test is a relatively cheap supplementary method.

Both single fluid and double fluid jet grouting were performed. For the single fluid system, a design diameter of 1.0 m was proposed, whereas for the double system a diameter of 1.7 m. The reason for assessing two dimensions and treatment systems were given by the possible economic benefits and the opportunity to collect material to support future investment decisions. Considering that the initial estimation suggested that about 2,100 columns are necessary in order to seal the sheet pile in all zones, a larger diameter can significantly reduce the number of required columns, as illustrated in Figure 30. Furthermore, the employed drilling hammer has a length of 1.8 m. This means that drilling of about 2 m into the bedrock is required for each soilcrete column, to ensure that the nozzle is leveled with the bedrock surface. A reduced number of required columns would therefore entail less drilling time, and thereby possible economic gains. Additionally, as pointed out by Strina (2020), a larger design diameter would also decrease the risk of not achieving a waterproof seal, as fewer columns result in a lower probability of defects. A larger diameter would, however, result in a need for greater cement volumes.

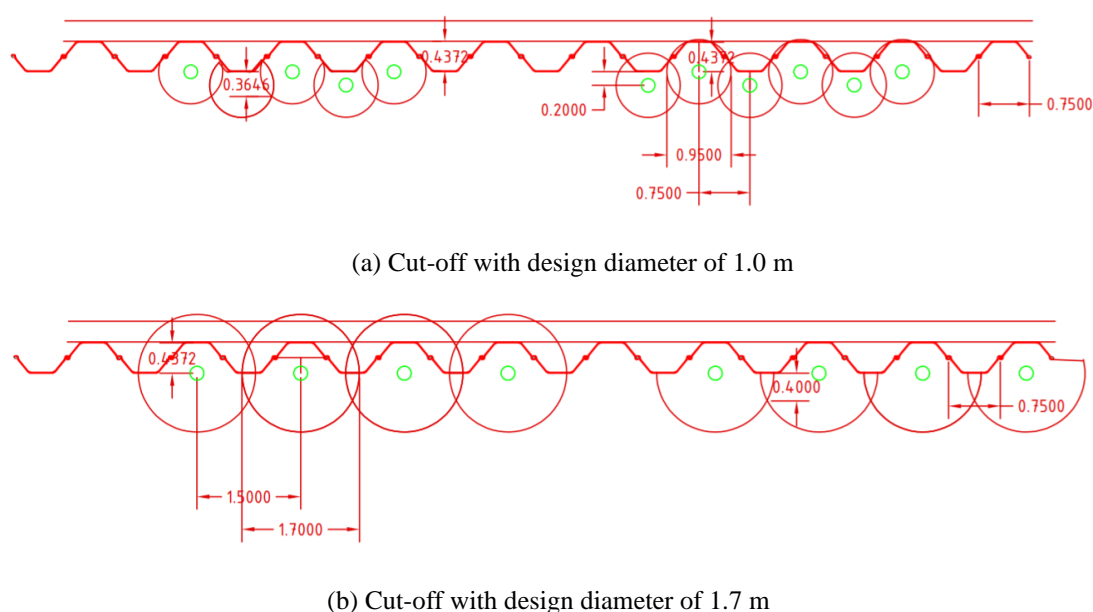


Figure 30 Blueprint of cut-off design utilizing columns with a diameter of (a) 1.0 m and (b) 1.7 m (unpublished material, Skanska, 2020a).

Finally, the tests were conducted using three different sets of operational parameters which were suggested by the project's jet grouting consultant (Strina, 2020). These sets were chosen to optimize the execution with regards to quality and economy.

5.3.1 Equipment

The equipment used in the trial followed the general jet grouting arrangement as described in Section 2.2.1. The photographs below do however demonstrate the set-up in more detail, see Figure 31.



Figure 31 Photographs of the equipment set-up in zone 2 including the three working stations; the mixing plant (top left), the water pump for the drill tip and air compressor (bottom left), and the jet rig (right).

The mixing plant used (top left picture) was a compact installation. The cement silo (A) had a volume of 28.5 m^3 and could contain up to 33 tons of cement. The blender (B.1) had a mixing capacity of 750 L, which corresponds to a maximum production of $15 \text{ m}^3/\text{h}$. The agitator (B.2) had a maximum capacity of 1,700 L, allowing for a continuous flow of grout. The grout pump (C) can obtain a maximum pressure of 650 bar, however, when in constant use, the manufacturer specifies 550 bar as the maximum pressure. Exceeding this pressure can otherwise result in abrasion of the pump. Furthermore, its maximum delivery is 500 L/min.

Since the majority of the bedrock in the southwest of Sweden consists of hard metamorphic rock (Larson & Tullborg, 2015), the drilling method used by the jet rig (F) was a water drilling system. It has a length of 1.8 m and a diameter of 0.13 m. As the drill utilizes water to power the hammer, a water pump (D.1) and a water tank (D.2) was also required. The pump requires about 120-130 bar when drilling into bedrock and 70-80 bar when drilling through coarse soil. This corresponds to about 175-445 L/min of water needed, according to the drill's technical specifications. When performing double-fluid jetting, an additional air compressor was used. All pumps and compressors utilize diesel as fuel.

Table 8 summarizes the main tasks and the operational parameters of concern for the different jetting stations. Note that the number of people required to perform the provided tasks varies with the experience and the qualifications of the personnel, but also the chosen treatment system and the equipment used. In this trial, a workforce of four people was employed. The tasks of operating the water pump and the air compressor, as well as the excavator, were performed by the same person. For all operations appropriate personal safety equipment was adopted. Communication was assisted by utilizing Bluetooth technology and radio, but also by locating the working stations in such a way so the personnel could have visual contact.

Table 8 Summary of the required tasks and input parameters of concern at each station

Station	Main tasks	Input parameters of concern
Jet rig	Operate the jetting rig; that is, moving the rig into position and to perform the drilling, jetting, and grouting.	Lifting speed Time Rotation speed Pressure Delivery
Water pump and air compressor	Make sure that the pre-determined water and air (during double-fluid jetting) pressures and deliveries are obtained	Pressure water Delivery water Pressure air (double fluid) Delivery air (double fluid)
Grout pump	Make sure that the pre-determined grout pressure and delivery are obtained. Cleans the mixing station when finished for the day	Pressure grout Delivery grout
Mixing plant	Blend the grout; track the volumes of cement and water that is used, counting the number of batches made, etc. Cleans the mixing station when finished for the day	W/C-ratio
Excavation	Helps to move the gear at the site and hoes, excavates the grouted columns in the trial, etc.	-

5.3.2 Excavation

For the excavation test, a total of 11 soilcrete columns were made. Three different kinds of operational schemes were utilized, as specified in Table 9. The reason for trying two different settings for the 1.0 m columns was to investigate if less time and energy could be used to still attain the same desired diameter (see test 1 and 2).

Table 9 Summary of the operational parameters used to produce the excavated columns.

	Test 1	Test 2	Test 3
Design diameter [m]	1.0	1.0	1.7
Installation	F-in-F	F-in-F	F-in-F
No. of columns	4	4	3
W/C-ratio [-]	0.91	0.91	0.91
Pressure of grout [bar]	400	350	400
Nozzle diameter [mm]	3.5	3.0	4.5
No. of nozzles [-]	1	2	1
Lifting step [cm]	4	4	4
Time [s/step]	8	6	14
Lifting speed [m/s]	0.005	0.0067	0.0029
Rotation speed [RPM]	(7.5) 8	(10) 10.5	(4.3) 4.5
Delivery of grout [L/min]	132	180	216
Air pressure [bar]	-	-	8
Delivery of air [m ³ /min]	-	-	10

Figure 32 illustrates the jet stream when flushing water through the system before performing the second test, where two nozzles were used. In this figure, it is also evident that the drilling tip is located 1.8 m below the nozzles, demonstrating the additional drilling length required for the grouting to start at the desired level.



Figure 32 The jet stream using two nozzles. Note that here only water is flushed through the system.

For all columns, the installation was performed fresh-in-fresh. The motivation for carrying out the work in this manner was to investigate if this approach would be applied without jeopardizing the quality of the columns, despite using the water-intensive hammer. To compensate for the increased volume of water in the soil, the W/C-ratio of the grout had to be lowered to 0.91.

Figure 33 illustrates the location of all test columns. As demonstrated, most of the columns were formed next to the sheet pile wall. However, for each test, one column was also installed free-standing. The sheet pile used was of AU-profile with a width of 750 mm, which is the same type that will be used throughout the project. Drilling was performed to a depth of 6 m below surface level leaving the nozzle at a depth of around 4 m, in order for the jet grouting to start at the pre-determined depth. Grouting was then executed, resulting in a column of 2 m ending 2 m below ground surface. To be noted was that when performing jet grouting using the double fluid system, substantial amounts of spoil were generated. Also, due to the large air pressures, some of the spoil started to splash, making the installation rather messy. Once all columns were installed they were excavated and measured.

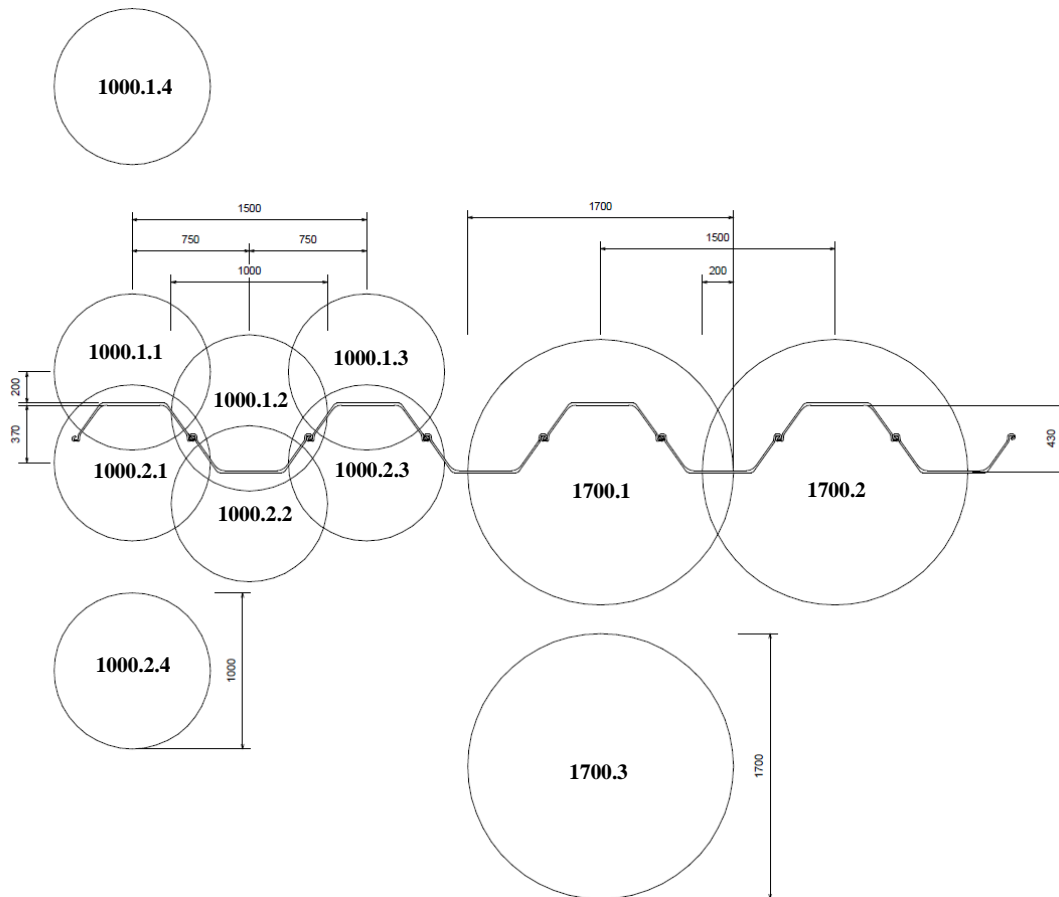


Figure 33 Illustration of the columns made for the excavation test.

5.3.3 Painted bars test

The painted bars test was performed according to the work sequence described in Section 3.4.2. However, in order for the spray-painted reinforcement bars to be installed, the boreholes first had to be pre-drilled. For test 1, investigating a column diameter of 1.7 m, the pre-drilling was performed with air. For test 2, the case of 1.0 m and a grout pressure of 400 bar, the pre-drilling was performed with water. Lastly, for test 3, now considering a pressure of 450 bar, the pre-drilling was performed using the water-intensive hammer. The reason for the variation in drilling methods was lack of preparation prior to the execution, resulting in the necessary equipment not being available for the entire test period.

As illustrated in Figure 34, bars with a length of over 9 m were installed at either -0.1 m, 0 m, or +0.1 m from the desired radius center. For the 1.0 m columns, this corresponds to radii of 0.4, 0.5, and 0.6 m, respectively, whereas for the 1.7 m columns the bars were located at radii of 0.75, 0.85, and 0.95 m. The operational parameters used for each test are given in Table 10.



Figure 34 Photographs taken during the painted bars test; measuring and installation (left) and uninstalled bars (right).

Table 10 Summary of the operational parameters used when producing the deep test columns.

	Test 1	Test 2	Test 3
Design diameter [m]	1.7	1.0	1.0
No. of columns	1	1	1
WC-ratio [-]	0.91	0.91	0.91
Pressure of grout [bar]	400	400	450
Nozzle diameter [cm]	4.5	3.5	3.5
No. of nozzles [-]	1	1	1
Lifting step [cm]	4	4	4
Time [s/step]	14	8	9
Lifting speed [m/s]	0.0029	0.005	0.004
Rotation speed [RPM]	4.3 (4.5)	7.5 (8)	6.67 (7)
Delivery of grout [L/min]	216	132	137
Air pressure [bar]	8	-	-
Delivery of air [m ³ /min]	10	-	-

The considered treatment zone for the columns in the painted bars test was at a depth of 8 m to 6 m. After the grouting had been performed, all bars were immediately removed to make sure that they did not harden inside the column. Before studying them more closely, remaining grout and sand were removed by gently hosing the bars off with water.

6 Results

In this chapter, the obtained results are presented in two sections. In Section 6.1, the predicted column diameters, calculated by using the three studied prediction models and the model provided by the manufacturer, are compared to the measured diameters excavated columns. In Section 6.2, the most predominant observations and measurements made in the case study are described.

6.1 Theoretical predictions models

Table 11 summarizes the average diameter of the excavated columns and the predicted diameters for the three calculations approaches that were described in Section 4.1-4.3 with input parameters from Table 6 and Table 7. A copy of one calculation for each model can be found in Appendix II. In the case of Wang et al. (2012), no predictions have been made for the columns made using the double fluid system. The reason for this is that the model is constrained to only be applicable for the single fluid system.

Table 11 Table summarizing the measured average diameter for the excavated columns and the predicted diameters calculated using the three semi-theoretical prediction models.

Column ID	Excavated diameter [m]	Predicted diameter [m]		
		Wang et al. (2012)	Shen et al. (2013)	Flora et al. (2013)
1000.1.1	1.00	1.20	1.92	0.92
1000.1.2	0.86			
1000.1.3	1.00			
1000.2.1	0.66	1.83	2.87	0.90
1000.2.2	0.80			
1000.2.3	0.46			
1000.2.4	0.70			
1700.1	3.08	N/A	3.65	1.63
1700.2	2.28			
1700.3	2.60			

By studying the table above, it is recognized that the general trend is that the prediction models overestimate the diameter. That is, the models predict a larger diameter than the diameter of the columns made in the field. Table 12 also illustrates this trend, in the format of a ratio between the predicted diameter and the measured diameter. A ratio larger than 1.00 indicates that the predicted value is larger than the measured value, that is the model overestimates. On the contrary, a ratio smaller than 1.00, indicates that the model underestimates the diameter. Hence, orange color indicates that the model overestimates the diameter, whereas blue color indicates that the model underestimates. A darker shade signifies that the prediction is farther away from a completely correct prediction.

Table 12 Table demonstrating the ratio between the predicted diameter and measured diameter for the case of the three prediction models.

Column ID	$D_{\text{predicted}}/D_{\text{measured}} [-]$		
	Wang et al. (2012)	Shen et al. (2013)	Flora et al. (2013)
1000.1.1	1.20	1.92	0.92
1000.1.2	1.40	2.24	1.07
1000.1.3	1.20	1.92	0.92
1000.2.1	2.77	4.35	1.37
1000.2.2	2.29	3.59	1.13
1000.2.3	3.98	6.24	1.97
1000.2.4	2.61	4.10	1.29
1700.1	N/A	1.18	0.53
1700.2	N/A	1.60	0.72
1700.3	N/A	1.40	0.63

A visual demonstration of the predicted and measured diameters for the single fluid and the double fluid systems can be observed in Figures 35 and 36, respectively. The solid line corresponds to the scenarios where the prediction is correct, that is $D_{\text{predicted}} = D_{\text{measured}}$. This means that markers found above this line correspond to the cases where the prediction approach overestimates the diameter, in other words when $D_{\text{predicted}} > D_{\text{measured}}$. Correspondingly, the markers observed under this line represents an underestimation. The dotted lines correspond to a ± 20 percent error margin. Moreover, blank markers are the predictions made for test 1 whereas filled markers are for test 2.

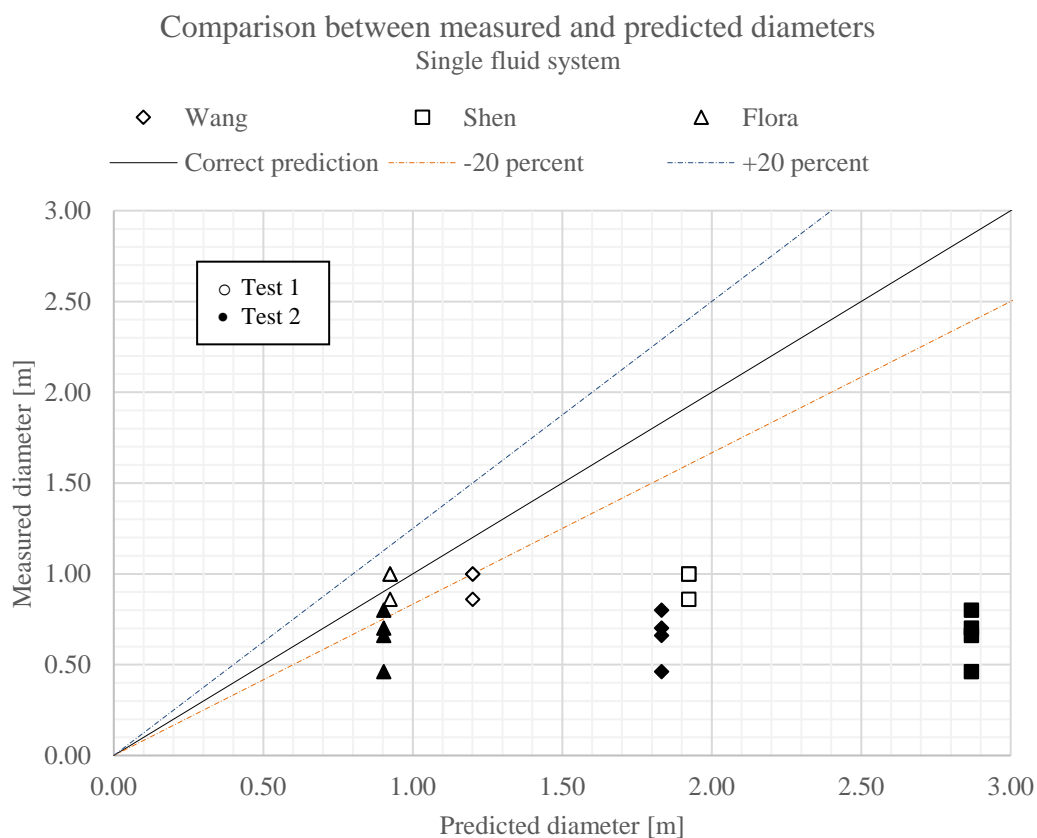


Figure 35 Cross-plot comparing the measured diameters for columns made using a single fluid system and the predicted diameters for the three prediction models.

Comparison between measured and predicted diameters
Double fluid system

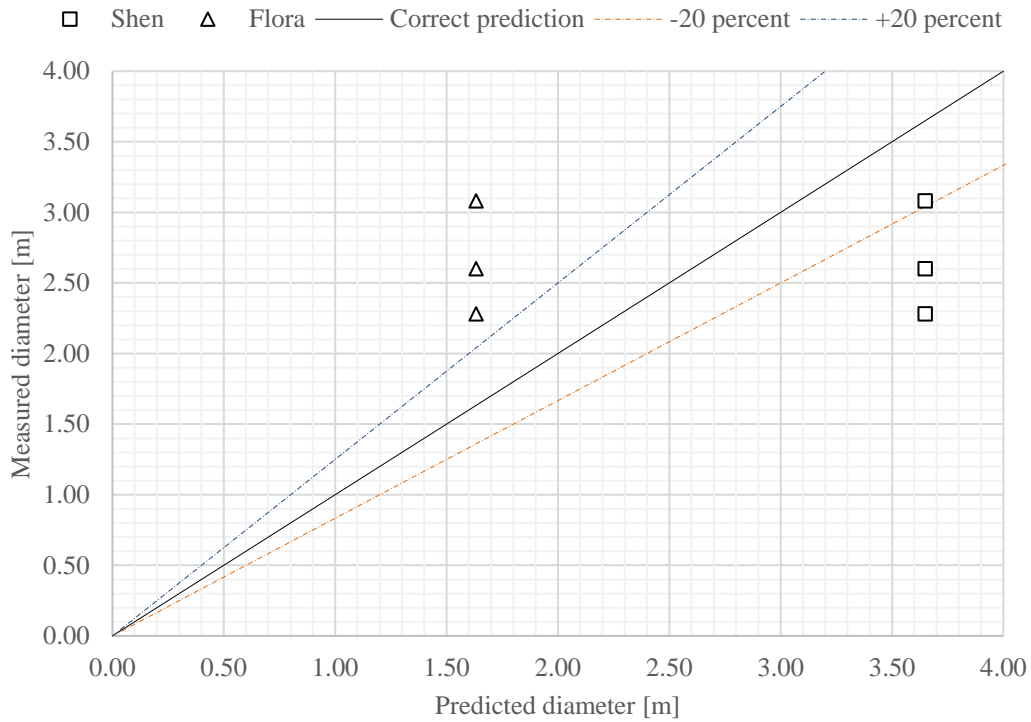


Figure 36 Cross-plot comparing the measured diameters for columns made using a double fluid system and the predicted diameters for the two prediction models.

The predictions made using the revised version of the manufacturer’s prediction model are summarized in Table 13. Moreover, a cross-plot for the single fluid system, now also including these predictions, is given by Figure 37.

Table 13 Table summarizing the measured average diameter found during excavation in comparison to the predicted diameters from the manufacture’s model.

Column ID	Excavated diameter [m]	Predicted diameter [m]	$D_{\text{predicted}}/D_{\text{measured}}$ [-]
		Manufacturer’s model	
1000.1.1	1.00	1.13	1.13
1000.1.2	0.86		1.31
1000.1.3	1.00		1.13
1000.2.1	0.66	1.15	1.74
1000.2.2	0.80		1.44
1000.2.3	0.46		2.50
1000.2.4	0.70		1.64

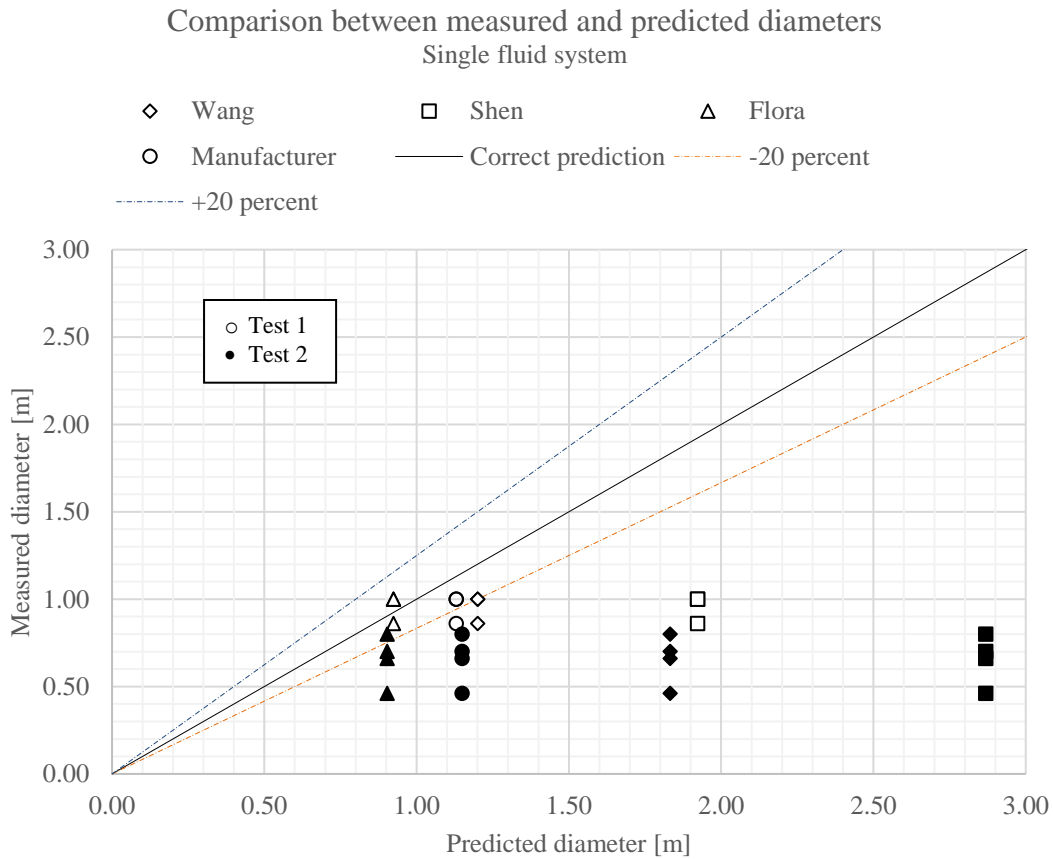


Figure 37 Cross-plot comparing the measured diameters for columns made and the predicted diameters for the revised version of the manufacturer’s model, but also the three prediction models.

6.2 Field trial

6.2.1 Excavation

The excavation of the test columns was performed on two separate occasions to comply with the project’s working hours. Column 1000.1.1-1000.1.3 were excavated less than 24 hours after installment, whereas columns 1000.2.1-1000.2.4 and 1700.1-1700.3 about 120 hours afterward. To be noted is that column 1000.1.4 could not be found during either one of the excavations.

A summary of the design and the measured average diameters are presented in Table 14. Furthermore, the ratio between the measured diameter and the design diameter is given. Note that a value larger than 1.00 denotes that the intended diameter was achieved, whereas a value below 1.00 means that the column did not achieve the design requirement. Also, due to shortcomings during the excavation, two columns were damaged. However, the measured average diameters are considered trustworthy.

Figure 38 demonstrates the physical appearance of columns 1000.1.1-1000.1.3. Graphical illustrations of all columns that were excavated can be found in Appendix III.

Table 14 Summary of the design diameter, the measured average diameter, and the calculated ratio for all excavated columns.

Column ID	Design diameter [m]	Measured average diameter [m]	$D_{\text{measured}}/D_{\text{design}} [-]$
1000.1.1	1.00	1.00*	1.00
1000.1.2	1.00	0.86	0.86
1000.1.3	1.00	1.00	1.00
1000.1.4	1.00	N/A	N/A
1000.2.1	1.00	0.66	0.66
1000.2.2	1.00	0.80	0.80
1000.2.3	1.00	0.46	0.46
1000.2.4	1.00	0.70**	0.70
1700.1	1.70	3.08	1.81
1700.2	1.70	2.88	1.69
1700.3	1.70	2.60	1.53

N/A: Column was not found during the excavation

*: Column was damaged vertically during the excavation, the average diameter have therefore been approximated

**: Column was cut horizontally in two, the measured average diameter is however believed to be true

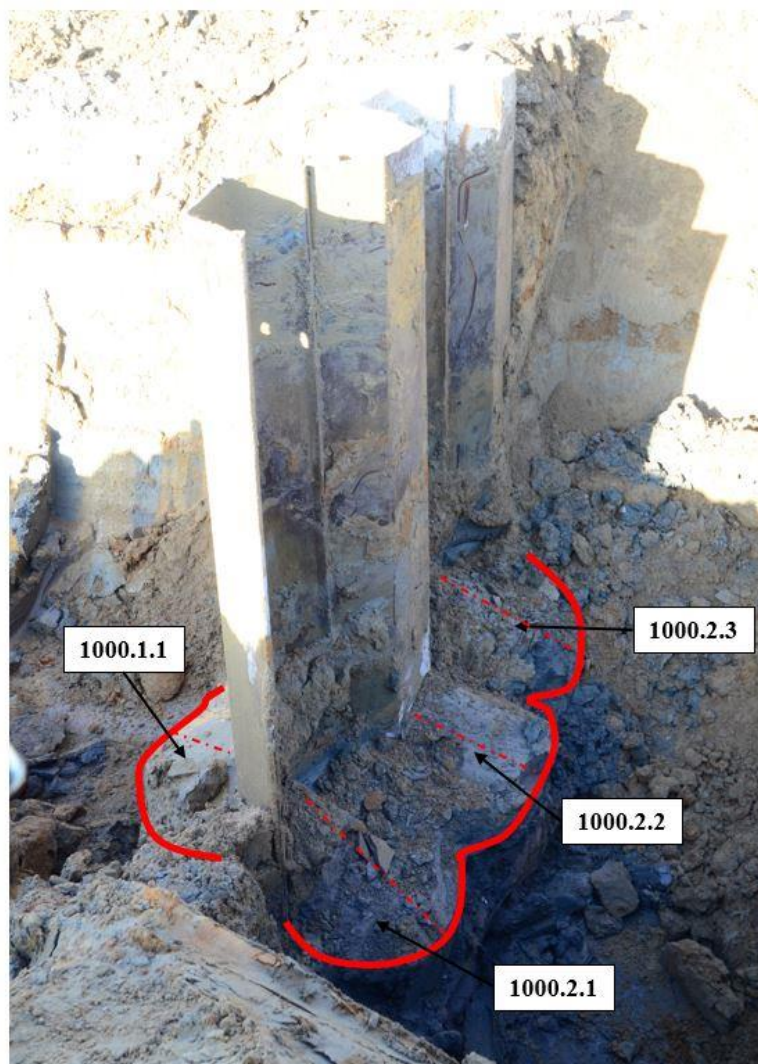


Figure 38 Photograph taken during the excavation of columns 1000.2.1-1000.2.3. Red lines illustrate the shape of the columns and the measurements gathered, taken from the center of the concave or the convex part of the sheet pile to the edge of the column.

Other important observations regarding the excavation are:

1. For the columns installed fresh-in-fresh, there were some difficulties to measure diameter, since the columns overlapped well, and thereby forming a continuous structure with no distinct boundaries. Therefore, only the measurement from the center of the sheet pile wall to the opposite end of the column could be measured. From there an average diameter could be estimated, taking into consideration the location of the center point of jet grouting.
2. For the columns installed fresh-in-fresh and made using the double fluid system, that is column 1700.1 and 1700.2, the diameter varied significantly. They obtained a more of an oval shape in the direction of the sheet pile wall, rather than a circular shape, as illustrated in Appendix II. Once again, the average diameters were used.
3. During the visual inspection, all test columns were determined to be stiff and consistent. Although, when walking on top of and physically examining the columns, it was, however, the general belief that the larger columns felt slightly more porous.
4. Despite the previous geological survey, all test columns turned out to be installed in clay, rather than in sand. This caused some issues to distinguish the hardened cement from the surrounding clay, as they both have a grey color.
5. The excavator was equipped with a too large bucket, resulting in two columns being damaged. The oversized bucket also caused difficulties to ensure sufficient removal of the soil above the columns grouted in the concave parts of the sheet pile wall. Consequently, the connection between the sheet pile surface and the 1.7 m columns was not fully visible and could not be assessed properly. The connection for the 1.0 m columns and the sheet wall were however adequate.
6. Finally, during the excavation of column 1700.3, a 10 cm layer of hardened cement, reaching as far as 5 m from the column, was discovered in a fissure between the filling material and the clay layer. See Appendix IV for a photograph.

6.2.2 Painted bars test

Figure 39 illustrates the painted rebars retrieved from test 1. As can be observed, most of the paint along the -0.1 m bar and the bar 0 m were scratched off by the jet. This implies that the design requirement to obtain a diameter of 1.7 m was fulfilled. For the bar installed at $+0.1$ m, the paint had only been removed for certain sections. This suggests at those depths a diameter of at least 1.9 m was obtained. However, for the sections where paint remained, a diameter of 1.9 m was not reached. Recognizing that the jet grouting started at a depth of -8 m and by measuring the sections of bare steel, it was possible to produce a theoretical profile of the column, as seen in Figure 40.

Also, the spoil return of all tests had a light brown color, indicating that the grout had replaced the sand well.

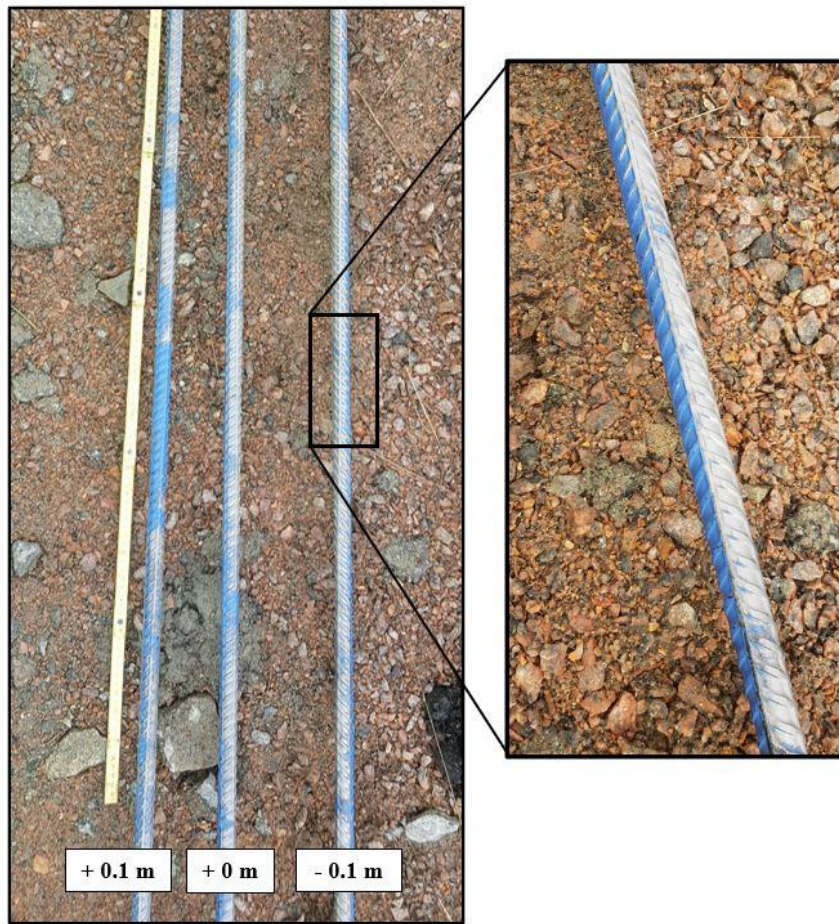


Figure 39 Photograph of the retrieved and washed rebar from test 1, including a close-up demonstrating where the jet has reached the bar.

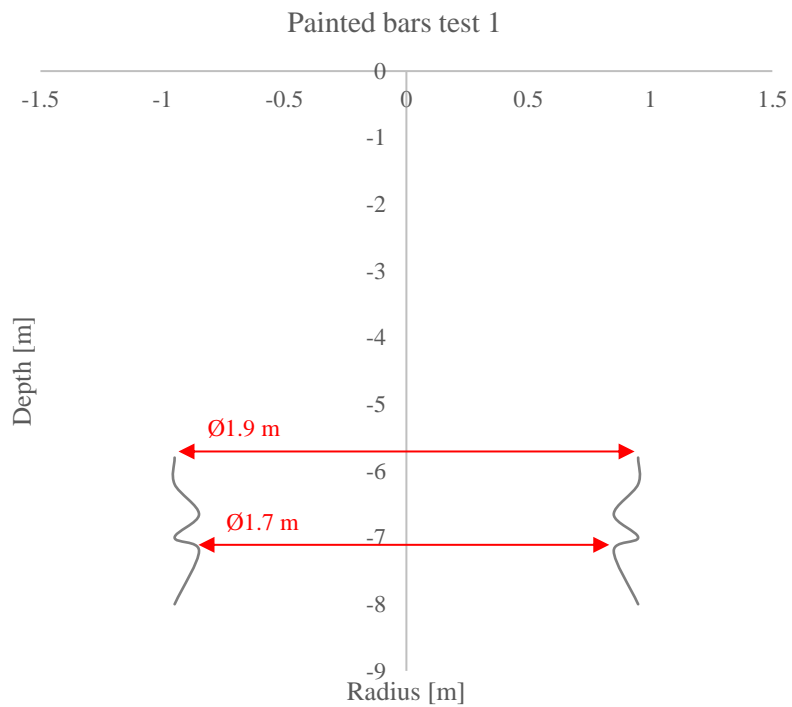


Figure 40 Graph illustrating the radius of test column 1 at different depths.

For test 2, where the aim was to achieve a 1.0 m diameter by using a jetting pressure of 400 bar, the test was considered as non-conclusive. The reason for this is given by the fact that the +0 m bar did not show any distinct signs of weathering, suggesting the jet stream only touched the bar. Moreover, the -0.1 m bar was unfortunately installed without allowing enough length remaining above the ground level. This resulted in the bar not being accessible for retrieval.

Due to the inconclusiveness of test 2, a third test was performed. This test still aimed for a diameter of 1.0 m, however, now applying a higher jetting pressure, a larger delivery, and a longer jetting time than in test 2. When recovering these bars, the -0.1 m and +0 m bar showed a more distinct sign of weathering, as steel was exposed along the bars' entire length. The +0.1 m bar was, on the other hand, to a large degree still painted. Nonetheless, it was concluded that the operational parameters in test 3 were enough to achieve the desired diameter of 1.0 m.

7 Discussion

This chapter has been divided into three sections. In Section 7.1 the results from the analysis of the prediction models are evaluated and discussed. Thereafter, in Section 7.2, the observations and the results obtained in the case study are reviewed and recommendations are given for future test programs. Lastly, in Section 7.3, the presented literature is discussed.

7.1 Theoretical prediction models

The most apparent finding from the analysis regarding the semi-theoretical prediction models is that the models generally overestimate the column diameter. This is problematic, as the models therefore predicted larger diameters than what was measured in the field. However, considering that these approaches are models, and thus only an attempt to describe the reality, a certain tolerance towards errors ought to be acceptable.

By studying Tables 11 and 12 and bearing this in mind, only the predicted values based on the method of Flora (2013) can be considered as acceptable. For this model, five out of eleven predictions underestimated the diameter. For the six overestimations, four of these are within a ± 20 percent error margin. It is debatable if this is a suitable margin or not, especially for the lower limit. Any overestimation in a sealing context would imply a possibility of untreated zones between adjacent columns and thereby increasing the risk of an inflow. However, as discussed in Section 4.4, this is the established error margin for the semi-theoretical prediction models. Only the most recent prediction methods, exemplified by the data mining approaches presented by Ochmański et al. (2015) and Tinoco et al. (2018), have demonstrated a lower error margin of about ± 15 percent.

For the two other prediction models, Wang et al. (2012) and Shen et al. (2013), larger deviations were obtained, implying that the models are inadequate. The predictions made using the method by Shen et al. (2013) are particularly poor; where almost all the predicted diameters are at least twice as large as the diameters measured in the field. The predictions according to the method by Wang et al. (2012) for test 1 is however near the suggested error margin of ± 20 percent.

The reason why the Asian models predict greater diameters can partly be explained by the assumptions made regarding the input parameters of which describes the characteristics of the soil. As summarized in Table 6 in Section 4.6, the models use different input parameters to describe the erosive action of the jet stream and the resistance of the soil. Due to the Asian models being developed by many of the same academics, similar input parameters are employed in these models. More specifically, they are dependent on the effective friction angle and the clay content of the soil. Furthermore, Shen et al. (2013) also consider the average particle size. In contrast, Flora et al. (2013) base the characteristics of the soil on data from CTP or STP measurements. Considering that no laboratory tests to determine the clay content were made, this value had to be assumed. The assumption of 15 percent (USDA, 2017) might therefore, in this case, be a great underestimation. This especially since the excavated columns turned out to be made in clay, instead of in the assumed sand layer. For example, if calculations had been based on the soil being a clay, assuming a clay content of 50

percent, the prediction according to Shen et al. (2013) would have been 1.24 m instead of 1.92 m for test 1. In Sweden, it is common practice to perform CTPs in the geological survey, and this was also the case for the Gothenburg Port Line. The reason that the predictions made using the method of Flora et al. (2013) approximated the diameter more accurately, can be derived to the fact that interpreted values from a CPT performed at the site were employed. A source of error is therefore the assumed value for the clay content, and consequently also the average particle size. Considering that the input values were assumed for the methods of Wang et al. (2012) and Shen et al. (2013), it cannot be concluded that the models are incomplete, only that the assumptions in this case did not correlate to the characteristics of the site.

Another interesting observation that can be made from Table 12 is that for all predictions, regardless of the model, the calculated predictions for test 2 are greatly incorrect. This is unexpected, considering that the predictions made for test 1, which also utilized a single fluid treatment system, are decent. The reason for this discrepancy is difficult to determine. By studying Table 6 which summarizes the model inputs and Table 9 over the chosen operational parameters in Section 5.3.2, a possible explanation is a potential fault during test 2, in combination with the use of two nozzles. As reported, the measured diameters for test 2 are much smaller than the intended design diameter of 1.0 m. If there was an oversight in the production of these columns, ultimately causing smaller diameters despite the chosen operational parameters, the $D_{\text{predicted}}/D_{\text{measured}}$ ratio would not be representative. More on this probable production error in test 2 is discussed in Section 7.2. Furthermore, the fact that this discrepancy is more predominant in the two Asian models, can likely be related to the fact that both Wang et al. (2012) and Shen et al. (2013) consider the number of nozzles as an input variable, in contrast to Flora et al. (2013). Using two nozzles instead of one increases the eroding capacity of the treatment and consequently the radius of influence. As the prediction model by Flora et al. (2013) does not consider this parameter, this model is not affected as much as the other two models if there were an issue in the production concerning the two nozzles.

Moreover, by comparing Figure 35 and Figure 36 an additional conclusion regarding the prediction models can be made. The cross-plots give the impression that the predictions for the double fluid system are more accurate in comparison to the predictions for the single fluid system. This is surprising, considering that previous research has found the errors to be larger for the double fluid system. The contradicting result may however be related to the few predictions that have been made. To be exact, for the single fluid system a total of 21 predictions were made, whereas only six predictions were made for the case of double fluid treatment. This finding must therefore be interpreted with caution. Nonetheless, all double fluid predictions made by Flora et al. (2013) underestimate the diameter, which is beneficial in the context of waterproofing. One downside though; if this model were to be used to determine the operational parameters, for a given soil and design diameter, these would be extremely conservative. As reported, a 30-50 percent larger diameter than necessary could likely be achieved, denoting a misuse in material and monetary funds.

A similar trend as for the semi-theoretical prediction models is observed for the predictions made by using the updated version of the manufacturer's model. As presented in Table 13, all predictions are overestimations; particularly for test 2, however, within the suggested error margin for test 1. Furthermore, from the cross-plot

given by Figure 37, it can be observed that the predictions using the revised version of the manufacturer's model provided a more accurate estimation than the methods of Wang et al. (2012) and Shen et al. (2013). In fact, the predictions are not far from those estimated using the method of Flora et al. (2013). This indicates that the manufacturer has a fair appreciation of the treatment system's performance and knowledge about the involved jetting mechanisms. Furthermore, both Flora et al. (2013) and the manufacturer's model employs the pressure of the grout as an input parameter. Flora et al. (2013) by using the injection pressure at the pump and assuming a 10 percent loss in the system, while the manufacturer's model utilizes the pressure at the nozzle. This can possibly explain why the predictions are more correct in contrast to the Asian models, which do not consider this parameter.

What also is noteworthy with this result, is that the revised manufacturer's model does not employ any inputs concerning the soil conditions at the site, but still provides adequate predictions. As mentioned repeatedly and similarly highlighted by the scholars who developed the semi-theoretical prediction models, the resistance of the soil is a crucial aspect to consider when describing the treatment performance. It could therefore be argued that these positive results should be accredited to the project's jet grouting consultant, Ludovico Strina, who used his expertise to professionally choose the operational parameters based on the conditions presented at the site. For example, Strina initially had one set of parameters in mind before the case study started, but after examining the sand, other parameters were chosen as it was more compact than he originally had thought. Moreover, it is to the authors' knowledge the first time this revised version of the method of the manufacturer's model has been assessed. The result may therefore be limited and should be interpreted with care.

7.2 Field trial

The two tests that were performed during the case study are both considered to be successful and valuable because both tests provided important knowledge and observations about the site and the equipment used. By excavating the columns, information regarding the uniformity of the individual columns as well as the merging of columns next to the sheet pile wall could be visually assessed. By performing the painted bars test, an understanding of the treatment effectiveness at greater depths could be acquired. It is the authors' belief that both tests are useful to perform during a jet grouting trial, as they combined provide the necessary information to perform an effective treatment. Furthermore, it is also recommended to install more test columns in order to improve the statistical reliability of the results.

Two column dimensions were assessed in both tests. This to evaluate the prospect of optimizing the design with regards to economic benefits and to gain knowledge to support future investments, considering that jet grouting is a new technology to the collaborating construction company. The tests disclosed the same result; that both diameters can be achieved, however, to obtain the larger diameter the double fluid system is required. At the Gothenburg Port Line project, the larger diameter would significantly reduce the number of columns needed. This would be advantageous because less drilling would result in shorter construction times, considering that most of the drilling must be made in the bedrock due to the length of the hammer. This could save the production money, despite an increased quantity of required cement. However, as observed during the excavation test, the double fluid system generated larger

volumes of spoil, which at low depths splashed up through the borehole. Considering that no harm is to be caused to the surrounding trees, the double fluid system might not be appropriate in these areas. Alternatively, practices to protect the trees and their sensitive root system, need to be considered. Furthermore, the risk of shadow effects can be greater with larger diameters, especially in soils with blocks such as till.

Another option to reduce the drilling time, if economically and technically possible, would be to use a shorter drill. To find equipment of which still can penetrate crystalline bedrock and at the same time facilitate the fluid strings might be difficult, considering that much of the jet grouting equipment originate from countries with soft bedrock. To develop a more practical drill together with a drilling or a mining manufacturer might be beneficial for the technology, as it could become more economical and competitive on the Nordic market.

Lastly, it was observed that continuous communication between the personnel is important to achieve satisfactory quality, as well as for safety reasons. This includes knowledge regarding the specific tasks and the operational parameters at each station. For example, the personnel at the mixing plant needs to employ a larger pressure and delivery to compensate for transportation losses to ensure that the correct value is employed by the driller. Furthermore, by locating the stations within sight of one another and utilizing Bluetooth technology or radio, swift measures can be taken if there is an obstacle or if any other change is observed.

7.2.1 Excavation

As summarized in Table 14, the excavation revealed that two out of three columns made in test 1 attained the design diameter of 1.0 m, whereas none of the four columns did in test 2. Due to that columns 1000.1.1-1000.1.1.3 were installed fresh-in-fresh and merged well, test 1 can be considered as successful.

The reason for the smaller diameters in test 2 can be derived from the fact that the columns were installed in clay and not in the sand, as intended when selecting the treatment zone and the operational parameters. This inaccuracy could however have been avoided, considering that the interpretation of borehole 4705, seen in Figure 28, illustrates a layer of clay at the depth of 2-4 m. There is a possibility that the supervisors who selected these depths as the treatment zone, might have interpreted tests from other boreholes in the area, of which instead suggested that this depth would comprise of sand. Furthermore, during the installation, it was observed that the spoil had a grey color indicating that the treatment indeed was made in clay. This shows how important it is to carefully analyze the results from the geological survey before performing a jet grouting trial, as well as to pay attention to the spoil.

The jet grouting in the excavation test was subsequently performed in a different soil than what is expected to be present later in the project. However, clays are more difficult to erode than sands. It can therefore be presumed that the columns would have obtained a larger diameter if they had been installed in sand. The fact that test 1 was a success despite being performed in clay, implies that those operational parameters can be used when the sealing is to be performed. The operational parameters used in test 2 can however not be recommended at this site.

It is noteworthy, that using two nozzles resulted in such a smaller diameter, in comparison to when using only one. The explanation to this might again be connected to the treatment being performed in clay, but also because of the modifications of the operational parameters; those being a lowered jetting time, lowered pressure, and a higher delivery. As described in Section 2.3.1, the primary interacting mechanism varies between soil types. In clay, cutting is the main mechanism, and therefore the number of rotations, consequently the time, is the most important parameter to break the adhesive forces. By lowering this variable, a smaller diameter can therefore be expected. In sands, erosion is the main interacting force and thus the pressure, but also delivery, are the most important parameters. If the jetting had been performed in sand, it is reasonable to believe that two nozzles and a higher delivery would have been an appropriate adjustment to still achieve the design diameter.

Another observation made when excavating the single fluid test columns was that the fresh-in-fresh method worked well, despite the use of the water-intensive hammer. The columns were merged into a unity, without any indications of the grout being “washed out”. Hence, the fresh-in-fresh method can be recommended, which is preferable considering the more straightforward installation.

For the columns made by using the double fluid system, that is column 1700.1-1700.3, all three turned out larger than expected. In fact, the measured diameters were between 50-80 percent larger than intended. Test 3 is therefore considered to be a success for the purpose of sealing. The columns did however obtain a somewhat oval shape along the sheet pile wall. The reason for this might be related to the additional air pressure “pushing” the grout along the wall. This could also be an explanation as to why the columns closest to the sheet pile obtained a larger diameter than the detached column. This “push-out effect” is advantageous for the case of sealing since it reduces the risk of the columns not merging. Considering the substantially greater diameters than intended, the energy and the efficiency of the double fluid system was underestimated. To compensate for this, a lower pressure, as well as a lower grout flow, should be used, especially as jetting in the project will be performed in sand and not in clay. Furthermore, the double fluid columns turned out to be slightly more porous than the single fluid columns. This is an expected consequence due to the large volumes of injected air when using a double fluid system. Still, they are in this case considered to have obtained a low enough permeability to create a water barrier. However, if this cut-off would have been intended as a permanent structure with the purpose of detaining water for a long time, this permeability would perhaps not be enough.

Another interesting finding when excavating the larger columns was the encounter of a thin layer of hardened cement that had been formed between the filling material and the clay, see Appendix IV. This layer had reached as far as 5 m from column 1700.3, where the grout originated, filling up the fissure between the two soil layers. This circumstance shows similarities to hydrofracking. During the desk study and the installment of columns, it is therefore important to be aware of low resistance layers, such as fissures, especially when using air.

During the excavation it was noticed that the excavator was equipped with a too large bucket. The authors believe that the insufficient removal closest to the sheet pile and the damaging of two columns could have been avoided if suitable equipment had been used. Furthermore, one column could not be found. It is likely that this column was

never, or very defectively, formed, considering that it was the first column to be installed using this new equipment and relatively inexperienced, in a jet grouting context, personnel. On the other hand, no distinct markers were used to recall the exact locations for the free-standing columns, so it is possible that it was lost. A more detailed excavation plan for jet grouting trials is therefore recommended in the future including a higher number of test columns and a construction surveyor taking coordinates directly after installment. An acceptable result could however be obtained with the equipment at hand, making the excavation method reasonable as no additional equipment had to be purchased to complete the test.

7.2.2 Painted bars test

The results obtained from the painted bars test confirm that the chosen operational parameters for double fluid jetting, that is test 1, is sufficient to achieve a diameter of at least 1.7 m, as illustrated in Figures 39 and 40. This is reassuring, considering that this test simulates the conditions of jet grouting being performed at a larger depth, but also treatment in sand. As the generated spoil during this test had more of a brown color, in comparison to the grey color during the excavation, it can be assumed that treatment took place in sand. This is also supported by studying Figure 40 where it can be observed that a smaller diameter at -7 m was obtained. This correlates to the interpretation made for borehole 4714, where a layer with clay at the same depth can be detected. As mentioned, clay does not erode as well as sand, and therefore a smaller diameter was obtained. Despite this layer, the design requirement was still fulfilled and there should not be any concern about a potential gap if these parameters were chosen.

In the test aiming for the 1.0 m diameter, that is test 2, the result was inconclusive. This was due to that the bar located at -0.1 m could not be retrieved. In this set-up, this bar was the most important one to recover, considering that the +0 m bar only showed signs of scratching. This test could therefore not confirm that the minimum diameter had been achieved and another test was consequently performed. For test 3, the pressure was increased to improve the jetting distance. This time all three bars could be recovered, and the conclusion could be made that the 1.0 m design diameter was obtained. The operational parameters used in this test are therefore recommended to be used during the actual jet grouting works.

The painted bars test is cheap and time-efficient, as rebars and paint easily can be purchased and prepared beforehand. Yet, there were a few complications during the execution. Firstly, one bar was installed too deep, leaving little of the bar left above ground for it to be recovered. The spoil consequently caused this bar to be buried, ultimately resulting in an inconclusive result and a need for an additional test considering that removal of all bars is essential. It is therefore crucial to ensure that at least 0.5 m of the bar is left above the ground surface. Secondly, the bars were installed by employing three different pre-drilling methods. This is an incitement for varying results, as the variation in drilling methods can lead to different disturbances of the surrounding soil. In this trial, some bars were installed using air, while others by using water. The lack of preparation before the installation of the bars is believed to be the reason for this, as not the same equipment or personnel were available for all three tests. To improve the reliability of this test, a more thorough trial plan is recommended, where the same drilling method is chosen and employed in order to disturb the soil as little as possible.

7.3 Literature and the jet grouting research community

Regarding the literature that has been presented in this thesis, much of the material about the technology and its applications are based on scientific findings and case studies. However, in the studied literature, the material found connected to the specific application of using jet grouting to seal the toe of sheet piles have been scarce. In other words, there is currently a deficit in information concerning specific design considerations and motivations for these. Therefore, some of the reasonings presented in this thesis are discussed in more detail below.

Firstly, in Section 3.2.1, the column length required to seal the toe of the sheet pile wall is examined. No information could be found in the literature of which specified how long the columns should be. More specifically, whether the jet grouting should begin in the bedrock or not, and how much of the column that should cover the toe of the sheet pile. The reason for this could be that jet grouting practices have been mostly developed by “trial and error” performed by specialist contractors, with no academic aspirations or the will to exchange information. For the two found Swedish projects, both did however specify that drilling into the bedrock is required, whereas for the case study project studied in this thesis, no requirements into the bedrock have been specified. The reason for this is unknown, however it can be derived from the quality of the rock. Thus, the authors have identified a gap in the field which should be studied further to provide supplementary material to optimize the design when sealing sheet pile walls.

Secondly, in Table 2 in Section 3.3.1 the coefficient of variation for column diameters is presented. Statistically is the variation much larger in gravels than in clays. For instance, the diameter can vary with 5-25 cm for gravels, 2-10 cm for sands, but only 2-5 cm for clays. In the same section, it is also suggested by Pan et al. (2019) and Strina (2020) that it is common practice to select the minimum overlap to be 20-30 cm. Hence, the safety margin is larger in fine-grained soils than in granular soils. Considering that the variance is larger for sands and gravels, it can be questioned if it is reasonable to employ this kind of “rule-of-thumb” approach. To exemplify; if the diameter for two adjacent columns in a clay turns out 3.5 cm smaller, the minimum overlap would be reduced to 14 cm instead of 20 cm. Similarly, in a sand the diameter would be reduced with 6 cm making the remaining overlap to be only 8 cm. Likewise, in a gravel, a gap of 10 cm would be formed. This generic interval of 20-30 cm has probably been acquired from professionals in the industry and has been proven to be sufficient in most cases. If this interval is based on overlapping with the purpose to seal or to increase the mechanical properties is unknown. Nonetheless, to optimize future designs and to evenly distribute the risk, it might be of interest to investigate if intervals for the minimum overlap could be specified for the soil type rather than being a generic value. This would be a suitable addition to the material presented, considering that this thesis discusses the sealing of sheet pile walls taking place in granular soils.

Bearing in mind the limitation of studying excavations utilizing steel sheet piles according to Swedish practices, it is also relevant to reflect on the installation sequence of the rock dowels. As the rock dowel is installed on the excavated side of the sheet pile, it can be installed either prior to or after the jet grouting works. By installing it before the jet grouting, there is no risk that the drilling would cause any movements or other disturbances to the sheet pile, which potentially could compromise the sealing capability of the cut-off. Nonetheless, when drilling the dowel hole there is a risk that the overlying granular material can fall into it. This is a known problem which is particularly troublesome when sand or gravelly till overlies the bedrock. If the jet grouting on the other hand was performed before the dowel installation, some of the material surrounding the borehole would instead be included in the grouted structure. The jet grouting could subsequently be used to decrease the risk of blockages to the dowel borehole.

Another topic presented in the literature, that should be considered with reservations, is Section 2.5 regarding the environmental impacts of jet grouting practices. Even though Yoshida (2012) provides important insights on the topic regarding CO₂ emissions, the results presented in the article are open for debate. This mainly because the author fails to disclose which years the statistics are considered and the number of projects that were included. Criticism can also be made to the data commentary, as neither labels nor categories are comprehensively defined, resulting in uncertainties regarding what the diagrams truly displays. Due to the lack of transparency, a true understanding of the most prominent factors for adverse effects on the environment cannot be defined. To develop an improved comprehension of the environmental impacts, additional studies are therefore encouraged. It would for instance be interesting to perform a life cycle assessment to identify which areas of the technology that can be improved further, whether it is the treatment of the spoil or the use of substitutes to cement. What also needs to be considered in the assessment is the intended lifespan of the constructed element, if it is acting as a permanent or temporary structure. By constructing a massive cut-off wall in a project that extends for vast distances, it can be debatable if this is a sustainable solution if the structure only is temporary.

Lastly, and perhaps something the reader of this thesis might already have noticed, is that the academic community within the field of jet grouting is rather limited. When using the literary databases' statistical tools, it is evident that most of the published documents are written by a handful of writers. Yet, most authors have published around ten papers each, suggesting a devotion to the field and years of professional experience. However, considering that two distinct research groups can be identified, one based in Europe consisting of mainly Italian academics and another team in China, the conducted research can be prone to bias. Scientists are generally encouraged to publish positive results to gain citations and status, but also continuous funding (Matosin et al., 2014). It can be argued though, that these academics to some degree is aware of the issue. For example, Croce et al. (2014) writes in their book that “[...] *publications on jet grouting tend to concentrate on the newest innovations and successful applications of the technique, being rarely focused on highlighting and understanding defective behavior or on developing effective design rules*”. Moreover, an extensive study performed by Wu et al. (2019) found that large team sizes of researchers tend to focus on existing and popular beliefs, whereas small size teams lean towards new prospects and improved understandings. Consequently, a balance of small-sized and larger research groups is required, to adapt existing techniques but also to promote research to new frontiers.

8 Conclusion and recommendations

The overall purpose of this thesis was to gain an in-depth knowledge about jet grouting and how the technology can be used to prevent groundwater from entering a sheet-piled excavation. This was achieved by conducting a literature review and by performing a case study.

In the literature review, jet grouting was described as a soil improvement technique because the practice enhances the strength of the treated soil and reduces the permeability. The procedure entails drilling to a pre-determined depth, followed by an injection of a cementing agent by a high-velocity jet. This results in a soilcrete column being formed. For the case of sheet-piled excavations, triangular gaps are often formed between the toe of the sheet pile and the sloping bedrock, which allows seepage to enter the excavation. To prevent this inflow of groundwater, jet grouting can be used as a sealant by merging individual columns into a so-called cut-off structure. These often comprises of one row of overlapping columns, with a length that at least covers the gap and some of the sheet pile above the toe. However, if the quality of the bedrock is considered as poor, treatment into the rock might also be necessary. The total performance of this water barrier is connected to the continuity and the uniformity of the structure, which in turn is dependent on the individual columns' geometry and position. More specifically, it is crucial to attain the design diameter and to follow the intended inclination, otherwise untreated zones may arise. A suitable design should therefore consider these deficiencies by allowing enough overlap but also recognizing the risk of shadow effects.

Several methods to verify the column diameter of the installed column exist and have been presented in this thesis. The methods of excavating test columns and the painted bars test have been identified as reliable, straightforward, and relatively affordable. These methods were employed in the case study to verify the accuracy of three semi-theoretical prediction models and one commercial prototype model for column diameters.

In the case study, it was disclosed that both verification methods provide essential information in order to achieve an effective treatment. Excavation of the test columns makes it possible for a visual inspection, thereby allowing an assessment of the continuity of the structure and the connection to the sheet pile. The painted bars test, on the other hand, confirms if the design diameter can be achieved at a greater depth. Likewise, by studying the results from both tests, the sought diameters of 1.0 m and 1.7 m, for the single- and double fluid system respectively, can be achieved at the site with carefully chosen input parameters. Hence are both tests recommended to be used in future trials. Excavation of columns provides the most valuable information, whereas the painted bars is a useful complementary method considering that excavation is limited to certain depths. It is however advised to install more columns to improve the statistical reliability of the results.

A problem that occurred during the field trial was that the excavated columns were installed in clay and not in sand as intended. This demonstrates the importance of carefully analyzing the findings in the geological survey before performing a jet grouting trial, but also to pay attention to the generated spoil. Other insights gained from this case study that may be of assistance when planning future test programs are:

- Considering that one column was not found during the excavation, it is advised to take note of the column's location directly after installment.
- As two columns were damaged during excavation and since the soil closest to the sheet pile was not completely removed, it is recommended to have a selection of buckets and shovels available.
- For the painted bars test it is essential to leave at least 0.5 m of the bars above the ground surface. This to ensure that the bars can be retrieved.
- The same pre-drilling method should employ when installing the bars. A variety of methods can cause different kinds of disturbances to the immediate soil and therefore compromising the reliability of the results.
- The jet grouting personnel must regularly discuss the practice and the employed parameters. This to ensure the quality of the work. It is also advantageous to set up the equipment in such a way that visual contact can be established.
- Lastly, a thorough strategy prior to the trial is essential to ensure that the test program provides the necessary linkage between the design and the execution. To be a success, the goal of the trial should clearly be defined and different scenarios of which refine the procedure that is to be implemented should be specified. Furthermore, the strategy should include a distinct excavation plan, in order to not jeopardize the result or the safety precautions. It is also valuable to ensure that the necessary drilling equipment and personnel are available to make the trial time effective.

In this thesis, the acquired measurements from the case study were also used to verify the accuracy of the studied prediction models. It was found that most of the calculated predictions did not correlate to the measured column diameter obtained in the trial. In fact, most of the predicted values were larger than the measured, indicating that the models overestimate the column diameter. The predictions made using the method of Shen et al. (2013) and Wang et al. (2012) were particularly poor. This implies that these two models are unsuitable for sealing purposes as overlapping of columns is crucial. These predictions were however made by assuming several of the soil parameters, whereas when employing the method by Flora et al. (2013) CPT data from the site was used. Hence, it cannot be concluded that the Asian models are incomplete, only that the assumptions made in this thesis did not correlate to the specific characteristics at the site. Thus, it is advised to use a model that employs input values that normally are obtained in the geological survey in the considered region. Furthermore, for the commercial prototype model, the predictions were similar to the calculated values according to Flora et al. (2013). This is noteworthy as the manufacturer's model does not employ any inputs relating to the soil conditions at the site, in contrast to Flora et al. (2013). As a result, this study has shown that the method of Flora et al. (2013) is the most accurate of the studied models for the conditions present at the Gothenburg Port Line.

Owing to the relatively limited number of trial columns made and the variance in the result, but also the fact that the trial was performed in clay, it is not recommended to use the prediction models to determine the operational parameters that are to be used to achieve a certain design diameter. The models can however offer valuable insight by indicating an appropriate parameter interval, but it is vital to perform a jet grouting trial at the site prior to execution. This as the trial might reveal that the proposed settings can result in an insufficient soil treatment. Moreover, a natural progression to this thesis would be to continue to gather data when performing other trials in similar and other

geological environments. This to further evaluate the accuracy of the models, especially the methods of Flora et al. (2013) and the revised model of the manufacturer. Even though this thesis provides a broad description of how jet grouting can be utilized to prevent groundwater intrusion, further research is mandated to establish more precise design guidelines for cut-offs used to seal to toe of sheet piles. A suggested research topic is therefore to assess the required column length. A reasonable approach would be to investigate this by reviewing the specified lengths in existing projects and to find the motivation for these lengths by conducting interviews with designers or by performing case studies. If trials are made, it would also be interesting to see if the working sequences can be optimized. For example, if the rock dowel should be installed prior to or after the jet grouting works. Another topic to be studied is the overlapping of columns, that is if the minimum overlap can be adapted to the specific soil types rather than be specified as a generic value. This would require considerable amounts of data gathering and analysis. Furthermore, there is also a need to study the environmental impacts of jet grouting more thoroughly.

As a final note, due to the time constraints of this thesis, the sealing of the project's excavations could not be assessed. Yet, due to the successful trial, the operational parameters to attain the sought design diameter could be determined and employed in the project. To this date, the jet grouting has, so far, been performed without any significant difficulties. It remains to see whether there will be reports of groundwater inflows into the jet grouted excavations and consequently if the groundwater level will be affected or not.

References

- Andréasson, P.-G. (2015). *Geobiosfären - en introduktion* (2nd ed.). Studentlitteratur AB.
- ArcelorMittal. (2018). *Rock Bolts: Horizontal toe support for steel sheet piles on bedrock*.
- Arroyo, M., Gens, A., Croce, P., & Modoni, G. (2012). Design of jet-grouting for tunnel waterproofing. *Geotechnical Aspects of Underground Construction in Soft Ground - Proceedings of the 7th International Symposium on Geotechnical Aspects of Underground Construction in Soft Ground, August 2014*, 181–188. <https://doi.org/10.1201/b12748-25>
- Bearce, R. G., Mooney, M. A., & Kessouri, P. (2015). Estimation of Jet Grout Column Geometry using a DC Electrical Resistivity Push Probe. *International Symposium Non-Destructive Testing in Civil Engineering (NDT-CE)*.
- Bellato, D., Schorr, J., & Spagnoli, G. (2018). Mathematical analysis of shadow effect in jet grouting. *Journal of Geotechnical and Geoenvironmental Engineering*, 144(12). [https://doi.org/10.1061/\(ASCE\)GT.1943-5606.0001975](https://doi.org/10.1061/(ASCE)GT.1943-5606.0001975)
- Brill, G. T., Burke, G. K., & Ringen, A. R. (2003). A Ten-Year Perspective of Jet Grouting: Advancements in Applications and Technology. *Third International Conference on Grouting and Ground Treatment*, 218–235. <https://doi.org/10.1061/40663%282003%29101>
- Broere, W. (2016). Urban underground space: Solving the problems of today's cities. *Tunnelling and Underground Space Technology*, 55, 245–248. <https://doi.org/10.1016/j.tust.2015.11.012>
- Burke, G. K. (2004). Jet grouting systems: advantages and disadvantages. *GeoSupport Conference*, 1–12. <https://doi.org/10.1061/40713%282004%2975>
- Burke, G. K. (2012). The State of Practice of Jet Grouting. *Proceedings of the Fourth International Conference on Grouting and Deep Mixing*, 74–88. <https://doi.org/10.1061/9780784412350.0003>
- Carlsson, L., & Gustafson, G. (1997). *Provpumpning som geologisk undersökningsmetodik* (2nd ed.). Chalmers University of Technology.
- Cheng, S.-H., Liao, H. J., Yamazaki, J., Wong, R. K. N., & Iwakubo, T. (2019). Alignment of vertical and inclined jet grout columns for waterproofing. *Geotechnical Testing Journal*, 43(2). <https://doi.org/10.1520/GTJ20180324>
- Comodromos, E. M., Papadopoulou, M. C., & Georgiadis, K. (2018). Design procedure for the modelling of jet-grout column slabs supporting deep excavations. *Computers and Geotechnics*, 100(April), 110–120. <https://doi.org/10.1016/j.compgeo.2018.04.008>
- Croce, P., Flora, A., & Modoni, G. (2014). *Jet Grouting Technology, Design and Control*. CRC Press.
- Croce, P., & Modoni, G. (2007). Design of jet-grouting cut-offs. *Ground Improvement*, 11(1), 11–19. <https://doi.org/10.1680/grim.2007.11.1.11>
- Eramo, N., Modoni, G., & Arroyo Alvarez De Toledo, M. (2012). Design control and monitoring of a jet grouted excavation bottom plug. *Geotechnical Aspects of Underground Construction in Soft Ground - Proceedings of the 7th International Symposium on Geotechnical Aspects of Underground Construction in Soft Ground, August 2014*, 611–618. <https://doi.org/10.1201/b12748-81>
- Ergun, M. (2008). Deep Excavations. *Electronic Journal of Geotechnical Engineering*, 13, 1–34.
- Flora, A., Modoni, G., Lirer, S., & Croce, P. (2013). The diameter of single, double and triple fluid jet grouting columns: Prediction method and field trial results. *Geotechnique*, 63(11), 934–945. <https://doi.org/10.1680/geot.12.P.062>
- Geological Survey of Sweden. (n.d.). *Morän – spår av inlandsisen*. Retrieved April 15, 2020, from <https://www.sgu.se/om-geologi/jord/fran-istid-till-nutid/inlandsisen/moran-spar-av-inlandsisen/>
- Geological Survey of Sweden. (2020). *Jordarter 1:25000-1:100000*. <https://apps.sgu.se/kartvisare/kartvisare-jordarter-25-100.html>
- GI-ASCE. (2009). *Jet Grouting Guideline*.

- Holmøy, K. H., Langford, J., Hansen, T. F., Holte, K. G., & Karlsrud, K. (2019). Challenges with water in underground projects in urban areas. Is it possible to avoid settlement damages? *Fjellsprenningsdagen, Bergmekanikkdagen Og Geoteknikkdagen*.
- Kaliampakos, D. (2016). Underground Development: A Springboard to Make City life Better in the 21st Century. *Procedia Engineering*, 165, 205–213.
<https://doi.org/10.1016/j.proeng.2016.11.792>
- Kimpritis, T., Standing, J. ., & Thurner, R. (2018). Estimating column diameters in jet grouting processes. *Proceedings of the Institution of Civil Engineers - Ground Improvement*, 3(171), 148–158. <https://doi.org/10.1680/jgrim.17.00001>
- Langford, J., Baardvik, G., & Karlsrud, K. (2016). Pore pressure reduction and settlements induced by deep supported excavations in soft clay. *Proceedings of the 17th Nordic Geotechnical Meeting*, 993–1002.
- Langhorst, O. S., Schat, B. J., de Wit, J. C. W. M., Bogaards, P. J., Essler, R. D., Maertens, J., Obladen, B. K. J., Bosma, C. F., Sleuwaegen, J. J., & Dekker, H. (2007). Design and validation of jet grouting for the Amsterdam Central Station. *14th European Conference on Soil Mechanics and Geotechnical Engineering*, 1299–1305.
- Larson, S. Å., & Tullborg, E.-L. (2015). *Sveriges berggrund: en geologisk skapelseberättelse* (1st ed.). Terralogica.
- Leoni, F. M., & Pianezze, G. (2017). Elliptical Jet Grouting: An Innovative, Viable, and Effective Solution: The Example of Bottom Plugs for the SELA Projects in New Orleans, LA. *Grouting 2017*, 11–20. <https://doi.org/10.1061/9780784480809.002>
- Lindström, M., Lundqvist, J., & Lundqvist, T. (2000). *Sveriges geologi från urtid till nutid* (2nd ed.). Studentlitteratur AB.
- Lu, Y., & Tan, Y. (2019). Overview of Typical Excavation Failures in China. *Eighth International Conference on Case Histories in Geotechnical Engineering*, 315–332.
<https://doi.org/10.1061/9780784482155.033>
- Matosin, N., Frank, E., Engel, M., Lum, J. S., & Newell, K. A. (2014). Negativity towards negative results: a discussion of the disconnect between scientific worth and scientific culture. *Disease Models & Mechanisms*, 7, 171–173.
<https://doi.org/10.1242/dmm.015123>
- Meinhard, K., Adam, D., & Lackner, R. (2010). Temperature measurements to determine the diameter of jet-grouted columns. *Proceedings of the International Conference on Geotechnical Challenges in Urban Regeneration*.
- Modoni, G., Flora, A., Lirer, S., Ochmański, M., & Croce, P. (2016). Design of jet grouted excavation bottom plugs. *Journal of Geotechnical and Geoenvironmental Engineering*, 142(7). [https://doi.org/10.1061/\(ASCE\)GT.1943-5606.0001436](https://doi.org/10.1061/(ASCE)GT.1943-5606.0001436)
- Nakanishi, W. (1974). *Method for forming a underground wall comprising a plurality of columns in the earth and soil formation*.
- Ni, J. C., & Cheng, W. C. (2014). Quality control of double fluid jet grouting below groundwater table: Case history. *Soils and Foundations*, 54(6), 1039–1053.
<https://doi.org/10.1016/j.sandf.2014.11.001>
- Niederleithinger, E., Galindo Guerreros, J. C., Mackens, S., & Fechner, T. (2015). Quality Assurance of Jet Grout Columns with Borehole Seismic Measurements. *21st European Meeting of Environmental and Engineering Geophysics*, 1–5.
<https://doi.org/10.3997/2214-4609.201413679>
- Niermann, M. J., Henevein, D. R., & Worst, S. L. (2017). Jet Grouting for Water Cutoff and Excavation Support. *Grouting 2017*, 124–134.
<https://doi.org/10.1061/9780784480809.013>
- Ochmański, M., Modoni, G., & Bzówka, J. (2015). Prediction of the diameter of jet grouting columns with artificial neural networks. *Soils and Foundations*, 55(2), 425–436.
<https://doi.org/10.1016/j.sandf.2015.02.016>
- Pan, Y., Liu, Y., Hu, J., Sun, M., & Wang, W. (2017). Probabilistic investigations on the watertightness of jetgrouted ground considering geometric imperfections in diameter and position. *Canadian Geotechnical Journal*, 54(10), 1447–1459.
<https://doi.org/10.1139/cgj-2016-0671>

- Pan, Y., Yib, J., Gohc, S.-H., Hud, J., Wange, W., & Liuf, Y. (2019). A three-dimensional algorithm for estimating water-tightness of cement-treated ground with geometric imperfections. *Computers and Geotechnics*, 115, 1–18.
- Port of Gothenburg. (2019). *Railport Scandinavia* (Issue 05, pp. 1–20). Port of Gothenburg.
- Puller, M. (2003). *Deep excavations: A practical manual* (2nd ed.). Thomas Telford.
- Ribeiro, D., & Cardoso, R. (2017). A review on models for the prediction of the diameter of jet grouting columns. *European Journal of Environmental and Civil Engineering*, 21(6), 641–669. <https://doi.org/10.1080/19648189.2016.1144538>
- Schoning, K. (2016). *Saltvattenavsatta leror i Sverige med potential för att bilda kvicklera*.
- Shen, S. L., Wang, Z. F., Yang, J., & Ho, C. E. (2013). Generalized approach for prediction of jet grout column diameter. *Journal of Geotechnical and Geoenvironmental Engineering*, 139(12), 2060–2069. [https://doi.org/10.1061/\(ASCE\)GT.1943-5606.0000932](https://doi.org/10.1061/(ASCE)GT.1943-5606.0000932)
- Shibazaki, M. (2003). State of Practice of Jet Grouting. *Third International Conference on Grouting and Ground Treatment*, 198–217. <https://doi.org/10.1061/40663%282003%297>
- Shirlaw, J. ., Page, R., Teoh, E. ., & Hsi, J. (2005). The interface friction between piles and Jet grout Slabs. *Underground Singapore, December 2005*, 118–125.
- Skanska. (2019). *Skanska to expand Harbor line at Hisingen, Gothenburg, Sweden, for about SEK 1.3 billion*. <https://group.skanska.com/media/237285/Skanska-to-expand-Harbor-line-at-Hisingen%2C-Gothenburg%2C-Sweden%2C-for-about-SEK-1.3-billion>
- Skanska. (2020a). *Blueprint of cut-off design utilizing columns with a diameter of (a) 1.0 m and (b) 1.7 m*.
- Skanska. (2020b). *Map demonstrating the different production zones for phase Eriksberg-Pölsebo*.
- Swedish Institute for Standards. (1999). *SS-EN 12063:1999*. [https://www.sis-se.proxy.lib.chalmers.se/produkter/byggstandardpaket/byggstandard-utforande-och-kontroll/mark-och-grundlaggningsarbeten/ssen12063/](https://www.sis.se.proxy.lib.chalmers.se/produkter/byggstandardpaket/byggstandard-utforande-och-kontroll/mark-och-grundlaggningsarbeten/ssen12063/)
- Swedish Institute for Standards. (2000). *SS-EN 12715:2000*. <https://www.sis.se/produkter/byggstandardpaket/byggstandard-utforande-och-kontroll/mark-och-grundlaggningsarbeten/ssen12715/>
- Swedish Institute for Standards. (2012). *SS-EN ISO 22282-2:2012*. <https://www.sis.se/produkter/miljo-och-halsoskydd-sakerhet/jordkvalitet-pedologi/hydrologiska-egenskaper-hos-jord/sseniso2228222012/>
- Swedish Institute for Standards. (2014). *SS-EN 16228-6:2014*. <https://www.sis.se/produkter/maskinsakerhet-3f1691ec/anlaggningsmaskiner/ssen1622862014/>
- Swedish Institute for Standards. (2018). *SS-EN 12716:2018*. <https://www.sis.se/produkter/byggstandardpaket/byggstandard-utforande-och-kontroll/mark-och-grundlaggningsarbeten/ssen12716/>
- Swedish National Board of Housing. (2017). *Urban density done right - Ideas on densification of cities and other communities*.
- Swedish National Land Survey. (2020). *Kartsök: Ortofoto 1960*. <https://kso.etjanster.lantmateriet.se/>
- Miljöbalk 1998:808, chapter 11, (1998).
- Miljöbalk 1998:808, chapter 29, (1998).
- Swedish Transport Administration. (2015). *Teknisk handling geoteknik: Hamnbanan Göteborg, dubbelspår Pölsebo-Eriksberg*.
- Swedish Transport Administration. (2016). *Miljökonsekvensbeskrivning: Hamnbanan Göteborg, dubbelspår Eriksberg-Pölsebo*.
- Swedish Transport Administration. (2018). *Markteknisk undersökningsrapport (MUR) Geoteknik*.
- Swedish Transportation Administration. (2016). *Bilaga 1: Trafikverket Ansökan om vattenverksamhet Hamnbanan, Eriksberg - Pölsebo*. [Image]. <https://www.trafikverket.se/contentassets/704ec2d97a0344b1ad5ab7ee2020035a/ovriga->

- dokument-vattenverksamhet/bilaga_1_oversiktskarta-pdf-fil-3-mb.pdf
- Swedish Transportation Agency. (2010). *E4/E20 Tomtebodavägen-Haga södra: Teknisk beskrivning*.
- Swedish Transportation Agency. (2017). *E4 Förbifart Stockholm: Teknisk beskrivning*.
- Tanaka, T., & Yokoyama, T. (2006). Effects of jet grouting under sheet piles on seepage failure stability of soil. *Geotechnical Aspects of Underground Construction in Soft Ground - Proceedings of the 5th International Conference of TC28 of the ISSMGE*, 923–929.
- Telling, R. M. (1975). *The Effectiveness of Cut-off Walls beneath Water Retaining Structures*.
- Tinoco, J., Gomes Correia, A., & Cortez, P. (2018). Jet grouting column diameter prediction based on a data-driven approach. *European Journal of Environmental and Civil Engineering*, 22(3), 338–358. <https://doi.org/10.1080/19648189.2016.1194329>
- USACE. (2017). *Engineering and Design: Grouting Technology*.
- USBR. (2009). *Procedure for Determining Permeability of Rock Core - Flow Pump Permeability Test: Vol. C*.
- USDA. (2017). *Examination and Description of Soil Profiles* (Soil Survey Division Staff (ed.); pp. 122–131). United States Department of Agriculture.
- Wang, Z.-F., Shen, S.-L., & Yang, J. (2012). Estimation of the Diameter of Jet-Grouted Column Based on Turbulent Kinematic Flow Theory. *Proceedings of the Fourth International Conference on Grouting and Deep Mixing, 2044–2051*. <https://doi.org/10.1061/9780784412350.0179>
- World Economic Forum. (2015). *Top Ten Urban Innovations*.
- Wu, L., Wang, D., & Evans, J. A. (2019). Large teams develop and small teams disrupt science and technology. *Nature*, 566(7744), 378–382. <https://doi.org/10.1038/s41586-019-0941-9>
- Yoshida, H. (2012). Recent Developments in Jet Grouting. In L. F. Johnsen (Ed.), *Fourth International Conference on Grouting and Deep Mixing* (pp. 1548–1561). <https://doi.org/10.1061/9780784412350.0130>

Appendices

Appendix I

Below is the data that were used to perform the borehole interpretation regarding the soil layers and their characteristics presented (Swedish Transport Administration, 2018). Borehole 4705 corresponds to the location of the excavation and 4714 for the painted bars test.

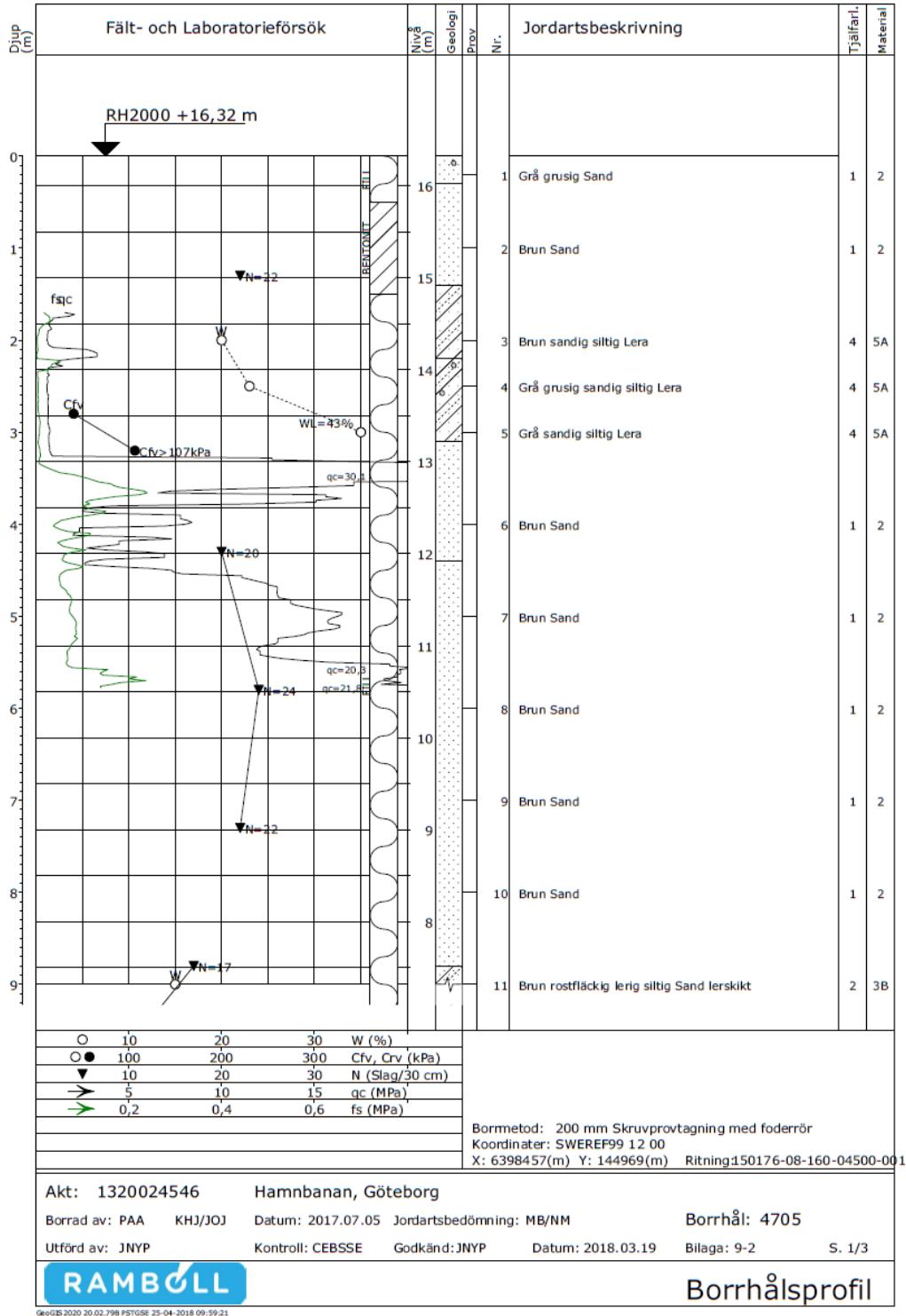


Figure I.1 Copy of the borehole profile for borehole 4705 at the first 11 m.

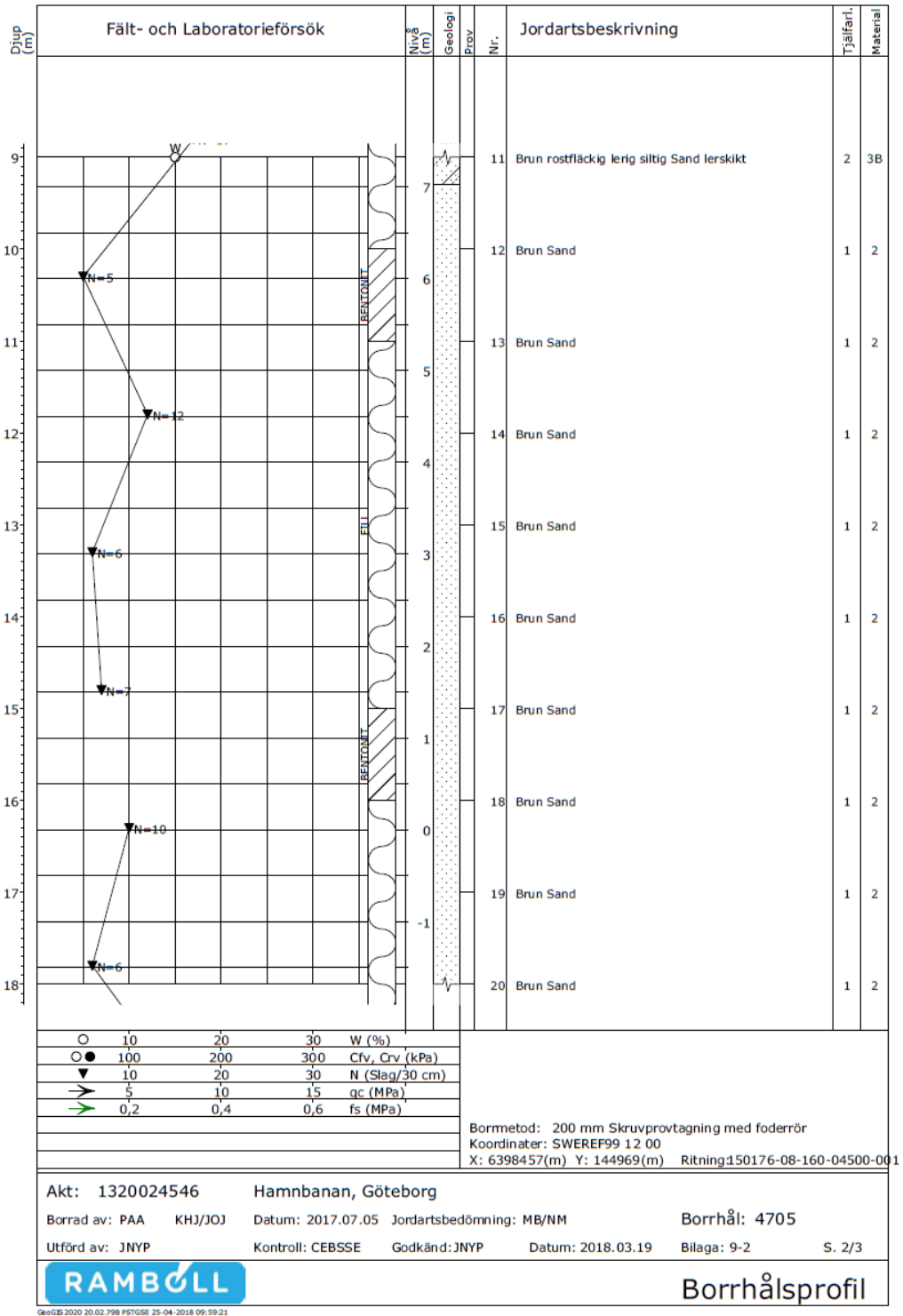


Figure I.2 Copy of the borehole profile for borehole 4705 at the depths 11-20 m.

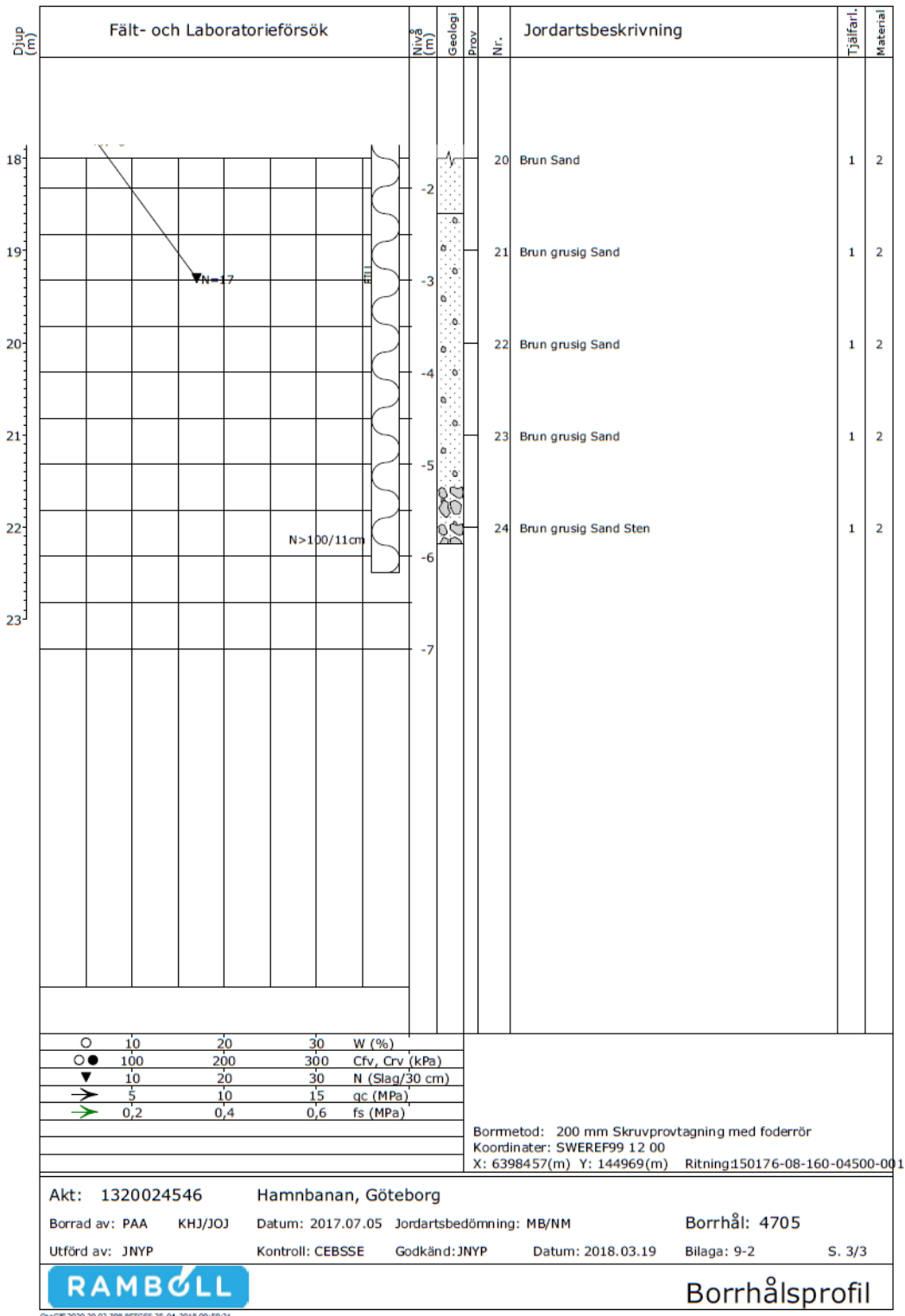


Figure I.3 Copy of the borehole profile for borehole 4705 at the depth 20-24 m.

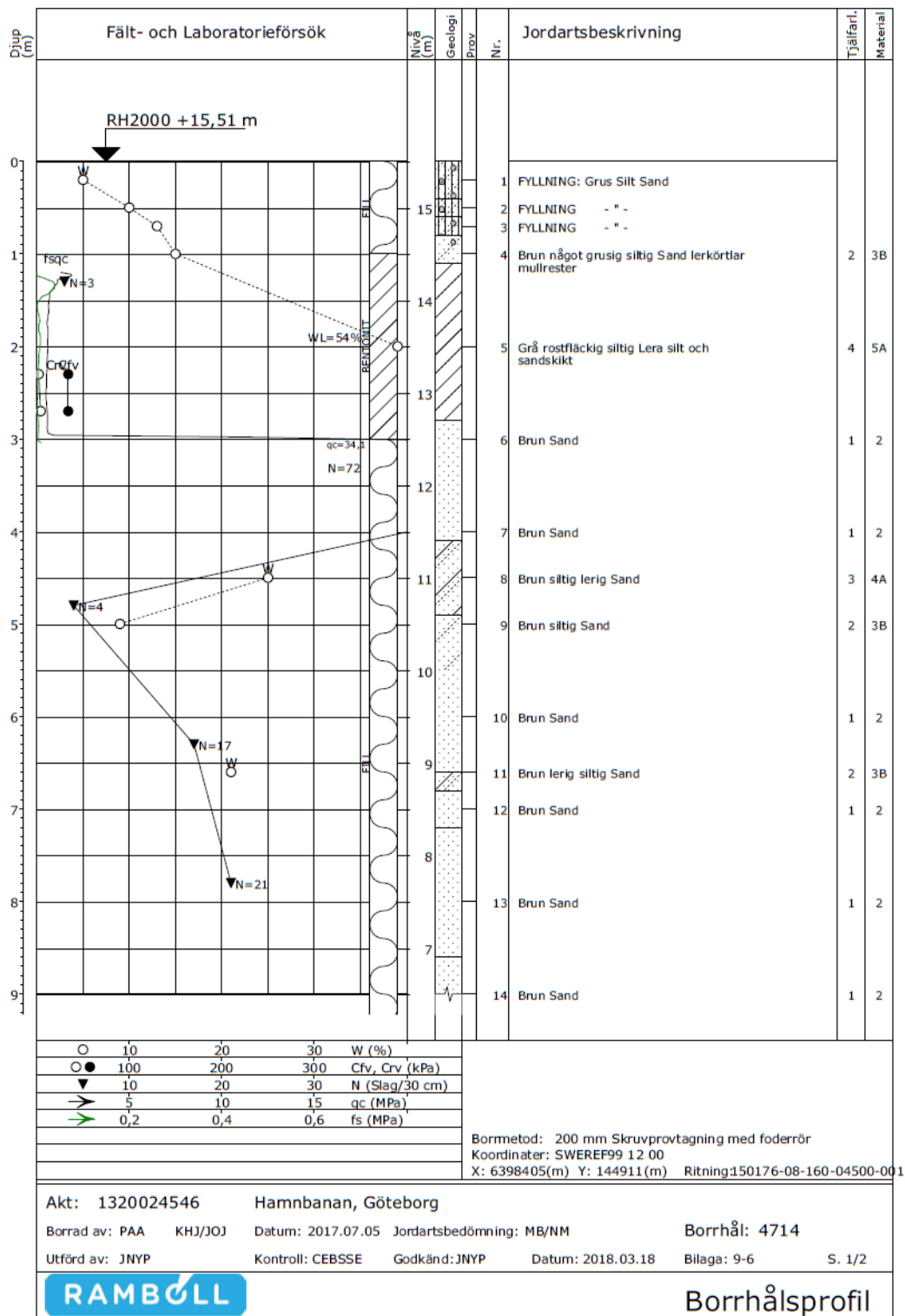


Figure I.4 Copy of the borehole profile for borehole 4705 for the first 14 m.

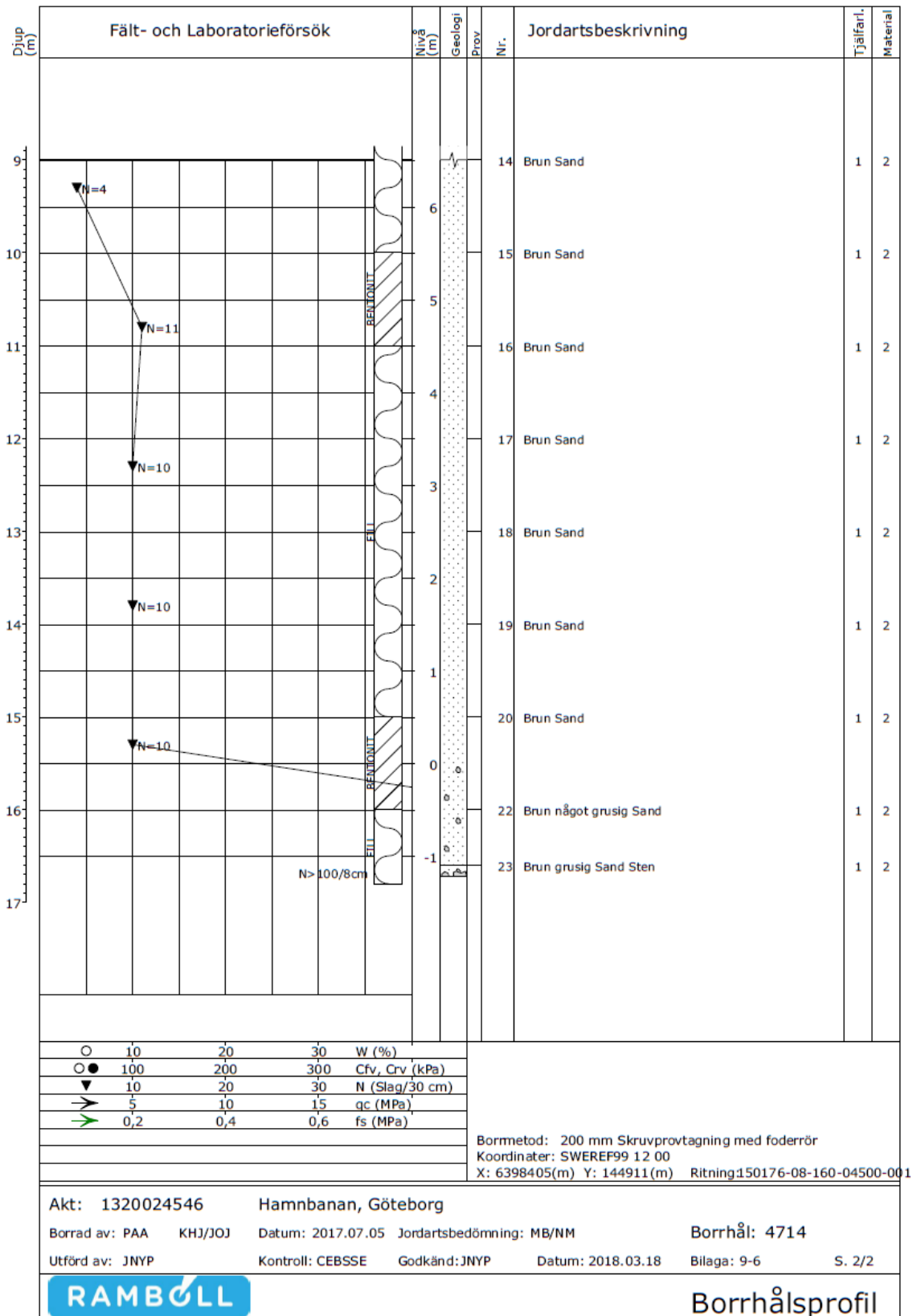


Figure I.5 Copy of the borehole profile for borehole 4705 at the depths 14-23 m.

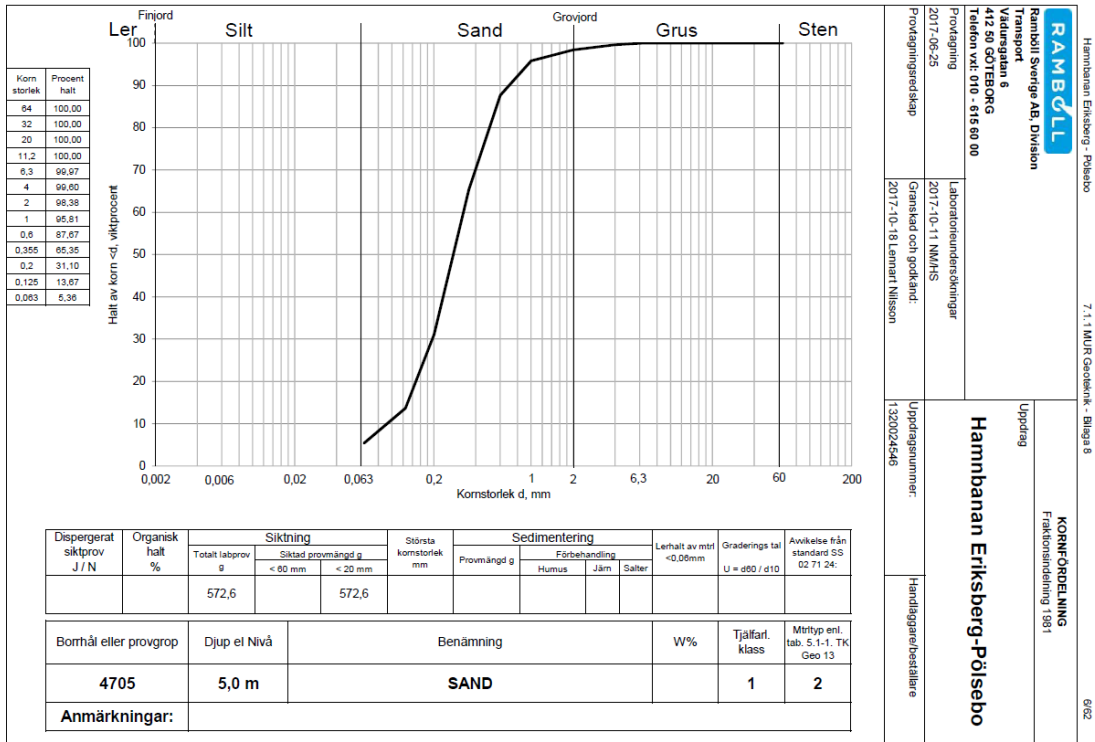


Figure I.6 Copy of the sieve analysis performed at depth 5.0 m for borehole 4705.

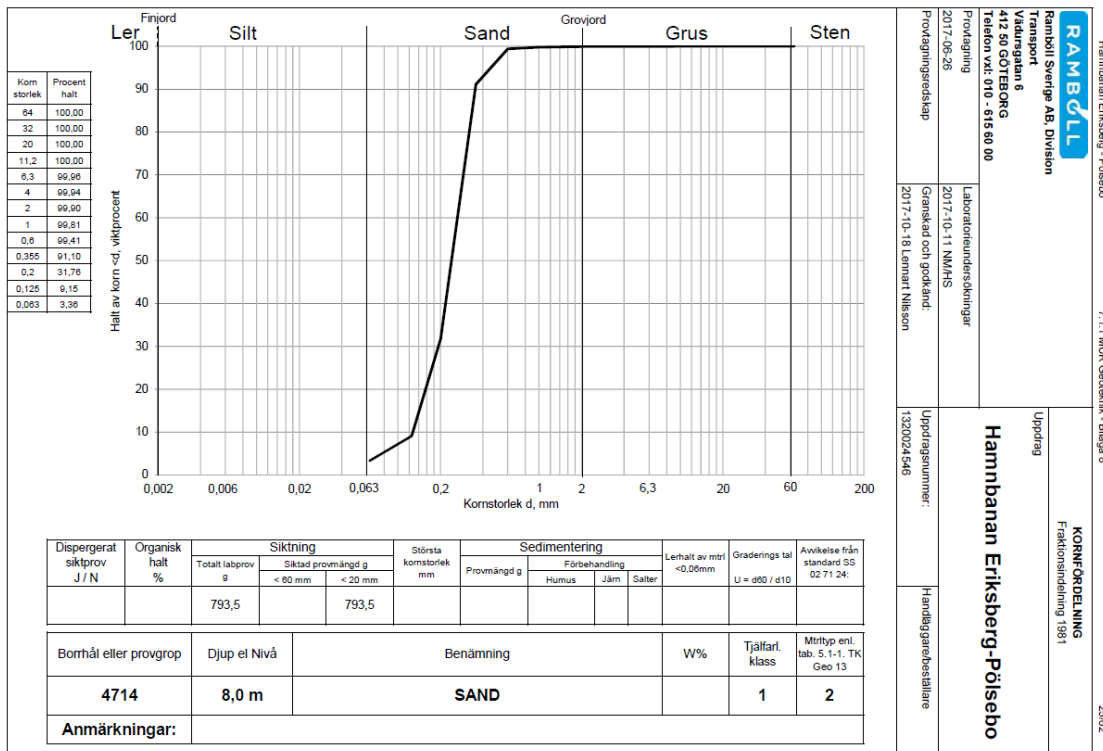


Figure I.7 Copy of the sieve analysis performed at depth 8.0 m for borehole 4714.

CPT - sondering

Sida 1 av 1

Projekt Hamnbanan, Eriksberg-Pölsebo 1320024546				Plats Sannegården Borrhål 4705 Datum 2017-09-04										
Djup (m)		Klassificering	ρ t/m ³	W_L	τ_{fu} kPa	ϕ °	σ_{vo} kPa	σ'_{vo} kPa	σ'_c kPa	OCR	I_D %	E MPa	M_{OC} MPa	M_{NC} MPa
Från	Till													
0,00	0,20	grSa	1,90				1,9	1,9						
0,20	1,00	Sa	1,80				10,8	10,8						
1,00	1,70	sasiLe	1,80				24,0	24,0						
1,70	1,90	Si v L	1,70	0,54	((52,4))		31,8	31,8			3,5	4,0	3,2	
1,90	2,10	CI L	OC	1,70	0,54	30,0	35,4	35,4	188,6	5,33				
2,10	2,30	Si L	1,70	0,54	((96,5))	(33,4)	38,6	38,6			6,0	7,2	5,8	
2,30	2,50	Si v L	1,70	0,54	((41,8))		41,8	41,8			2,9	3,2	2,6	
2,50	2,70	CI L	OC	1,70	0,54	30,1	45,4	45,4	178,1	3,93				
2,70	2,90	CI L	OC	1,70	0,54	31,0	48,7	48,7	181,3	3,72				
2,90	3,10	CI L	OC	1,70	0,54	32,7	52,0	52,0	190,3	3,66				
3,10	3,30	CI L	OC	1,70	0,54	36,3	55,4	55,4	214,0	3,86				
3,30	3,50	Sa v D	1,70	0,54		45,5	59,0	59,0			105,2	90,0	145,4	78,1
3,50	3,70	Sa D	1,70	0,54		38,7	62,2	62,2			86,1	54,6	76,8	50,7
3,70	3,90	Sa Med	1,70	0,54		37,0	65,4	65,4			59,9	23,8	31,5	25,2
3,90	4,10	Sa L	1,70	0,54		35,6	68,7	68,7			48,5	16,9	21,7	17,4
4,10	4,30	Sa L	1,70	0,54		35,8	72,0	72,0			51,1	18,8	24,4	19,5
4,30	4,50	Sa Med	1,70	0,54		36,1	75,4	75,4			54,4	21,3	28,0	22,4
4,50	4,70	Sa D	1,70	0,54		38,2	78,9	78,9			76,0	44,0	60,9	44,4
4,70	4,90	Sa D	1,70	0,54		38,3	82,2	82,2			78,5	48,5	67,7	47,1
4,90	5,10	Sa D	1,70	0,54		38,5	85,5	85,5			83,0	57,1	80,7	52,3
5,10	5,30	Sa D	1,70	0,54		38,2	88,9	88,9			77,5	48,6	67,9	47,2
5,30	5,50	Sa D	1,70	0,54		38,0	92,2	92,2			74,6	45,2	62,7	45,1
5,50	5,66	Sa D	1,70	0,54		38,6	95,2	95,2			86,9	68,1	97,5	59,0

Figure I.8 Copy of the CPT performed for borehole 4705.

CPT - sondering

Sida 1 av 1

Projekt Hamnbanan, Eriksberg-Pölsebo 1320024546				Plats Sannegården Borrhål 4714 Datum 2017-09-05										
Djup (m)		Klassificering	ρ t/m ³	W_L	τ_{fu} kPa	ϕ °	σ_{vo} kPa	σ'_{vo} kPa	σ'_c kPa	OCR	I_D %	E MPa	M_{OC} MPa	M_{NC} MPa
Från	Till													
0,00	1,20	grsiSa	1,90				11,2	11,2						
1,20	1,40	Si v L	1,70	0,54	((66,6))	(33,8)	23,9	23,9			4,3	4,9	4,0	
1,40	1,60	Si v L	1,70	0,54	((43,1))	(30,9)	27,3	27,3			2,9	3,3	2,6	
1,60	1,80	Si v L	1,70	0,54	((39,8))		30,6	30,6			2,7	3,0	2,4	
1,80	2,00	Si v L	1,70	0,54	((40,8))		33,9	33,9			2,8	3,1	2,5	
2,00	2,20	Si v L	1,70	0,54	((38,5))		37,3	37,3			2,7	3,0	2,4	
2,20	2,40	CI L	OC	1,70	0,54	25,3	40,6	40,6	146,9	3,62				
2,40	2,60	CI L	OC	1,70	0,54	24,4	43,9	43,9	138,2	3,14				
2,60	2,80	CI L	OC	1,70	0,54	27,7	47,5	47,5	158,4	3,33				
2,80	2,93	CI H	HOC	1,70	0,54	75,6	50,3	50,3	548,1	10,90				

Figure I.9 Copy of the CPT performed for borehole 4714.

Appendix II

Illustrations of the Excel computations made to calculate the predicted column diameter for the three semi-theoretical models and the manufacturer's model.

Column diameter estimation according to Wang et al. (2012)

Project no. 206082
Project name Hammabaran
Column ID 1000_1,1-1000_1,4

Date: 2020-04-20

General settings

Treatment system: Single fluid
 Installation type: Fresh-in-fresh
 Design diameter: Ø1000
 Level, bottom of column: 4,0 [m]
 Length of column: 2,0 [m]

Notes

Interpretation from borehole data suggest jetting is performed in a non-cohesion soil. Overlying soil is assumed to be 1 m crust and 3 m saturated sand. Ground water table located at -1 m. No samples collected to evaluate clay content, therefore assuming b value according to table.

Input parameters

Operational parameters	Unit	Notation
Nozzle diameter	[mm]	d ₀
No. of nozzles	[1]	M
Delivery of grout	[L/min]	Q
Diameter of monitor	[cm]	D ₀

Soil parameters	Unit	Notation
Content of clay particles, <5µm	[%]	M _c
Undrained shear strength	[kPa]	c _u
Effective friction angle	[°]	φ'
Unit weight, crust	[kN/m ³]	γ _c
Unit weight, saturated soil	[kN/m ³]	γ _s

Input parameters, SI

Operational parameters	Unit	Notation
Nozzle diameter	[m]	d ₀
No. of nozzles	[1]	M
Delivery of grout	[m ³ /s]	Q
Diameter of monitor	[m]	D ₀

Soil parameters	Unit	Notation
Content of clay particles, <5µm	[%]	M _c
Undrained shear strength	[Pa]	c _u
Effective friction angle	[Rad]	φ'
Unit weight, moist	[N/m ³]	γ _c
Unit weight, saturated	[N/m ³]	γ _s
Unit weight, water	[N/m ³]	γ _w
Atmospheric pressure	[Pa]	P _{atm}

Figure II.1 Illustration of the input parameters used in the calculations to predict the diameter according to the method by Wang et al. (2013)

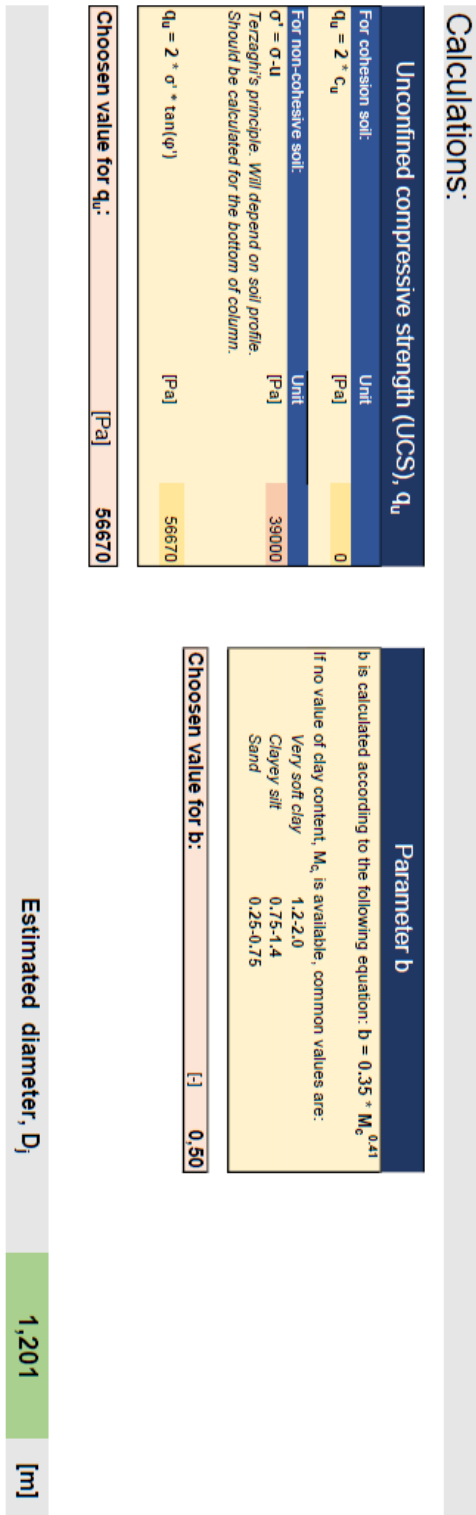


Figure II.24 Illustration of the calculations used to predict the diameter according to the method by Wang et al. (2013)

Column diameter estimation according to Shen et al. (2013)

Date:

2020-04-20

Project no. 206082
 Project name Hammabanan
 Column ID 1000_1.1-1000_1.4

General settings	
Treatment system	Single fluid
Installation type	Fresh-in-fresh
Design diameter	Ø1000
Level: bottom of column	4,0 [m]
Length of column	2,0 [m]

Notes
 Interpretation from borehole data suggest jetting is performed in a non-cohesion soil. Overlying soil is assumed to be 1 m crust and 3 m saturated sand. Ground water table located at -1 m. No samples collected to evaluate clay content, assuming 15 percent as it is the suggested max. clay content in a sand. Average size particle determined to be 0.3 mm from sieve analysis performed by consultant.

Input parameters		
Operational parameters		
Nozzle diameter	[mm]	3,5
No. of nozzles	[-]	1
Delivery of grout	[L/min]	132
Diameter of monitor	[cm]	13
Lifting step	[cm]	4
Time	[s]	8
Air pressure	[bar]	
Water pressure	[bar]	
Grout parameters		
Water	[kg]	100
Cement	[kg]	110
Density of cement	[ton/m ³]	3,15
Soil parameters		
Content of clay particles, <75µm	[%]	15
Average size of soil particles	[mm]	0,3
Undrained shear strength	[kPa]	
Effective friction angle	[°]	36
Unit weight, crust	[kN/m ³]	18
Unit weight, saturated soil	[kN/m ³]	17

Input parameters, SI		
Operational parameters		
Nozzle diameter	[m]	0,0035
No. of nozzles	[-]	1
Delivery of grout	[m ³ /s]	0,0022
Diameter of monitor	[m]	0,13
Lifting step	[m]	0,04
Time	[s]	8
Air pressure	[Pa]	0
Water pressure	[Pa]	0
Rotation speed	[RPS]	0,125
Withdrawal rate	[m/s]	0,005
Exit velocity	[m/s]	229
Grout parameters		
W/C ratio	[kg/kg]	0,91
Density of cement	[kg/m ³]	3150
Soil parameters		
Content of clay particles, <75µm	[%]	15
Average size of soil particles	[mm]	0,3
Undrained shear strength	[Pa]	0
Effective friction angle	[rad]	0,628
Unit weight, moist	[N/m ³]	18000
Unit weight, saturated	[N/m ³]	17000
Unit weight, water	[N/m ³]	10000
Atmospheric pressure	[Pa]	101325

Figure II.3 Illustration of the input parameters used in the calculations to predict the diameter according to the method by Shen et al. (2013)

Calculations:

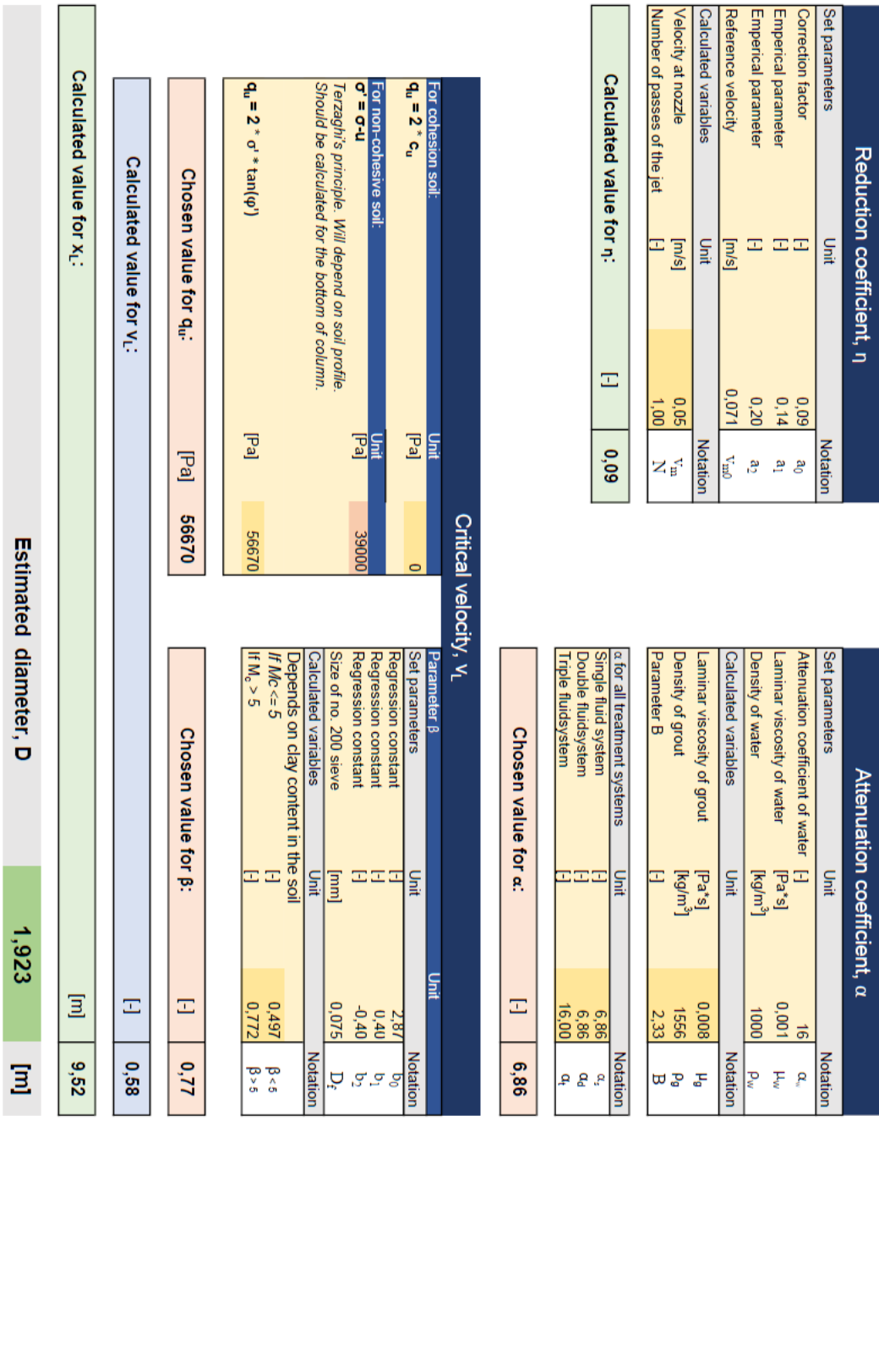


Figure II.4 Illustration of the calculations used to predict the diameter according to the method by Shen et al. (2013)

Column diameter estimation according to Flora et al. (2013)

Date: 2020-04-21

Project no. 206082
 Project name Hammanan
 Column ID 1000.1-1000.1.4

General settings

Treatment system Single fluid
 Installation type Fresh-in-fresh
 Design diameter Ø1000
 Level: bottom of column 4.0 [m]
 Length of column 2.0 [m]

Notes

Interpretation from borehole data suggest jetting is performed in a non-cohesion soil. Protocol from CPT suggest unit tip resistance 2 m below surface 1 MPa.

Input parameters

Operational parameters	Unit	Notation
Nozzle diameter	[mm]	d_n
Delivery of grout	[L/min]	Q
Lifting step	[cm]	Δs_1
Time	[s]	t
Pressure of grout	[Bar]	p

Grout parameters	Unit	Notation
Water	[kg]	W
Cement	[kg]	C
Density of cement	[ton/m ³]	ρ_c

Soil parameters	Unit	Notation
Number of blows in SPT	[]	N_{spt}
Unit tip resistance in CPT	[MPa]	q_c

Input parameters, SI

Operational parameters	Unit	Notation
Nozzle diameter	[m]	d_n
Delivery of grout	[m ³ /s]	Q
Lifting step	[m]	Δs_1
Time	[s]	t
Pressure of grout	[Pa]	p
Withdrawal rate	[m/s]	v_w

Grout parameters	Unit	Notation
W/C ratio	[kg/kg]	w
Density of cement	[kg/m ³]	ρ_c

Soil parameters	Unit	Notation
Number of blows in SPT	[]	N_{spt}
Unit tip resistance in CPT	[MPa]	q_c

Figure II.5 Illustration of the input parameters used in the calculations to predict the diameter according to the method by Flora et al. (2013)

Calculations:

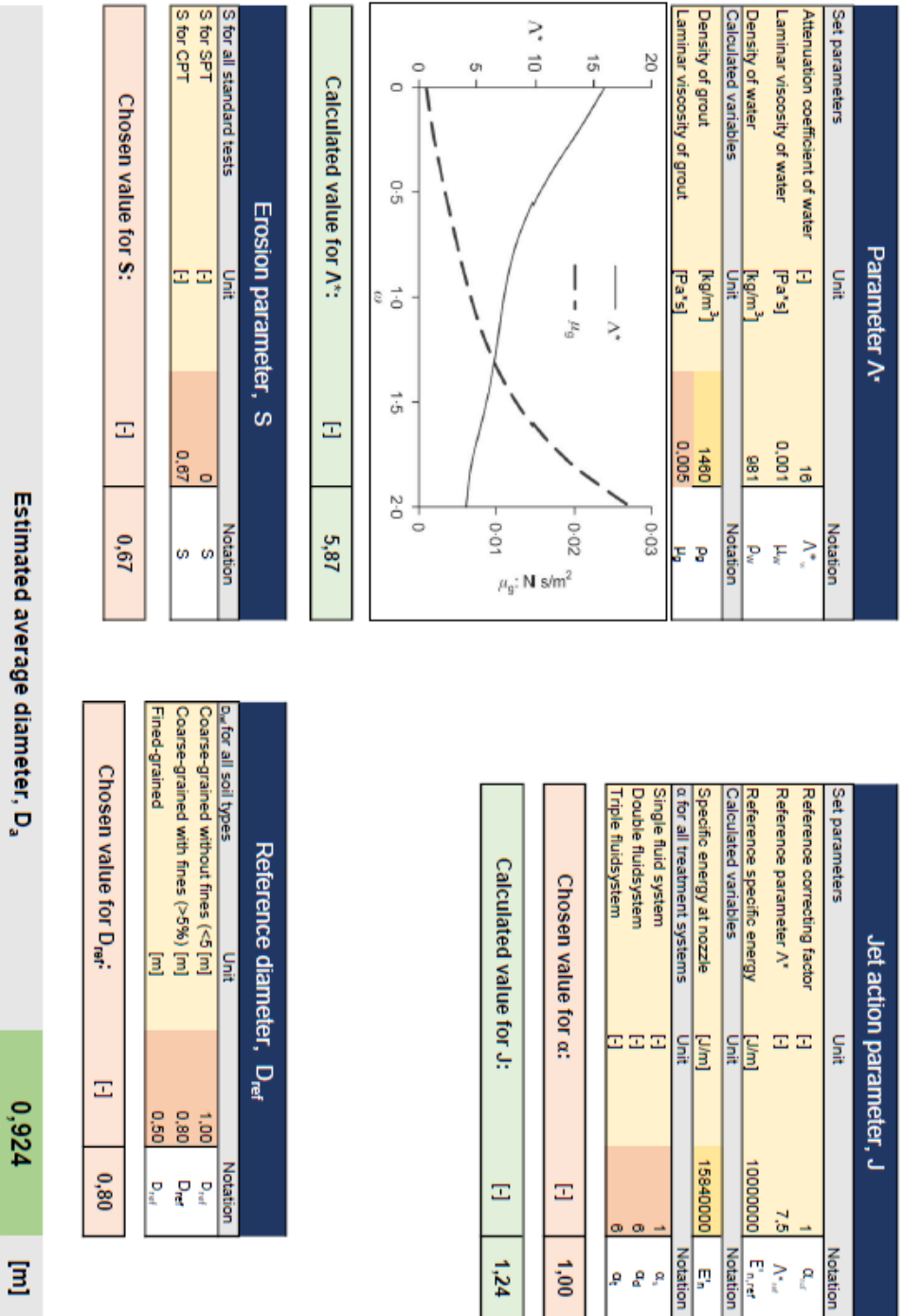


Figure II.6 Illustration of the calculations used to predict the diameter according to the method by Flora et al. (2013)

Column diameter estimation according to the converted manufacturer's model Date: 2020-04-21

Project no. 206082
 Project name Hamnbanan
 Column ID 1000.1.1-1000.1.4

General settings		
Treatment system	Single fluid	
Installation type	Fresh-in-fresh	
Design diameter	Ø1000	
Level: bottom of column	4,0	[m]
Length of column	2,0	[m]

Notes

Input parameters			
Operational parameters		Unit	Notation
Nozzle diameter	[mm]	3,5	d_0
No. of nozzles	[-]	1	M
Rotation per step	[-]	1	R
Lifting step	[cm]	4	Δs_t
Time	[s]	8	t
Pressure of grout	[Bar]	400	p
Grout parameters		Unit	Notation
Water	[kg]	100	W
Cement	[kg]	110	C
Density of cement	[ton/m ³]	3,15	ρ_c
Cement / m ³ treated soil	[kg]	350	CT

Figure II.7 Illustration of the input parameters used in the calculations to predict the diameter according to the revised version of the manufacturer's model.

Calculations:

Conversions			
Parameter	Unit		Notation
Nozzle area	[mm ²]	9,62	N_{area}
Total lifting steps /m	[-]/m	25	S
W/C ratio	[-]	0,91	W/C
Rotations per minute	[RPM]	7,5	RPM

Grout parameters			
Parameter	Unit		Notation
Specific gravity grout	[-]	1,56	SG_g
Grout flow velocity	[m/s]	225	v_g
Grout delivery	[l/s]	2,16	Q
	[l/min]	130	Q
Total grout needed /m	[l]/m	432	V_g
Total cement needed /m	[kg]/m	352	V_c

Estimated diameter, D	1,132	[m]
------------------------------	--------------	------------

Figure II.8 Illustration of the calculations used to predict the diameter according to the revised version of the manufacturer's model.

Appendix III

The illustrations below demonstrate the appearance of the columns that were excavated and the measurements that were gathered.

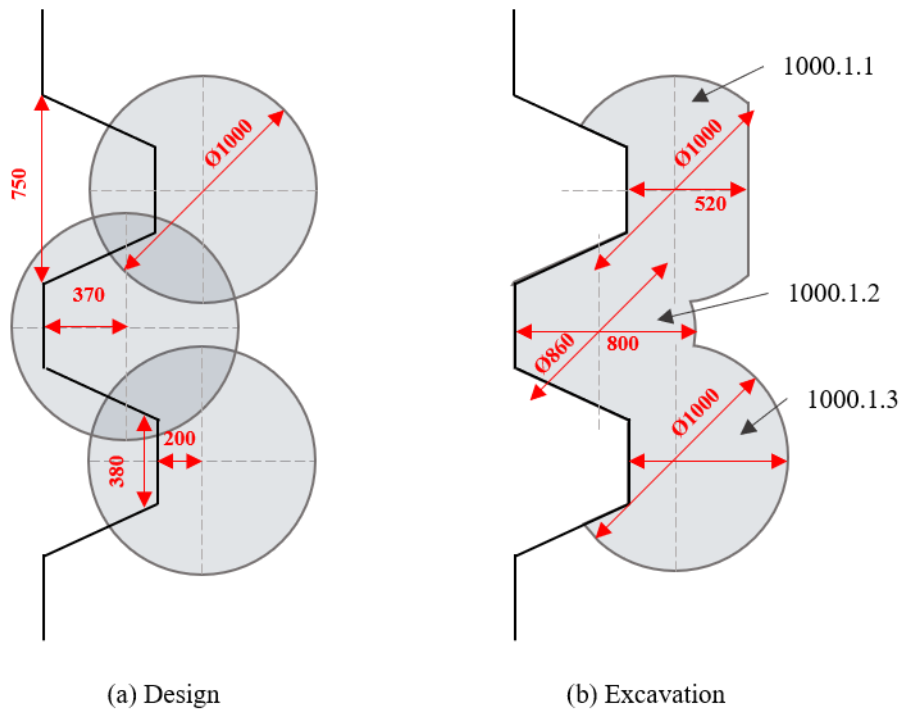


Figure III.1 Excavation test 1.

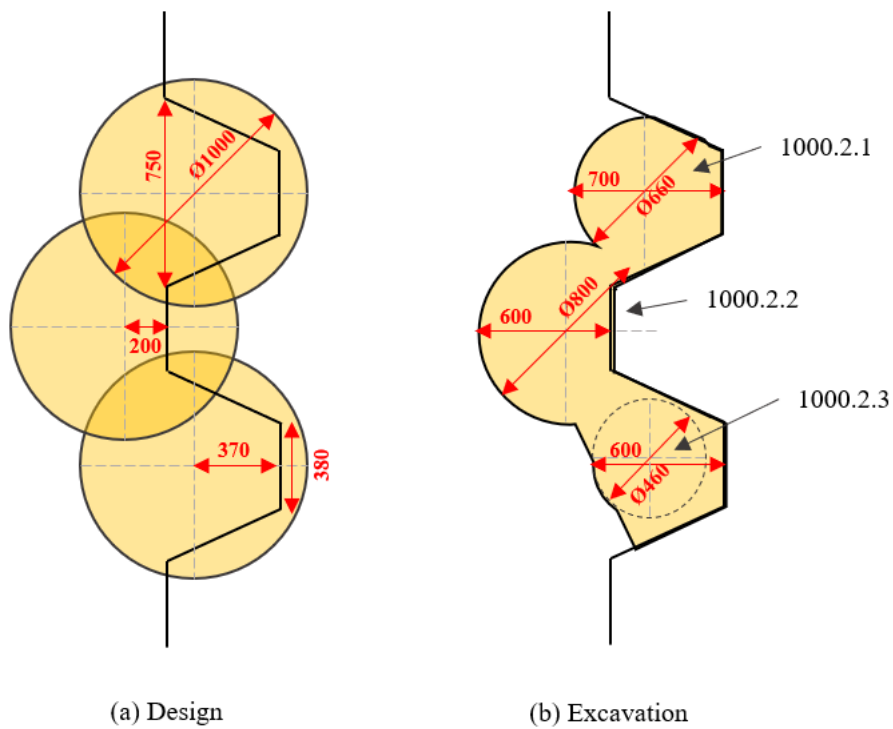
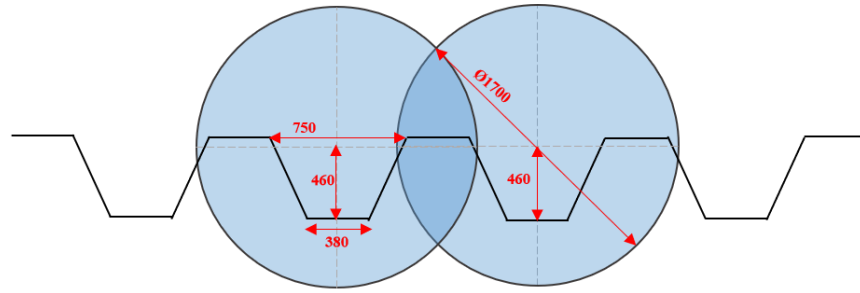
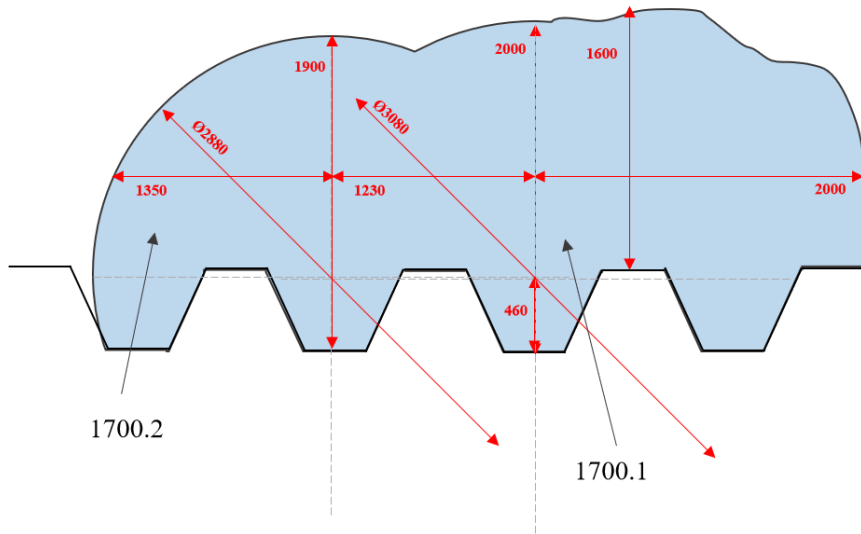


Figure III.2 Excavation test 2.



(a) Design



(b) Excavation

Figure III.3 Excavation test 3.

Appendix IV

Below is a photograph that was taken during the excavation of column 1700.3 displaying the fissure between two soil layers of which was filled up with grout.



Figure IV.1 The “plate of cement” found during the excavation in zone 2 (March 16, 2020).

DEPARTMENT OF ARCHITECTURE AND CIVIL ENGINEERING
DIVISION OF GEOLOGY AND GEOTECHNICS
CHALMERS UNIVERSITY OF TECHNOLOGY

Gothenburg, Sweden
www.chalmers.se



CHALMERS
UNIVERSITY OF TECHNOLOGY